NOVA SCHOOL OF SCIENCE & TECHNOLOGY

DEPARTMENT OF CHEMISTRY

POLYHYDROXYALKANOATE (PHA) BIOSYNTHESIS FROM FRUIT WASTE AT PILOT SCALE: PRODUCTIVITY MAXIMISATION AND POLYMER TAILORING

MARIANA CAMPOS DE MATOS

Master in Chemical and Biochemical Engineering

DOCTORATE IN CHEMICAL AND BIOCHEMICAL ENGINEERING

NOVA University Lisbon

September, 2021

NOVA SCHOOL OF SCIENCE & TECHNOLOGY

DEPARTMENT OF CHEMISTRY

POLYHYDROXYALKANOATE (PHA) BIOSYNTHESIS FROM FRUIT WASTE AT PILOT SCALE: PRODUCTIVITY MAXIMISATION AND POLYMER TAILORING

MARIANA CAMPOS DE MATOS
Master in Chemical and Biochemical Engineering

Adviser: Gilda de Sousa Carvalho Oehmen, Senior Lecturer
University of Queensland, Australia

Co-adviser: Maria D'Ascensão Carvalho Fernandes Miranda Reis, Full Professor, NOVA University Lisbon, Portugal

Examination Committee:

President: José Paulo Barbosa Mota, Full Professor, NOVA University Lisbon

Rapporteurs: Marianna Villano, Assistant Professor, Sapienza University of Rome

Bruno Sommer Ferreira, Chief Executive Officer, Biotrend SA

Co-adviser: Maria Ascensão Carvalho Fernandes Miranda Reis, Full Professor, NOVA University Lisbon

Members: Maria Teresa Ferreira Cesário Smolders, Invited Assistant Professor, Instituto Superior Técnico

Nídia Dana Mariano Lourenço, Researcher
UCIBIO - Unidade de Ciências Biomoleculares Aplicadas of NOVA School of Science & Technology

DOCTORATE IN CHEMICAL AND BIOCHEMICAL ENGINEERING
NOVA University Lisbon
September, 2021

Polyhydroxyalkanoate (PHA) biosynthesis from fruit waste at pilot scale: productivity maximisation and polymer tailoring

Agradecimentos

A elaboração deste projeto não seria possível sem o auxílio de várias pessoas tanto a nível científico como pessoal. Por isso, queria agradecer a todos aqueles que, de uma forma ou de outra, acompanharam, contribuíram e ajudaram à sua concretização.

Desta forma, em primeiro lugar, gostaria de agradecer às minhas orientadoras Doutora Gilda Carvalho e Professora Doutora Maria Ascensão Reis pelo apoio que me deram ao longo de todo o doutoramento e pelos valiosos ensinamentos que sempre estiveram dispostas a partilhar. Fico eternamente grata às minhas orientadoras por me terem inspirado com a vossa dedicação à profissão e, acima de tudo, por me terem transmitido confiança nos momentos em que mais precisei. Mais do que uma excelente orientação, não posso deixar de reforçar o agradecimento à Professora Ascensão pelas ótimas condições de trabalho que me foram proporcionadas, e, acima de tudo, por ter sempre acreditado no meu potencial integrando-me em inúmeros projetos de investigação durante os nove anos que temos de colaboração.

Agradeço também o apoio financeiro da Fundação para a Ciência e Tecnologia através da bolsa de doutoramento SFRH/BD/104767/2014 e às instituições que me acolheram FCT/UNL e UCIBIO.

Parte do trabalho desta tese não seria possível de realizar sem a contribuição dos vários colegas (e co-autores de publicações científicas) com quem tive o prazer de trabalhar, deixo um obrigado especial a todos pela vossa ajuda e dedicação a este projeto. Primeiro, quero agradecer aos meus companheiros da piloto, Rafaela Cruz, Pedro Cardoso e Fernando Silva pelo vosso empenho neste trabalho e também pelos momentos de diversão que vivemos juntos. À minha colega Elisabete Freitas deixo um obrigado pela ajuda preciosa nas análises de microbiologia. Por último agradeço à Doutora Nilay Uçar, ao Doutor Jorge Santos e ao Doutor Adrian Oehmen pela colaboração no trabalho de modelação, Adrian obrigada pelas correções e sugestões de última hora. Mais do que um colega de trabalho, não posso deixar de realçar o meu amigo Jorge Santos que além de co-autor de publicações científicas me ajudou com inúmeras sugestões e conselhos e me inspirou ao longo de todo este percurso!

Quero também agradecer aos colegas do grupo BioEng pelo apoio no laboratório, pelo companheirismo, pelos momentos de descontração e pelas horas de almoço animadas.

Por último, um muito obrigado à família e aos amigos que estiveram sempre lá nos momentos mais difíceis e que me apoiaram durante todo o percurso académico com uma palavras de coragem e incentivo.

Um muito obrigado a TODOS pela ajuda, pela paciência, pela compreensão e pela força que deram em todos os momentos que precisei!

Abstract

Bio-based and biodegradable plastics are an ecological alternative to conventional petroleum-derived polyolefins. Polyhydroxyalkanoates (PHA) have drawn significant attention as one of the most promising biopolymers due to its biocompatibility and biodegradable character. In particular, the copolymer poly(3-hydroxybutyrate-*co*-3-hydroxyvalerate) – P(3HB-*co*-3HV) – has exceptional thermal and mechanical properties, which can be manipulated by varying its monomeric composition. PHA production using non-aseptic mixed microbial cultures (MMCs) enables the use of waste/surplus feedstocks, contributing simultaneously to the implementation of a circular economy approach and to reduce the process operational costs associated to the traditional pure cultures' PHA production. The MMC process usually comprises three steps: the acidogenic fermentation, the enrichment of a MMC in PHA-storers and finally the PHA production. The monomeric composition of the P(3HB-*co*-3HV) produced by MMCs largely depends on the fraction of each soluble fermentation product (SFP) produced in the first step of the process, which can be precursors of either 3-hydroxybutyrate (3-HB) or 3-hydroxyvalerate (3-HV). This Thesis project was focused on solving, at pilot scale, the main difficulties (at the production level) that currently prevent industrial implementation of the PHA production process by MMC: the high manufacturing costs associated to the low process performance and the ability to consistently manipulate and tailor the polymer composition (and thus its properties).

A three-stage MMC process was implemented at pilot scale. Fruit waste (FW) was selected as feedstock, since it contains high concentration of carbon and is globally generated in large volumes, causing several environmental and economic problems. FW is a nutrient-deficient feedstock, thus enabling the implementation of an uncoupled carbon and nitrogen feeding strategy in the selection reactor. The first study conducted in this PhD assesses, for the first time, the impact of the sludge retention time (SRT) (2 and 4 days) and the organic loading rate (OLR) (from 2.6 to 14.5 $gCOD.L^{-1}.d^{-1}$) on the growth versus polymer storage dynamics of PHA-storers selected under the uncoupled feeding strategy. The results showed that, similar biomass volumetric productivities were achieved for each OLR tested, regardless the SRT. However, the culture selected at 4 d SRT showed superior specific storage rates and accumulation capacity resulting in a global PHA productivity (4.6 ± 0.3 $g.L^{-1}.d^{-1}$) that was 80% above that of 2 d SRT (2.6 ± 0.2 $g.L^{-1}.d^{-1}$). This study underlined the importance of achieving a good balance between culture growth and accumulation capacity to increase the viability of the PHA-producing process from wastes.

The same pilot plant set-up and feedstock (FW) were used to incorporate different effective operating conditions in the three stages of the process with the objective of boosting the overall PHA production performance (namely, PHA content on biomass, global productivity and overall yield). The OLR and pH of the acidogenic reactor were successfully adjusted targeting a high fermentation yield (0.74

gCOD.gCOD^{-1}) and the production of a fermentate highly enriched in butyrate (56.8%, gCOD-basis), resulting in enhanced PHA production steps. A well selected MMC was obtained as a result of uncoupling the carbon to the nitrogen feeding, and the biomass volumetric productivity attained the unprecedented value of 1.96 g.L^{-1}.d^{-1} as a response to the high OLR (8.7 gCOD.L^{-1}.d^{-1}) imposed. The culture selected at the optimal OLR achieved a high storage yield (0.98 gCOD.gCOD^{-1}), and the continuous feeding strategy led to a maximum PHA content of 80.5% (w/w) at the end of accumulation assays. The obtained global PHA productivity (8.1 g-PHA.L^{-1}.d^{-1}) and overall process yield (0.45 gCOD.gCOD^{-1}) are the highest values reported for MMC using a real waste feedstock at pilot scale. Moreover, a P(3HB-*co*-3HV) copolymer with a 3-HV content of 0.24 (g-basis) and a molecular weight of 311 KDa was produced, making this material an ideal candidate for packaging applications, the largest market of plastic usage.

Lastly, the possibility of tailoring the precursors that influence the P(3HB-*co*-3HV) composition was investigated, by controlling the operating pH (between 4.69 and 6.34) of a continuous upflow anaerobic sludge blanket (UASB) reactor fed with FW. The impact of the operating conditions imposed was assessed by evaluating the microbial community profile, the corresponding performance and the impact on polymer composition. The fermentation yield of the UASB was maintained quite stable (between 0.72 and 0.79 gCOD.gCOD^{-1}) during the entire operational period. On the other hand, the 3-HV bioprecursors fraction in effluent was highly affected by pH, resulting in the production of P(3HB-*co*-3HV) copolymers with quite different monomeric compositions. Overall, the 3-HV content of the produced polymers varied from 0.16 to a maximum of 0.44 (gCOD-basis) when the pH of the acidogenic reactor increased from 4.69 to 5.92. Moreover, the end-stream SFP composition were similar for identical operational pH values tested in different periods, showing that despite the changes occurring in the system, the selected cultures were resilient and able to produce a consistent profile of fermentation products (and thus a constant PHA monomeric composition). Additionally, the IWA Anaerobic Digestion Model No. 1 (ADM1) was expanded to include the pathway of valerate production from lactate, aiming to dynamically predict the profile of the PHA bioprecursors produced. Calibration and validation procedures were done against data from two distinct pilot-scale UASB reactors fed with FW and describing different pH and OLR dynamics. The model was capable to predict the different PHA bioprecursors production in the UASB reactors with overall strong correlations with the experimental data for different OLRs over the pH range between 4.20 and 5.16, providing a useful tool for process optimisation and tailoring of the PHA monomer composition.

This thesis highlights the importance of understanding in-depth the impact of key operating conditions on the PHA production process with MMC to increase its overall viability. Moreover, it shows that predicting and regulating the acidogenic process is essential to promote an adequate PHA bioprecursors composition production, which are both promising results towards the full-scale implementation of the PHA production from MMC.

Keywords: polyhydroxyalkanoates (PHA); mixed microbial cultures (MMC); fruit waste; pilot plant; productivity maximisation; polymer tailoring;

Resumo

Plásticos biodegradáveis de origem biológica são uma alternativa ecológica às poliolefinas convencionais derivadas do petróleo. Os polihidroxialcanoatos (PHAs) têm vido a ganhar prestígio como um dos bioplásticos mais promissores devido ao seu carater biocompatível e biodegradável. Em particular, o copolímero poli(3-hidroxibutirato-*co*-3-hidroxivalerato) – P(3HB-*co*-3HV) – tem excelentes propriedades mecânicas e térmicas, que podem ser manipuladas variando a sua composição monomérica. A produção de PHA usando culturas microbianas mistas (MMCs) não assépticas permite o uso de resíduos/sub-produtos como substratos, contribuindo simultaneamente para a implementação de uma economia circular e para reduzir os custos operacionais associados ao tradicional processo de produção de PHA com culturas puras. O processo de produção com MMC envolve normalmente 3 passos: uma fermentação acidogénica, o enriquecimento de uma MMC em bactérias acumuladoras de PHA e, por último, a produção de PHA. A composição monomérica do P(3HB-*co*-3HV) produzido por MMCs depende fortemente da fração de cada produto de fermentação solúvel (SFP) produzido no primeiro passo do processo, que podem ser precursores de 3-hidroxibutirato (3-HB) ou de 3-hidroxivalerato (3-HV) Este projeto de Tese teve como foco principal resolver, à escala piloto, as principais dificuldades (ao nível da produção) que impendem a implementação do processo de produção de PHAs a partir de MMCs à escala industrial: os custos de produção altos associados à baixa performance do processo e a habilidade de manipular consistentemente a composição do polímero (e portanto as suas propriedades).

O processo de três passos de produção de PHAs foi implementado à escala piloto. Resíduos de fruta estragada (FW) foram selecionados como substrato, visto que contêm altas concentrações de carbono e são globalmente gerados em grandes volumes, causando diversos problemas ambientais e económicos. FW são um substrato deficiente em nutrientes, o que permite implementar uma estratégia de alimentação em que o fornecimento de carbono é desacoplado do azoto no reator de seleção. O primeiro estudo realizado durante este PhD teve como objetivo estudar, pela primeira vez, o impacto do tempo de retenção de lamas (SRT) (2 e 4 dias) e da taxa de carga orgânica (OLR) (de 2.6 a 14.5 $gCOD.L^{-1}.d^{-1}$) nas dinâmicas de crescimento versus armazenamento de polímero de culturas produtoras de PHA sujeitas ao regime de alimentação desacoplado. Os resultados mostraram que, semelhantes produtividades volumétricas de biomassa são observadas para cada OLR imposta, independentemente do SRT. No entanto, a cultura selecionada a um SRT de 4 d mostrou uma taxa especifica de produção de polímero e uma capacidade de acumulação superiores, apresentando uma produtividade global de PHA (4.6 ± 0.3 $g.L^{-1}.d^{-1}$) 80% superior ao atingido pela cultura selecionada a um SRT de 2 d (2.6 ± 0.2 $g.L^{-1}.d^{-1}$). Este estudo realçou a importância de conseguir um bom equilíbrio entre o crescimento da cultura e a sua capacidade de acumulação, de forma a aumentar a viabilidade do processo de produção de PHA a partir de resíduos.

A mesma instalação piloto e substrato (FW) foram usados no seguinte estudo, onde várias condições de operação eficazes foram incorporadas de uma só vez nos três passos do processo com o objetivo de impulsionar a performance global da produção de PHA (nomeadamente, o conteúdo de PHA na biomassa, a produtividade global e o rendimento global). A OLR e o pH do reator acidogénico foram ajustados com sucesso de forma a atingir um elevado rendimento de fermentação (0.74 $gCOD.gCOD^{-1}$) e produzir um fermentado enriquecido em butirato (56.8%, base gCOD), que irá beneficiar a performance da cultura nos próximos passos do processo. Uma MMC bem selecionada foi obtida como resultado da aplicação da estratégia de desacoplamento do carbono do azoto, e a produtividade volumétrica de biomassa atingiu o valor sem precedentes de 1.96 $g.L^{-1}.d^{-1}$, como resposta à alta OLR (8.7 $gCOD.L^{-1}.d^{-1}$) imposta. A cultura selecionada à OLR ótima mostrou um elevado rendimento de produção de PHA (0.98 $gCOD.gCOD^{-1}$), e a estratégia de alimentação continua levou à obtenção de um conteúdo máximo de PHA na biomassa de 80.5% (w/w) no final dos ensaios de acumulação. A produtividade global de PHA (8.1 $g\text{-}PHA.L^{-1}.d^{-1}$) e o rendimento global do processo (0.45 $gCOD.gCOD^{-1}$) obtidos foram os valores mais altos reportados para MMC usando um resíduo real como substrato à escala piloto. Alem disso, foi produzido um copolímero P(3HB-*co*-3HV) com 0.24 (base g) de monómeros 3-HV e um peso molecular de 311 KDa, o que faz deste material um excelente candidato para ser usado em embalagens, o sector de mercado que apresenta o consumo de plástico mais elevado.

Por último, a possibilidade de controlar a produção dos percursores que influenciam a composição do P(3HB-*co*-3HV) foi investigada através da manipulação do pH (entre 4.69 e 6.34) de um reator anaeróbio de fluxo ascendente (UASB) alimentado com FW. O impacto das diferentes condições de operação impostas foi avaliado através da observação do perfil da comunidade microbiana selecionada, da sua performance e do impacto na composição dos diferentes polímeros produzidos. O rendimento de fermentação do UASB manteve-se relativamente estável (entre 0.72 e 0.79 $gCOD.gCOD^{-1}$) durante todo o período de operação. Por outro lado, a fração de precursores de 3-HV no efluente foi bastante afetada pelo pH, o que resultou na produção de copolímeros P(3HB-*co*-3HV) com diferentes composições monoméricas. De forma global, o conteúdo de 3-HV nos polímeros produzidos variou de 0.16 até um máximo de 0.44 (base gCOD) quando o pH do reator acidogénico aumentou de 4.69 para 5.92. Além disso, a composição das correntes de SFP produzidas a valores de pH semelhantes, mas testados em diferentes períodos da operação, foram idênticas, mostrando que, apesar das mudanças que ocorrem no sistema, as culturas selecionadas foram resilientes a capazes de produzir um perfil de produtos de fermentação consistente (resultando numa composição monomérica de polímero constante). Além do trabalho experimental relatado, o modelo de digestão anaeróbia No. 1 (ADM1) foi expandido de forma a incluir a via de produção de valerato a partir de lactato, com o objetivo de se prever dinamicamente o perfil de precursores de PHA produzido no reator UASB descrito. Os procedimentos de calibração e validação foram realizados usando dados de dois reatores UASB piloto distintos, ambos alimentados com FW e sujeitos a diferentes dinâmicas de pH e OLR. O modelo foi capaz de prever a produção dos

diferentes precursores de PHA nos reatores UASB e atingir fortes correlações com os dados experimentais obtidos para várias OLRs dentro do intervalo de pH de 4.20 a 5.16, providenciando uma ferramenta útil para otimização do processo e para manipular a composição monomérica de PHA.

Esta tese realça a importância de efetivamente perceber o impacto de condições de operação chave no processo de produção de PHA com MMC de forma a aumentar a sua viabilidade global. Alem disso, mostrou que prever e regular o processo acidogénico é essencial para promover a produção de precursores de PHA com uma composição adequada, o que são ambos resultados promissores no sentido da implementação à escala industrial do processo de produção de PHA a partir de MMC.

Palavras-chave: polihidroxialcanoatos (PHA), culturas microbianas mistas (MMC); resíduos de fruta; instalação piloto; maximização da produtividade; manipulação da composição do polímero;

Table of contents

Agradecimentos III

Abstract V

Resumo IX

List of figures XVII

List of tables XIX

List of abbreviations XXI

1 INTRODUCTION 1

1.1 From petroleum derived plastics to new alternatives 2

1.2 Increasing demand for bioplastics: towards a closed loop cycle 3

1.3 Polyhydroxyalkanoates: a promising eco-friendly bioplastic 5

1.3.1 Applications 7

1.4 PHA production by bacteria 7

1.4.1 Pure cultures process – the current commercial approach 8

1.4.2 Mixed microbial cultures process using waste feedstocks – the eco-efficient approach 9

1.4.3 Impact of operating conditions on three-stage process performance 10

1.4.3.1 Acidogenic fermentation 10

1.4.3.2 Selection reactor 11

1.4.3.3 PHA production reactor 12

1.5 Scaling-up PHA production using MMCs: case studies and research needs 13

1.6 Motivation and thesis outline 15

1.7 References 17

2 SLUDGE RETENTION TIME IMPACTS ON POLYHYDROXYALKANOATE PRODUCTIVITY IN UNCOUPLED STORAGE/GROWTH PROCESSES 25

2.1 Introduction 27

2.2 Materials and methods 29

2.2.1 Experimental set-up and operation of the reactors 29

2.2.1.1 Acidogenic fermentation ... 29
2.2.1.2 Culture selection reactor ... 30
2.2.1.3 PHA accumulation fed-batch assays ... 31
2.2.2 Analytical methods ... 31
2.2.3 Microbiological analyses ... 32
2.2.4 Calculations ... 32
2.3 Results ... 33
2.3.1 Culture selection ... 33
2.3.1.1 SRT of 4 d ... 33
2.3.1.2 SRT of 2 d ... 34
2.3.2 PHA accumulation assays ... 36
2.3.3 Microbial community analysis ... 37
2.4 Discussion ... 39
2.4.1 Growth vs storage response ... 39
2.4.2 Impact of the operational conditions on PHA production process ... 42
2.5 Conclusions and prospects ... 44
2.6 References ... 44
3 COMBINED STRATEGIES TO BOOST POLYHYDROXYALKANOATE PRODUCTION FROM FRUIT WASTE IN A 3-STAGE PILOT PLANT ... 49
3.1 Introduction ... 51
3.2 Materials and methods ... 53
3.2.1 Waste feedstock for PHA production ... 53
3.2.2 Set-up and operation of the reactors ... 53
3.2.2.1 Acidogenic fermentation ... 53
3.2.2.2 Culture selection reactor ... 54
3.2.2.3 Maximum accumulation potential (MAP) tests ... 54
3.2.3 Analytical methods ... 54
3.2.4 Microbiological analyses ... 55

3.2.5 Calculations 55
3.3 Results and discussion 55
3.3.1 Acidogenic reactor performance: impact of OLR and pH 55
3.3.2 Selection reactor 58
3.3.2.1 Impact of loading rate in biomass concentration and productivity 58
3.3.2.2 Impact of substrate concentration and profile on substrate uptake and polymer storage 61
3.3.3 Accumulation step: maximum accumulation potential (MAP) 64
3.3.4 Overall PHA yield 66
3.4 Conclusions 67
3.5 References 67
4 UNDERSTANDING THE POLYHYDROXYALKANOATE (PHA) BIOPRECURSORS PRODUCTION FROM FRUIT WASTE BY MIXED MICROBIAL CULTURES THROUGH PILOT SCALE EXPERIMENTS AND METABOLIC MODELLING 73
4.1 Introduction 75
4.2 Materials and methods 77
4.2.1 Acidogenic reactor setup 77
4.2.2 PHA production assays 78
4.2.3 Analytical methods 79
4.2.4 Microbiological analyses 79
4.2.5 Calculations 80
4.3 Model description and development 81
4.3.1 Stoichiometric coefficients calculation 82
4.3.2 Plant model setup 83
4.3.3 Influent fractionation 84
4.3.4 Model calibration and validation 85
4.4 Results and discussion 86
4.4.1 Impact of acidogenic pH on the PHA precursors composition 86
4.4.2 UASB microbial community dynamics as a function of pH 89
4.4.3 Impact of pH on the polymer composition 92

4.4.4 Model simulation results 93
4.4.4.1 Model calibration 93
4.4.4.2 Model validation 95
4.5 Conclusions 97
4.6 References 97
5 GENERAL CONCLUSIONS AND FUTURE WORK 105
5.1 General conclusions 106
5.2 Future work and perspectives 107
APPENDIX A 111
APPENDIX B 119
APPENDIX C 129

List of figures

Figure 1.1 – Plastics demand by segment in Europe in 2019. Adapted from (Plastics Europe, 2020). 3

Figure 1.2 - Bioplastics demand by segment in 2020. Adapted from (European Bioplastics, 2020). 4

Figure 1.3 - General chemical structure of PHAs. n variable number of carbon atoms in the linear structure; R1 and R2 are the variable hydrocarbon side chains. 5

Figure 1.4 - Typical 3-stage process for PHA production by MMCs. Adapted from (Reis et al., 2011). 9

Figure 2.1 - Configuration of the pilot plant unit adopted in this study. 29

Figure 2.2 - PCA ordination highlighting the differences in OTUs abundance between the microbial communities selected in SBR 4d and SBR 2d (data labels correspond to the operational OLR). The relative contribution (eigenvalue) of each axis to the total inertia in the data is indicated in percent at the axis titles..... 38

Figure 2.3 – Storage yields ($Y_{PHA/SFP}$) as a function of (A) the different OLR values applied and (B) the relative abundance of known putative PHA-storers, determined in the SBR 4d and SBR 2d. 40

Figure 2.4 - Specific storage rates (q_{PHA}) obtained in the SBRs and accumulation assays as a function of (A) the different OLR values applied in SBRs and (B) the relative abundance of known putative PHA-storers of the cultures selected at the different OLRs in SBR 4d and SBR 2d. The orange and yellow rectangles highlight q_{PHA} obtained for the same culture inoculated in the SBR and Acc reactors..... 41

Figure 2.5 – Influence of the OLR values in the biomass volumetric productivity (P_X) obtained for the SBR 4d and SBR 2d. 43

Figure 3.1 – Profiles of OLR, pH and SFP in the UASB reactor using fruit waste as feedstock. (A) pH conditions applied and fraction of produced HLac and HBut, (B) Imposed OLR and effluent SFP profiles..... 56

Figure 3.2 – Correlation between pH in the UASB reactor and the fraction of HBut produced (excludes the values obtained for the initial start-up period of 37 days)..... 57

Figure 3.3 – Specific uptake rates of total SFP (A), HLac (B), HAce (C) and HBut (D) as a function of their concentrations in SBR. Estimated mean (standard deviation) values of $-q_{max}$ and K_m for each corresponding substrate are also represented. [a] in $gCOD.gCOD\text{-}Xa^{-1}.h^{-1}$; [b] in $Cmol.Cmol\text{-}Xa^{-1}.h^{-1}$; [c] in $gCOD.L^{-1}$; [d] in $Cmmol.L^{-1}$..... 61

Figure 3.4 – Correlation between butyrate (HBut) fraction observed in SBR and storage yield ($Y_{PHA/SFP}$). 63

Figure 4.1 – Layout of the UASB system in the Sumo 21 software 84

Figure 4.2 - SFP profiles and 3-HV precursors fraction obtained at each different pH setpoint. 87

Figure 4.3 –Dynamics of the most relevant bacteria (A) and PCA ordination highlighting the differences/similarities in microbial communities (B) selected in the UASB reactor at the different pH setpoints (period – pH are represented in the data labels in B). The relative contribution (eigenvalue) of each axis to the total inertia in the data is indicated in percent at the axis titles. 90

Figure 4.4 – HBut fraction as a function of the relative abundace of *Clostridium sensu stricto 12 and Ruminiclostridium 5* (A) and 3-HV precursors fraction relation with *Prevotella 7* and *Megasphaera* relative abundance (B) 91

Figure 4.5 – 3-HB (A) and 3-HV (B) monomer fractions produced in the PHA production assays as a function of the corresponding different precursors present in the feed. 92

Figure 4.6 – Measured pH and observed total SFP (A), 3-HB (B) and 3-HV (C) bioprecursors production in calibration reactor and performance comparison between original ADM1 model and the modified ADM1 model developed in this study. 94

Figure 4.7 – Observed reactor pH and predicted versus measured results for total SFP (A), 3-HB (B) and 3-HV (C) precursors production in the validation UASB. 96

Figure A1 - Feast to famine ratio and OLR change over time in SBR 4d (A) and SBR 2d (B). 112

Figure A2 - Δ3-HB (A) and Δ3-HV (B) monomers produced during SBR cycles and accumulation assays as a function of the corresponding 3-HB and 3-HV precursors molar fraction in the feed. 116

Figure B1 - Experimental setup of the pilot PHA production process using fruit waste as feedstock. Grey circles with 1, 2 and 3 identify the sampling points of the UASB (only effluent), SBR and accumulation reactors, respectively. 119

Figure B2 - COD flow in the 3-step PHA production process using fruit waste as carbon source and applying the combined effective strategies. 125

List of tables

Table 1.1 – Properties of PHAs compared to other bio-based plastic (PLA) and to petroleum-derived polymers (PP, high-density PE and low-density PE). 6

Table 1.2 – Performance of PHA production pilot-scale studies using MMCs and waste-based feedstocks. 15

Table 2.1 - Characteristics of the clarified fermented feedstock. Ranges of the key parameters are presented as minimum/maximum values detected in the feedstock. 30

Table 2.2 – Main parameters monitored and determined for SBR operation at SBR 4d and SBR 2d for each OLR tested. Values presented are mean (standard deviation). 35

Table 2.3 - Main parameters determined in the accumulation reactor inoculated with culture selected at the maximum OLR tested in SBR 4d (Acc 4d) and SBR 2d (Acc 2d). Values presented are mean (standard deviation). 37

Table 2.4 - Relative abundance (% of total reads) and concentration of putative PHA-storers calculated for the cultures present in SBR 4d and SBR 2d. Values of putative PHA-storers concentration are mean (standard deviation). 38

Table 3.1 – Operating conditions and performance parameters of the PHA-accumulating mixed culture subjected to different OLR values. Parameters determined for pseudo steady state phases. Values presented are mean (standard deviation). 60

Table 3.2 – Calculated kinetic parameters of the maximum accumulation potential test and comparison with literature studies. Values presented are mean (standard deviation). 64

Table 4.1 – Performance of the UASB reactor fed with FW and operated under dynamic operating pH. The values listed are average (standard deviation). 78

Table 4.2 – SFP profiles used for the PHA production assays. 79

Table 4.3 – Stoichiometric equations of monosaccharides and lactate fermentation implemented in the extended ADM1 model developed in this study. 82

Table 4.4 - Stoichiometric coefficients from monosaccharides and lactate uptake. 83

Table 4.5 - Estimated fractions per total COD, total nitrogen and total phosphorous. 85

Table 4.6 – Yields of the different fermentation products on monosaccharides and lactate calculated from the experimental data reported by Matos et al. 2021 versus the values proposed by Batstone, 2002. 86

Table 4.7 – Qualitative FISH analysis using probe ARC915 to target Archaea. 90

Table 4.8 – Model accuracy assessment for the period from day 41 onwards of the calibration reactor. Values are mean (standard deviation). 94

Table A1 - High throughput 16S sequencing data of the most abundant bacterial populations present in the selection reactor at the different OLR tested and SRT of 4 days. (P_Phylum, c_class; genus level). 113
Table A2 - High throughput 16S sequencing data of the most abundant bacterial populations present in the selection reactor at the different OLR tested and SRT of 2 days. (P_Phylum, c_class; genus level). 114
Table A3 - Identification of putative PHA-storers and respective relative abundance (% of total reads) determined by high throughput 16S sequencing. For each identified taxonomic group, a reference (Ref.) reporting the suggested PHA storing ability is provided. 115
Table A4 - FISH analysis of the bacterial community over time..... 116
Table B1 - Operating conditions applied and performance parameters determined at pseudo-steady-state of UASB reactor. Values presented are mean (standard deviation)..... 122
Table B2 - Most abundant bacterial populations present in the microbial community identified by 16S rRNA gene amplicon sequencing of the cultures enriched in the selection reactor at the different OLR tested. (P_Phylum, c_class; genus level)..... 123
Table B3 - FISH analysis of the bacterial community over time during the increased OLR imposed in the SBR. 124
Table B 4 - Process parameters used in the calculation of the overall PHA yield and comparison with literature studies. 125
Table C1 - Kinetic matrix of the model. Description of kinetic and stoichiometric parameters can be found in Table C2..... 129
Table C2 - Description of kinetic and stoichiometric parameters and values used in the simulations. 132
Table C3 - Saturation and inhibition terms used in the process rates. 134
Table C4 - Measurements needed for the characterisation of the influent..... 135
Table C5 - Equations used in total COD, total nitrogen and total phosphorous mass balances. ... 135
Table C6 - State variables of the modified ADM1 model developed..... 136

List of abbreviations

μ_{max}	maximum specific growth rate	$f_{PROP,SUG}$	coefficients of propionate on monossacharides
3-HB	3-hydroxybutyrate	**fr_NH,TN**	fraction of ammonia
3-HHx	3-hydroxyhexanoate	**fr_PO4,TP**	fraction of orthophosphate
3-HV	3-hydroxyvalerate	**fr_S_{AC}**	fraction of soluble total Acetate
ADF	aerobic dynamic feeding	**fr_S_{BUT}**	fraction of soluble total Butyrate
ADM1	IWA Anaerobic Digestion Model No. 1	**fr_S_{ET}**	fraction of soluble total Ethanol
C	carbon	**fr_S_{LAC}**	fraction of soluble total Lactate
COD	chemical oxygen demand	**fr_S_{PROP}**	fraction of soluble total Propionate
C_{SFP}	concentration of soluble fermentation products on reactor broth	**fr_S_{SUG}**	fraction of soluble monosaccharides
CSTR	continuous stirred tank reactor	**fr_S_{VAL}**	fraction of soluble total Valerate
Cy3	cyanine 3	**fr_X_{CH}**	fraction of particulate carbohydrates
DO	dissolved oxygen	**fr_X_{LIP}**	fraction of particulate lipids
EtOH	ethanol	**fr_X_{PROT}**	fraction of particulate proteins
$f_{AC,LAC}$	coefficients of acetate on lactate	**fr_X_U**	fraction of particulate Inerts
$f_{AC,SUG}$	coefficients of acetate on monossacharides	$f_{VAL,LAC}$	coefficients of valerate on lactate
$f_{BUT,SUG}$	coefficients of butyrate on monossacharides	**FW**	fruit waste
f-CW	fermented cheese whey	**GC**	gas chromatography
$f_{ET,SUG}$	coefficients of ethanol on monossacharides	**HA**	hydroxyalkanoate
FF	feast to famine length	**HAce**	acetate
$f_{H2,LAC}$	coefficients of hydrogen on lactate	**HBut**	butyrate
$f_{H2,SUG}$	coefficients of hydrogen on monossacharides	**HLac**	lactate
FISH	fluorescence in situ hybridization	**HPLC**	high performance liquid chromatography
FITC	fluorescein isothiocyanate	**HPro**	propionate
$f_{LAC,SUG}$	coefficients of lactate on monossacharides	**HRT**	hydraulic retention time
f-PMW	fermented paper mill wastewater	**HVal**	valerate
$f_{PROP,LAC}$	coefficients of propionate on lactate	K_m	affinity constant

MAE	mean absolute error
MAP	maximum accumulation potential
M-M	Michaelis-Menten
N	nitrogen
OFMSW	organic fraction of municipal solid waste
OLR	organic load rate
OTU	operational taxonomic unit
P(3HB-*co*-3HV)	poly(3-hydroxybutyrate-*co*-3-hydroxyvalerate)
PA	polyamide
PBAT	polybutylene adipate-co-terephthalate
PBS	polybutylene succinate
PC	principal component
PCA	Principal component analysis
PCL	polycaprolactone
PE	polyethylene
PET	polyethylene terephthalate
PHA	polyhydroxyalkanoate
PHB	polyhydroxybutyrate
PLA	polylactic acid
PP	polypropylene
$\mathbf{P_x}$	biomass volumetric productivity
$\mathbf{-q_{max}}$	maximum specific uptake rate
$\mathbf{q_{PHA}}$	specific PHA storage rate
$\mathbf{-q_{PHA}^{famine}}$	maximum specific PHA consumption in the famine phase
$\mathbf{-q_{SFP}}$	specific substrate uptake rate
RMSE	root mean square error
$\mathbf{r_{SFP}}$	Soluble fermentation products volumetric productivity
SBR	sequential batch reactor
SCFA	short chain fatty acids
SEC	size exclusion chromatography
SFP	soluble fermentation products
SRT	sludge retention time
$\mathbf{T_m}$	melting temperature
TSS	total suspended solids
UASB	upflow anaerobic sludge blanket
VFA	volatile fatty acids
VSS	volatile suspended solids
WAS	waste activated sludge
$\mathbf{X_a}$	active biomass
$\mathbf{Y_{PHA/FW}}$	overall PHA yield on fruit waste
$\mathbf{Y_{PHA/SFP}}$	storage yield
$\mathbf{Y_{SFP/FW}}$	fermentation yield
$\mathbf{Y_{X/PHA}}$	growth yield on PHA
$\boldsymbol{\eta_{1,lac}}$	fraction of lactate that degrades via reaction 1
$\boldsymbol{\eta_{1,sug}}$	fraction of monosaccharides that degrades via reaction 1
$\boldsymbol{\eta_{2,lac}}$	fraction of lactate that degrades via reaction 2
$\boldsymbol{\eta_{2,sug}}$	fraction of monosaccharides that degrades via reaction 2
$\boldsymbol{\eta_{3,lac}}$	fraction of lactate that degrades via reaction 3
$\boldsymbol{\eta_{3,sug}}$	fraction of monosaccharides that degrades via reaction 3
$\boldsymbol{\eta_{4,sug}}$	fraction of monosaccharides that degrades via reaction 4

1

INTRODUCTION

1.1 From petroleum derived plastics to new alternatives

Approximately 100 years ago, plastics started a new era, supporting the expansion of a modern society. During the second World War, the annual plastic production in the United States nearly triplicated, making this synthetic material a central element in military supply chains (Meikle, 1995). At the post-war period, plastics became very widespread and competitive when compared with traditional used material, such as wood, metal or glass (Fra-Vázquez et al., 2020).

The plastic industry continues to grow, and in 2018 global plastics production reached about 360 million tonnes worldwide (European Bioplastics, 2019). The reason for this is the fact that plastics are a cheap material, that combine versatility and both excellent strength to weight ratio and long durability, being used in a wide number of applications, such as in the building, packaging and medical sectors (Klemeš et al., 2021). However, as for all other materials, the plastic brings welfare but also difficulties and weaknesses. First, over 99% of the plastics production still relies on the finite fossil fuel resources, if the same trend continues to be observed, by 2050 this industry will be responsible for the consumption of 20% of the total fossil feedstock availability (Ellen MacArthur Foundation, 2016). On the other hand, single-use and non-biodegradable character of most polymers, together with poor collection and deficient recycling systems, are leading to several environmental and human health concerns related to the accumulation of plastic waste into the ecosystems (Koller and Braunegg, 2018; Lebreton and Andrady, 2019).

The global and cumulative scenario of plastic disposal is significantly negative, as from the total plastic produced between 1950 and 2015 only 9% was recycled, 12% was incinerated and nearly 80% was accumulated in landfills or on the natural environment (Geyer et al., 2017). Plastic pollution is found in all major ocean basins around the world, including poles, deep seas and remote islands, and it is estimated that additional 5 to 13 million tonnes of plastic waste are still being introduced annually (Jambeck et al., 2015). Particularly in Europe, where the recycling rates are considerable higher than for the rest of the world (OECD, 2018), the tendency of recycling increased 100% between 2006 and 2018. However, the values are still low with only 32% of the collected plastic being recycled in 2018 and the remaining amount still being burned for energy recover (43%) or disposed-off in landfills (25%) (Plastics Europe, 2020). Additionally, the total collected plastics only represent 47% of total production, meaning that the potential for plastic recovery and recycling continues largely unexploited (Plastics Europe, 2020).

From the 51 million tonnes available for the European plastic converters in 2019, 40% was used by the packaging sector, the largest market for plastic usage, followed by building & construction (20%) and the automotive industry (10%) (Figure 1.1) (Plastics Europe, 2020). In particular, the packaging plastic is almost exclusively composed by single-use materials with 32% escaping from the collection system, making it one of the most common items found in beaches (Ellen MacArthur Foundation, 2016).

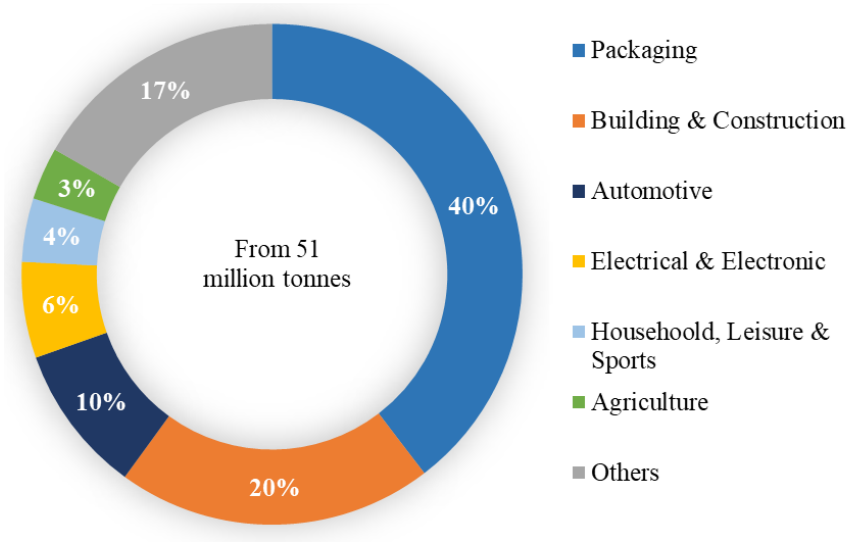

Figure 1.1 – Plastics demand by segment in Europe in 2019. Adapted from (Plastics Europe, 2020).

Bioplastics appear as a widely acceptable possibility to replace fossil-based plastics, they are used for an increased variety of applications, ranging from packaging and textiles to automotive and toys (European Bioplastics, 2020). These alternative polymers fit perfectly into the circular economy loop of the plastic industry, representing a way of reducing the carbon footprint associated to the traditional plastics and allowing to explore additional waste management options, such as industrial composting (European Bioplastics, 2019).

1.2 Increasing demand for bioplastics: towards a closed loop cycle

Bioplastics are a family of highly diversified products composed by biobased and/or biodegradable/compostable polymers.

Concerning the feedstock, some types of biopolymers, such as polybutylene succinate (PBS), polycaprolactone (PCL) and polybutylene adipate-co-terephthalate (PBAT), are still derived from crude oil and are considered bioplastics due to their biodegradable character (Cooper, 2013). On the other hand, for example the bio-based polyamide (PA), polypropylene (PP), polyethylene (PE), and polyethylene terephthalate (PET) are produced from renewable carbon sources, but they are similar to their petrochemical-based counterparts, not showing any biodegradability capacity (Lambert and Wagner, 2017).

The biopolymers that are most promising and a truly sustainable alternative to traditional plastics are the ones that are both biobased and biodegradable. From this sector, there are currently three main biobased polymer types on the market: the starch blends, the polylactic acid (PLA) and the polyhydroxyalkanoates (PHAs) (European Bioplastics, 2020).

Currently, bioplastics market represents less than 1% of the total annual plastic production with the packaging field remaining on top of the market segments, followed by consumer goods and textiles Figure 1.2). According to the latest market data from European Bioplastics, the global biopolymers production capacity is set to increase from 2.11 million tonnes in 2020 to around 2.87 million tonnes in 2025.

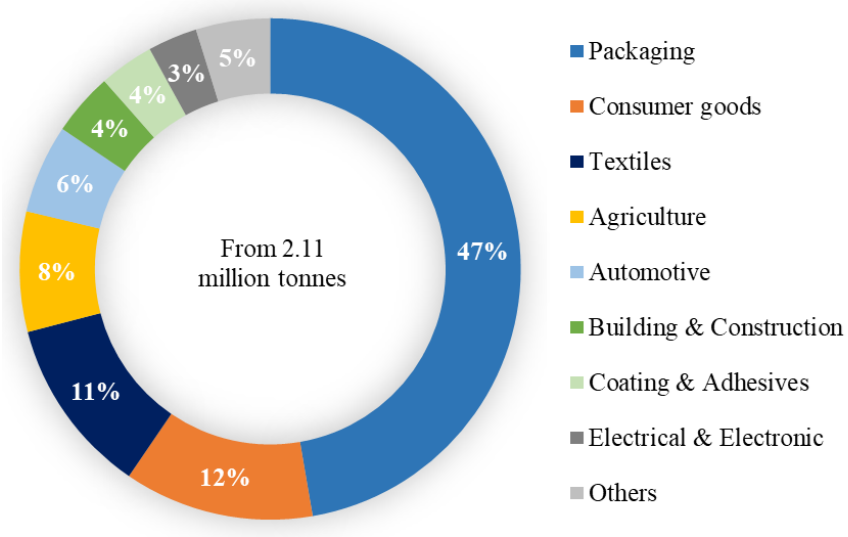

Figure 1.2 - Bioplastics demand by segment in 2020. Adapted from (European Bioplastics, 2020).

From those 2.11 million tonnes produced in 2020, starch-blends (18.7%), PLA (18.7%), PBAT (13.5%), and biobased PA (11.9%) represent the biggest fractions of the total bioplastic market. Furthermore, it was reported that the biodegradable plastics account for almost 60% of the biopolymer production capacities, and that this percentage shows higher predictable levels of growth than the forecast for biobased, non-biodegradable plastics. (European Bioplastics, 2020)

Among the different biodegradable/biocompostable bioplastics, PLA is estimated to double its market share and PHAs are estimated to increase almost tenfold within the next five years (from 2020 until 2025) (European Bioplastics, 2020). PHAs are the bioplastics which show the highest relative growth rate due to their very versatile properties and to the fact they are industrially and home compostable, marine and soil naturally biodegradable, anaerobically digestible, and also biodegradable in wetlands and in septic and municipal solid waste systems. On contrary PLA, is not so versatile in terms of characteristics and only degrades under specific conditions, such as industrial composting (Cooper, 2013).

1.3 Polyhydroxyalkanoates: a promising eco-friendly bioplastic

PHAs are a group of biobased and biodegradable polyesters that are fully biocompatible and show thermoplastic and elastomeric properties similar to those of conventional petroleum-derived plastics (e.g., PP and PE). Their high versatility makes them a very promising bulk material for a significant number of applications.

PHAs were first discovered by Lemoigne, 1926, a French scientist which observed polyhydroxybutyrate (PHB) being accumulated as intracellular granules in *Bacillus megaterium*. PHB is, up to date, the most observed and well-studied type of PHA. Although, since then, over 150 different types of hydroxyalkanoate (HA) monomers and more than 90 PHA-producing genus have been identified (Kim et al., 2007).

PHAs can be classified into three categories according to the length of their monomeric units, Figure 1.3 shows the general PHA chemical structure. Short-chain length PHAs (scl-PHA) contain 3 to 5 carbon atoms in each monomer, the most common monomers within this category are 3-hydroxybutyrate (3-HB) and 3-hydroxyvalerate (3-HV). Medium-chain length PHA (mcl-PHA) have monomers with 6 to 14 carbon atoms, such as 3-hydroxyhexanoate (3-HHx), and lastly long-chain length PHAs (lcl-PHA) are composed by monomers with more than 14 carbons (e.g., 3-hydroxyhexadecanoate – 3-HHD) (Lu et al., 2009; Singh and Mallick, 2009). Typically, the number of repeating monomers can range from 100 to 30000 monomeric units (Figure 1.3), which means that the polymer molecular weight (M_w) can increase up to 3000 kDa (Lee, 1996). M_w can have an impact on the melting and crystallization behavior, on the thickness and on crystal structures of the polymers, it is estimated that the PHA mechanical properties are ideal when the average M_w is higher than 400 kDa (Lorini et al., 2020b).

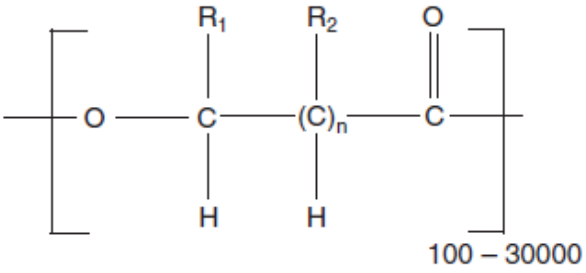

Figure 1.3 - General chemical structure of PHAs. n variable number of carbon atoms in the linear structure; R1 and R2 are the variable hydrocarbon side chains.

PHAs structure can be composed of the same type of HA monomer (homopolymers) or of two or more different HA subunits (copolymers). The homopolymer PHB is highly crystalline and have a melting temperature (T_m) close to 180ºC (Table 1.1). It exhibits good thermoplastic properties being processed as the traditional thermoplastics, however its highly crystalline structure makes it fairly stiff

and brittle (lower elongation at break, higher Young's modulus than for petroleum-derived plastics – Table 1.1) limiting its applications.

On the other hand, copolymers can incorporate endless monomeric compositions possibilities which allow the tuning of PHAs physical properties such as melting point and crystallinity, originating a wide range of materials that can be used for different application (Akaraonye et al., 2010; Steinbüchel and Lütke-Eversloh, 2003). For instance, the copolymer poly(3-hydroxybutyrate-co-3-hydroxyvalerate) – P(3HB-*co*-3HV) – display reducing T_m and crystallinity as long as the 3-HV monomers increase in its structure (Table 1.1). These copolymers exhibit improved mechanical properties compared with PHB and PLA (Table 1.1), such as higher toughness and flexibility (higher elongation at break and lower Young's modulus) facilitating further chemical and mechanical processing. Furthermore, similarly to petrochemical plastics, P(3HB-*co*-3HV) presents an extreme resistance to water and have a very low oxygen permeability (Table 1.1), which are considered major advantages over PLA when intending to use the polymer for example for packaging applications.

Table 1.1 – Properties of PHAs compared to other bio-based plastic (PLA) and to petroleum-derived polymers (PP, high-density PE and low-density PE).

	T_m (°C)	**Tensile strength (MPa)**	**Young's Modulus (GPa)**	**Elongation at break (%)**	**Water resistance**	**O_2 permeability**
PHB[1]	179	40	3.5	5	Yes	Very low
P(3HB-*co*-3HV)[a]						
3% 3-HV[1]	170	38	2.9			
9% 3-HV[1]	162	37	1.9			
14% 3-HV[1]	150	35	1.5	3.6 – 50[5,6]	Yes	Very low
20% 3-HV[1]	145	32	1.2			
25% 3-HV[1]	137	30	0.7			
43% 3-HV[2]	169	n.a.	0.8	58		
Other polymers						
PLA[3]	120/170[b]	53 - 70	0.35 - 0.45;	2.4	No	High
PP[3,4]	170	12 - 43	0.6 - 1.2	150 - 400	Yes	Low
High-density PE[3,4]	120 - 130	25 - 32	0.7 - 1.2	600 - 900	Yes	Low
Low-density PE[3,4]	105 - 115	15 - 20	0.15 - 0.45	600	Yes	Low

n.a. – not available; [a]3-HV in mol-basis; [b]amorphous/crystalline PLA; [1](Lee, 1996); [2](Arcos-Hernández et al., 2013); [3](Crank, M.; Patel, 2005); [4](Brandrup, J.; Immergut, E. H.; Grulke, 2003); [5](Bossu et al., 2020); [6](Kumar et al., 2015)

1.3.1 Applications

Over the last decade, several partnerships and collaborations were developed aiming to increase the commercial versatility of PHAs. Main applications reported for this biopolymer comprise: flexible and rigid packaging, coating applications, consumer goods (e.g., single-use containers for cosmetic and hygiene materials), durable goods, compostable bags for solid waste and agriculture/horticulture bags and films (e.g. mulch films) (European Bioplastics, 2020; Philip et al., 2007). Moreover, the unique biocompatible and biodegradable properties of PHA make it suitable to be used in high value applications on the medical field, such as in bone plates, surgical sutures, patches and as delivery systems for slow release of hydrophobic drugs (Philip et al., 2007).

Besides the functions mentioned above, PHAs demonstrated to be promising in endless other fields (e.g., as biofuels, raw material for paints, paper waterproof coating and as fibre material), however limitations that hinder the PHA usage at a higher level still persist, such as the elevated cost of the commercial PHA production cost and the reduced market availability (Mathuriya and Yakhmi, 2017).

1.4 PHA production by bacteria

More than 300 identified species with different biosynthetic pathways are able to accumulate PHA as intracellular carbon reserves (Sudesh et al., 2000).

The most common pathway for PHA production starts with the carbohydrate catabolic degradation through glycolysis. The resulting pyruvate is converted to acetyl-CoA which can serve as precursor for 3-HB monomers production when the culture is subjected to growth restrict conditions (Reis et al., 2011; Serafim et al., 2008).

There are however other pathways used by some microorganisms, for example short chain fatty acids (SCFAs), such as acetate, propionate, butyrate or valerate, that can also be used as substrates for PHA biosynthesis. In this case, acetate and propionate are transported across the cell membrane and activated to the corresponding acyl-CoA molecule. Acetyl-CoA serve as precursor for 3-HB production, while propionyl-CoA can be combined with 2 units of acetyl-CoA to form 3-HV monomers or decarboxylated to acetyl-CoA to form 3-HB (Dias et al., 2008; Reis et al., 2011). Butyrate and valerate have a higher number of carbons and can be directly converted into 3-HB and 3-HV monomers, respectively (Reis et al., 2011). When a mixture of substrates is fed, the monomeric composition of the polymer produced generally reflects the relative amount of the different carbon sources (Reis et al., 2011).

Regardless of whether the PHA-storing microorganism used for production presents all or just some of these pathways, PHA accumulation is internally regulated and can therefore be promoted through the activation of specific enzymes involved in the process and/or through the inhibition of some biochemical

pathways that compete for PHA precursors consumption. Consequently, several strategies and different microbial cultures and systems can be used to boost PHA production.

1.4.1 Pure cultures process – the current commercial approach

All the industrial processes for PHA production so far implemented use pure cultures of wild or genetically modified microorganisms as inoculum. The most well-studies species at industrial level include *Cupriavidus necator*, *Alcaligenes latus*, *Pseudomonas putida* and genetically modified strain of *Escherichia coli*. These cultures are usually fed with pure substrates (e.g., glucose, corn steep liquor and commercial grade SCFA) at sterile conditions in a two-step process: at a first stage, culture growth is promoted aiming to achieve high/ideal cell densities, and then in a second phase growth limiting conditions are applied to induce PHA accumulation (Keshavarz and Roy, 2010; Lee, 1996; Reis et al., 2011).

Considerable efforts have been devoted in the past 30 years to increase the economic viability of the PHA production by pure cultures. Research activities were set on increasing the PHA yield, on maximising cell growth and polymer production rate, to increase cell density and PHA productivity and on maximising PHA cell content, to increase process productivity and improve PHA recovery yield. One of the most successful cases was reported for *Cupriavidus necator* fed with glucose, which showed cell densities above 200g.L^{-1} and a PHB accumulation capacity over 80% (w/w) (Chen, 2009). P(3HB-*co*-3HV) production was also reported for this strain fed with a mixture of glucose and propionate, where the culture was able to accumulate the copolymer until 75% of its dry weight (Chen, 2009). Even though considerable high volumetric productivities were already achieved (typically range between 1 and 3 g-PHA.L^{-1}.h^{-1} (Kourmentza et al., 2017)), production costs remain too high limiting the large-scale production and the usage of PHA as a commodity polymer.

Cost analyses referred that the main responsibility for the high expenses can be attributed to the energy consumption for sterilisation, mixing and aeration and to the high cost of the pure substrates and downstream process (Nielsen et al., 2017). Alternative solutions have been tested, such as the design of genetic engineered strains that are able to use agro-industrial wastes/by-products as feedstock (Koller et al., 2017). This approach is very promising since it is a vehicle that leads to a greater sustainability and economic viability, however pure cultures metabolism often suffer instability with the high variable characteristics of waste substrates (Chen, 2009).

1.4.2 Mixed microbial cultures process using waste feedstocks – the eco-efficient approach

Over the past 20 years, an alternative PHA production process based on open mixed microbial cultures (MMCs) and carbon-rich wastes/by-products has been intensively studied (Kourmentza et al., 2017; Mannina et al., 2020; Valentino et al., 2017). PHA-producing MMCs are microbial populations with unknown composition, that can be obtained from activated sludge systems by applying certain feeding and cultivations conditions that favour the growth of PHA-storers over other microorganisms.

These types of systems provide simultaneously a means of reducing the overall operational costs and contributes to the implementation of a circular economy approach reducing the environmental footprint associated to the commercial process using pure cultures (Mannina et al., 2020; Valentino et al., 2017). Indeed, life cycle assessment and cost analysis have indicated MMC PHA production as financially attractive in comparison with the traditional process due to the operation under open conditions (no sterilization is required), to the reduced equipment costs and to the usage of cheap/costless carbon sources (Gurieff and Lant, 2007).

As schematically represented in Figure 1.4, the MMC PHA production process usually comprises three stages: (1) the anaerobic acidogenic fermentation, to convert the wasted organic carbon into a mixture of soluble fermentation products (SFP) that are precursors for PHA biosynthesis (such as the SCFAs); (2) the selection and continuous production of a MMC enriched in PHA-storers; and lastly (3) the PHA production, where the previously selected culture is fed with the SFP and accumulate PHA up to its maximum capacity (Reis et al., 2011).

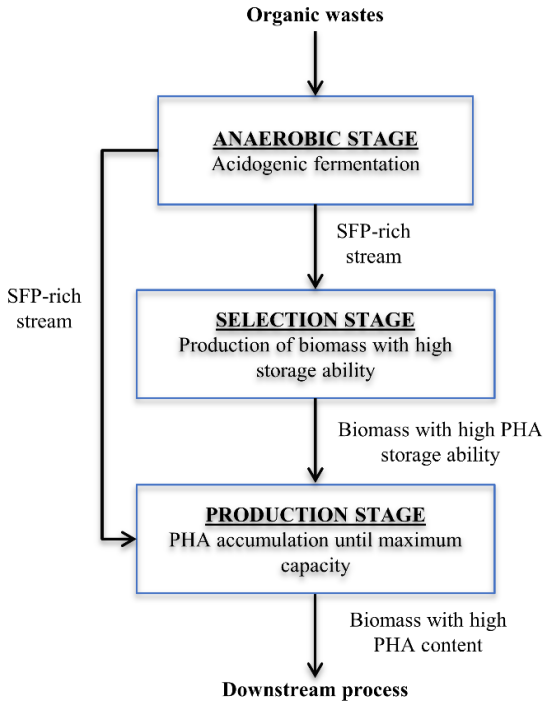

Figure 1.4 - Typical 3-stage process for PHA production by MMCs. Adapted from (Reis et al., 2011)**.**

1.4.3 Impact of operating conditions on three-stage process performance

1.4.3.1 Acidogenic fermentation

Regarding the culture metabolism, unlike pure cultures which typically use carbohydrates as carbon source, organic acids (such as SCFAs) are the preferred PHA bioprecursors for MMCs.

Anaerobic digestion has been used for decades to treat a wide range of organic waste streams. Within this process the complex organic substrates can be microbially hydrolysed and then sequentially converted into organic acids (acidogenesis), acetate (acetogenesis) and finally into biogas (methanogenesis) (Abbasi and Abbasi, 2012). The extent to which the substrate is degraded depends on the operating conditions imposed (Carvalheira and Duque, 2021). When organic acids production is desired, such as for the PHA production by MMCs, the anaerobic digestion conditions must be designed in order to stop the process before the organic acids being oxidised to CO_2 and methane (Carvalheira and Duque, 2021). Selecting and operating a MMC under low sludge retention time (SRT), low hydraulic retention time (HRT), low temperature and low pH demonstrated to favour acidogenic bacteria over methane producers (Carvalheira and Duque, 2021).

Continuous stirred tank reactors (CSTRs) are typically used to perform the acidogenic fermentation step (Albuquerque et al., 2007; Campanari et al., 2017; Duque et al., 2014; Jiang et al., 2012; Moretto et al., 2020). Although not so frequently observed within the PHA production process, other configuration reactors are also used, such as upflow anaerobic sludge blanket (UASB) reactors (Tamis et al., 2014) or anaerobic membrane bioreactors (Duque et al., 2014). Those reactors allow to increase the SRT to values that led to increased fermentation stability and performance keeping the HRT at low values (Carvalheira and Duque, 2021; Parawira et al., 2006).

The acidogenic fermentation of organic matter results in the production of different mixtures of SFP. Acetate, propionate and butyrate are the most common organics acids found alongside with lower amounts of lactate, ethanol and valerate (Albuquerque et al., 2007; Campanari et al., 2017; Duque et al., 2014; Jiang et al., 2012; Moretto et al., 2020).

Manipulating the operation conditions of the bioreactor can lead to a wide variety of SFP compositions which, in turn, can be used to produce PHAs with different monomeric compositions, suitable for different market applications (Albuquerque et al., 2007; Gouveia et al., 2017). Several studies demonstrated that HRT, SRT, pH, temperature, organic loading rate (OLR), and also reactor configuration are the most important factors influencing the effluent composition profile (Carvalheira and Duque, 2021). For instance, propionate fraction was found to increase with both pH and HRT for paper mill wastewater and cheese whey (Bengtsson et al., 2008), while butyrate and valerate were produced in higher amounts at lower pH for sugar cane molasses (Albuquerque et al., 2007).

The increase in the OLR usually supports the production of SFP in higher concentrations by increasing the substrate availability (Carvalheira and Duque, 2021) and indeed it can highly affect the

SFP profile. Carvalheira et al. 2018 observed that at an OLR of 21.2 $gCOD.L^{-1}.d.^{-1}$ acetate and propionate were equally produced in the higher amounts (19.65% and 19.11%), while at an OLR of 51.1 $gCOD.L^{-1}.d.^{-1}$ propionate was the prevailing organic acid (10.07%) and acetate concentration considerably decreased (5.48%). In its turn, Jiang et al. 2013 observed increasing concentrations of acetate and valerate and decreasing propionate and butyrate relative amounts for OLRs increasing in the range of 5 to 16 $gTS.L^{-1}.d.^{-1}$.

In sum, the literature is highly rich in conflicting and discrepant results achieved for acidogenic reactors fed with wastes/by-products, and it seems that the relationships found between operating conditions and SFP production profile is highly dependent on the type of feedstock used (Carvalheira and Duque, 2021).

1.4.3.2 Selection reactor

The culture selection is a critical step of the three-stage PHA production process, to maximise the global process performance (i.e., increase PHA productivity/yield and facilitate downstream stage) it is essential to select a stable and robust culture with a significant PHA accumulation potential and a high volumetric biomass productivity. At this stage, the main objective is to produce a homogeneous microbial population highly enriched in efficient PHA-storers, rather than to maximise PHA cell content, which will be further desired in the subsequent stage.

A good enrichment in PHA-storers can be generally obtained by applying an aerobic dynamic feeding (ADF) strategy, where transient periods of feast (carbon excess) and famine (carbon absence) are cyclically established in a sequencing batch reactor (SBR). The long starvation period acts as a physiological selective pressure, reducing the cell metabolic activity and the intracellular components required for cell growth (RNA and enzymes) to minimum values. When the new cycle starts with the feast phase, a slow growth response is observed leaving more external carbon available for PHA storage, which can be rapidly produced since PHA synthase remains active. When the microbial metabolism is ready to promote growth, the nitrogen source starts to be consumed and eventually, if nitrogen is supplied in sufficient amounts, cell growth on stored PHA is observed, creating a high selective pressure for organism with this capability (De Donno Novelli et al., 2021; Sabapathy et al., 2020). After a few cycles, microorganisms with no storage ability are unable to thrive along the long famine phase and will be eliminated from the reactor (Reis et al., 2011).

More recently, Oliveira et al. (2017) and Silva et al. (2017) proposed to completely uncouple the availability of carbon and nitrogen during the selection process while maintaining the ADF regime. This approach was demonstrated to be particularly interesting when operating the process at high OLRs using wastes as feedstock, since it effectively enhances the PHA storage response by significantly limiting the growth of flanking populations (Argiz et al., 2021; Campanari et al., 2017; Oliveira et al., 2017). Under these conditions, PHA is stored during feast and the growth occurs exclusively during famine using the

stored PHA, creating a double selective pressure that favours PHA-storers. Therefore, the implementation of this strategy in cases of nutrient-limited substrates is highly recommended.

The selection reactor operating conditions should be tuned for the culture enrichment success. The impact of several parameters, such as the pH, temperature, substrate type, feast to famine length (FF) ratio, OLR, SRT, C/N ratio, to name a few, were investigated by previous authors.

For example, it was found that pH can impact on microbial community selection and on polymer composition although an acceptable polymer production can be maintained within the range 6.5 to 9.5 (Dionisi et al., 2005; Villano et al., 2010). Culture selection is also sensitive to temperature, but PHA production performance can be maintained for a temperature range of 20 to 30 ºC (Jiang et al., 2011).

Regarding the established FF ratio, it is one of the key elements to ensure proper culture selection. Low FF ratios (<0.33) usually mean a good enrichment in PHA-storers since the famine phase is long enough to guarantee that the growth internal limitation occurs (Dionisi et al., 2006).

The specific substrate uptake and storage rates were found to tend to a maximum when the substrate concentration inside the reactor achieve a certain threshold and then decrease due to substrate inhibition phenomena (Reis et al., 2011). Additionally, until a certain extent where the proper selection is not compromised, high values of biomass productivity are usually obtained for higher OLRs (Albuquerque et al., 2010; Dionisi et al., 2006; Lorini et al., 2020a). The specific substrate rate vs substrate concentration dependency curves and the limit OLRs values are highly dependent on the feedstock characteristics.

The SRT also plays an important role in the culture selection since the effective culture specific growth rate is highly dependent on this parameter. On one hand, keeping this parameter shorter means faster growth rates and growth yields, thus driving a higher amount of carbon for growth, and less for PHA storage (Lemos et al., 2008). On the other hand, shorter SRTs may promote the selection of a MMC which shows an apparent enhanced accumulation capacity due to the lower fraction of inert cells present in the reactor (Chua et al., 2003). Other studies were conducted to find the ideal operating SRT for the selection stage, however contradicting results did not allow to conclude about the impact of this parameter on the culture's real storage ability (Chen et al., 2017; Chua et al., 2003; Johnson et al., 2010; Lemos et al., 2008), suggesting that further studies are still required on this field.

1.4.3.3 PHA production reactor

The efficiency of the PHA production step is strongly dependent on the good selection achieved in the previous selection stage. In this step, the main goal is to exploit the maximum accumulation potential of the selected culture by feeding the SFP produced in the acidogenic fermentation under growth limiting conditions.

This stage is commonly carried out in pulse-wise fed-batch mode controlled by the dissolved oxygen (DO). An increase in the respiration rate occurs when the substrate is added, corresponding to a decrease

in the DO levels. When the carbon source is depleted an increase of the DO is observed, demanding the next pulse of feedstock. Pulse feeding is repeated until no variation in the DO level is observed, meaning that a maximum PHA content on cells was achieved. Pulse-wise addition strategy is used due to the necessity of avoiding substrate inhibitions at high SFP concentrations, however this method often leads to polymer consumption in between pulses, decreasing the final PHA content on cells (Albuquerque et al., 2011; Oliveira et al., 2017).

A key opportunity that shows potential to simplify the process control lays on using a continuous feeding mode by maintaining a residual substrate concentration in the bulk, which avoids the consumption of polymer during the accumulation process. For instance, using the SFP solution to correct pH (pH-stat) induces a continuous feeding of external carbon which prevents polymer consumption in between pulses. This strategy was shown to increase the substrate uptake rates, the storage yields and finally the maximum PHA accumulation, thus increasing the PHA productivity when comparing with the traditional approach (Albuquerque et al., 2011; Chen et al., 2015)

Additionally, previous research has indicated that the bioprecursors profile can influence the PHA producing rate and yield. For example, butyrate and valerate have been indicated as preferred substrates for PHA production since they are more energetically favourable at a metabolic level than other SFP, such as acetate and propionate (Kourmentza and Kornaros, 2016; Marang et al., 2013; Wang et al., 2017).

1.5 Scaling-up PHA production using MMCs: case studies and research needs

Most of the studies reported thus far were performed at laboratory scale. Such studies have led to a greater awareness of the potential of producing PHA using MMCs and have disclosed important information for further process scale-up. Research in this field is continuously being developed and new feedstocks and operating conditions are being tested to bring forward this sustainable approach for PHA production.

Pilot plant studies represent an important bridge between bench and industrial production, as the results obtained at this stage are key to optimise the full-scale plants. These assays are often very challenging since some operational factors (e.g., homogeneity, fluid dynamics, equipment selection, control facility) change widely when equipment size scales up, especially between lab and pilot scale plants.

In the past 10 years, the feasibility of the PHA production process using MMCs and waste feedstocks has been demonstrated in various European projects performed at pilot scale, e.g. RES URBIS, SMART Plant, INCOVER, PHARIO, YPACK and VOLATILE (Mannina et al., 2020). These projects represent a major step forward for the MMC PHA industrialisation, since the pilot-scale studies allow to quantify a reasonable range of key performance parameters (e.g., PHA content on biomass, global productivity, overall yield) that are crucial to evaluate full-scale production feasibility, and also enable the production

of larger amounts of polymer to address product characteristics in the context of commercial applications (Estévez-Alonso et al., 2021)

Several different wastewater streams from food processing residues/wastewaters to urban waste have been used at pilot scale (Table 1.2), such as tomato waste centrate (Bengtsson et al., 2017), starch-rich wastewater (Morgan-Sagastume et al., 2020), candy factory wastewater (Tamis et al., 2014), paper mill wastewater (Tamis et al., 2018) and a mixture of organic fraction of municipal solid waste (OFMSW) and waste activated sludge (WAS) (Moretto et al., 2020). However, most of the studies were focused on simply evaluating the effect of specific operating parameters on the process performance, or on enhancing each one of key performance parameters once at a time, instead of trying to incorporate different optimal individual strategies that enhance all the performance indicators for a determined system. As can be observed in Table 1.2, all the presented pilot-scale studies tried to address maximum PHA content on biomass, but global productivity is often overlooked and only one study reported values for this parameter (1.09 – 1.34 $g.L^{-1}.d^{-1}$ for OFMSW). The overall yield (corresponding to the amount of polymer produced per total feedstock consumed in the 3 stages) is more frequently evaluated, and ranged between 0.30 – 0.34 $gCOD.gCOD^{-1}$ (Table 1.2), which is still quite lower than that the 0.42 $gCOD.gCOD^{-1}$ estimated by Valentino et al. 2017 as the theoretical value that may be achieved considering best laboratory scale results (at that time) using synthetic feedstock as substrate.

Additionally, only Conca et al. 2020 reported a wider range of 3-HV monomers in the polymers produced (21 – 41%, Table 1.2), this variation happened using similar operating conditions in all the reactors, possible due to fluctuations in the real feedstock. Thus, 3-HV content of PHA was never intentionally manipulated at pilot-scale, so the possibility of consistently producing different P(3HB-*co*-3HV) copolymers depending on the application demand using the same system and feedstock was never evaluated at a larger scale.

Despite the pilot plant successful operations to date and the positive indications for PHA usage that benefit the environmental ecosystems, breakthrough with commercial PHA production using MMCs is still not yet realized. In this sense, and considering the performance information described above, further studies at pilot-scale are still needed to overall reduce the production costs of the PHA production process using MMCs (by maximising all the key performance parameters). Additionally, the ability of consistently tailor polymer composition at a higher scale level needs to be proven to further foster the process full-scale implementation.

Table 1.2 – Performance of PHA production pilot-scale studies using MMCs and waste-based feedstocks.

Feedstock	Max. PHA content (%, w/w)	3-HV (%, w/w)	Global productivity ($g.L^{-1}.d^{-1}$) [a]	Overall yield ($gCOD.gCOD^{-1}$)[b]
Tomato waste centrate[1]	34 - 42	42 - 49	n.a.	n.a.
Potato-starch factory wastewater[2]	45	1.9	n.a.	n.a.
Candy factory wastewater[3]	70 - 76	16	n.a.	0.30
Paper mill wastewater[4]	65 - 76	25	n.a.	0.34
Cellulosic primary sludge liquid[5]	44	21 - 41	n.a.	0.32
OFMSW and WAS mix[6]	40 - 59	n.a.	n.a.	187 [c]
OFMSW [7]	38 - 49	11 - 13	1.09 – 1.34	n.a.

n.a. – not available; [a] related to selection and production reactors; [b] 3-stage yield; [c] in gCOD-PHA.Kg-VS^{-1}; [1](Bengtsson et al., 2017); [2](Morgan-Sagastume et al., 2020); [3](Tamis et al., 2014); [4](Tamis et al., 2018); [5](Conca et al., 2020); [6](Moretto et al., 2020).; [7](Valentino et al., 2019)

1.6 Motivation and thesis outline

PHAs are well known biobased and biodegradable polyesters, which are an ecological and promising alternative to some of the most used conventional petroleum-derived plastics. In particular, the copolymer P(3HB-*co*-3HV) is suitable to apply for a wide variety of applications due to its broader and exceptional thermal and mechanical properties, that can be manipulated by tuning its monomeric composition.

Currently, the commercial PHA production is still performed using pure cultures of natural or genetically modified PHA-producing bacteria. This approach is highly costly since it requires axenic conditions, and very specific fermentation and control equipment, hindering the PHA usage as a commodity polymer and limiting its expansion in the bioplastics market.

In order to reduce the PHA production cost, one alternative based on the usage of non-aseptic MMCs and waste/surplus feedstocks was proposed. This strategy contributes simultaneously towards the implementation of an eco-efficient circular economy and to reduce the operational costs associated with the traditional PHA production process. From the introduction given in Chapter 1, it can be observed that during the last decades, research on PHA production using MMCs was centred on laboratory-scale studies, trying to understand well the mechanisms of PHA synthesis and the impact of several operating parameters on the cultures' performance with the objective of process optimisation. This approach was also recently implemented at pilot-scale, however a full optimisation of all the key performance parameters and a consistent ability to control the polymer composition (and thus its properties) were never achieved and are considered major bottlenecks for industrial implementation. This Thesis was

focused on solving those difficulties, proposing a process approach that will potentially reduce the operational costs and decrease the PHA price to more affordable values.

Chapter 2 is focused on clarifying the impact of different SRTs and OLRs on the dynamics of growth versus PHA storage of a PHA-producing culture selected under uncoupled carbon and nitrogen availabilities. These two parameters are known to have a great impact on the process productivity and were poorly studied for processes where the uncoupled feeding strategy was applied. Fruit waste was used as substrate since it is globally generated in large volumes, causing several environmental and economic problems. Moreover, it is a real nutrient deficient feedstock that allows the implementation of the uncoupled feeding approach. This study was conducted at pilot scale to ensure the results have a direct applicability in an industrial setting. This work was published in an international peer reviewed scientific journal as: Matos, M., Cruz, R.A.P., Cardoso, P., Silva, F., Freitas, E.B., Carvalho, G., Reis, M.A.M., 2021. Sludge retention time impacts on polyhydroxyalkanoate productivity in uncoupled storage/growth processes. Sci. Total Environ. 799, 149363. https://doi.org/10.1016/j.scitotenv.2021.149363

The same pilot plant set-up and feedstock (fruit waste) were used in the work described in Chapter 3 where different effective operating conditions, in different points of the three-stage process, were simultaneously implemented with the objective of enhancing the overall PHA production performance, namely PHA content on biomass, global productivity, and overall yield. This work was published in an international peer reviewed scientific journal as: Matos, M., Cruz, R.A.P., Cardoso, P., Silva, F., Freitas, E.B., Carvalho, G., Reis, M.A.M., 2021. Combined Strategies to Boost Polyhydroxyalkanoate Production from Fruit Waste in a Three-Stage Pilot Plant. ACS Sustain. Chem. Eng. acssuschemeng.1c02432. https://doi.org/10.1021/acssuschemeng.1c02432

The possibility of tailoring the PHA precursors production, and thus the P(3HB-*co*-3HV) composition, was investigated on Chapter 4. The operational pH of a pilot-scale UASB reactor fed with the same fruit waste was manipulated and its impact on the microbial community profile, corresponding performance and effective influence on polymer composition were evaluated. Additionally, the IWA Anaerobic Digestion Model No. 1 was modified aiming to dynamically predict the PHA bioprecursors production composition, providing a successful approach for process regulation and PHA composition manipulation. This work will be submitted to an international peer reviewed scientific journal as: Matos, M.; Uçar, N., Cardoso, P., Carvalho, G., Reis, M.A.M.,. Santos, J.; Oehmen, A., Understanding the Polyhydroxyalkanoate (PHA) Bioprecursors Production from Fruit Waste by mixed Microbial Cultures through Pilot Scale Experiments And Metabolic Modelling .

Lastly, Chapter 5 describes the general outcomes from the study and addresses suggestions for future research studies.

Other relevant publications not included in this thesis:

- Silva, F., Matos, M., Pereira, B., Ralo, C., Pequito, D., Marques, N., Carvalho, G., Reis, M.A.M., 2022. An integrated process for mixed culture production of 3-hydroxyhexanoate-rich polyhydroxyalkanoates from fruit waste. Chem. Eng. J. 427, 131908. https://doi.org/10.1016/j.cej.2021.131908
- Meléndez-Rodríguez, B., Torres-Giner, S., Reis, M.A.M., Silva, F., Matos, M., Cabedo, L., Lagarón, J.M., 2021. Blends of Poly(3-Hydroxybutyrate-co-3-Hydroxyvalerate) with Fruit Pulp Biowaste Derived Poly(3-Hydroxybutyrate-co-3-Hydroxyvalerate-co-3-Hydroxyhexanoate) for Organic Recycling Food Packaging. Polymers (Basel). 13, 1155. https://doi.org/10.3390/polym13071155
- Bossu, J., Angellier-Coussy, H., Totee, C., Matos, M., Reis, M., Guillard, V., 2020. Effect of the Molecular Structure of Poly(3-hydroxybutyrate- co -3-hydroxyvalerate) (P(3HB-3HV)) Produced from Mixed Bacterial Cultures on Its Crystallization and Mechanical Properties. Biomacromolecules 21, 4709–4723. https://doi.org/10.1021/acs.biomac.0c00826
- Riccardi, C., Buiarelli, F., Castellani, F., Di Filippo, P., Lorini, L., Majone, M., Matos, M., Pomata, D., Simonetti, G., Sommer Ferreira, B., Valentino, F., 2020. Polychlorinated Biphenyl Profile in Polyhydroxy-alkanoates Synthetized from Urban Organic Wastes. Polymers (Basel). 12, 659. https://doi.org/10.3390/polym12030659
- Silvestre, S.L., Araújo, D., Marques, A.C., Pires, C., Matos, M., Alves, V., Martins, R., Freitas, F., Reis, M.A.M., Fortunato, E., 2020. Microneedle Arrays of Polyhydroxyalkanoate by Laser-Based Micromolding Technique. ACS Appl. Bio Mater. 3, 5856–5864. https://doi.org/10.1021/acsabm.0c00570
- Carvalho, M., Matos, M., Roca, C., Reis, M.A.M., 2014. Succinic acid production from glycerol by Actinobacillus succinogenes using dimethylsulfoxide as electron acceptor. N. Biotechnol. 31, 133–139. https://doi.org/10.1016/j.nbt.2013.06.006

1.7 References

Abbasi, T., Abbasi, S.A., 2012. Formation and impact of granules in fostering clean energy production and wastewater treatment in upflow anaerobic sludge blanket (UASB) reactors. Renew. Sustain. Energy Rev. 16, 1696–1708. https://doi.org/10.1016/j.rser.2011.11.017

Akaraonye, E., Keshavarz, T., Roy, I., 2010. Production of polyhydroxyalkanoates: The future green materials of choice. J. Chem. Technol. Biotechnol. 85, 732–743. https://doi.org/10.1002/jctb.2392

Albuquerque, M.G.E., Eiroa, M., Torres, C., Nunes, B.R., Reis, M.A.M., 2007. Strategies for the development of a side stream process for polyhydroxyalkanoate (PHA) production from sugar cane molasses. J. Biotechnol. 130, 411–421. https://doi.org/10.1016/j.jbiotec.2007.05.011

Albuquerque, M.G.E., Martino, V., Pollet, E., Avérous, L., Reis, M.A.M., 2011. Mixed culture polyhydroxyalkanoate (PHA) production from volatile fatty acid (VFA)-rich streams: Effect of substrate composition and feeding regime on PHA productivity, composition and properties. J. Biotechnol. https://doi.org/10.1016/j.jbiotec.2010.10.070

Albuquerque, M.G.E., Torres, C.A.V., Reis, M.A.M., 2010. Polyhydroxyalkanoate (PHA) production by a mixed microbial culture using sugar molasses: Effect of the influent substrate concentration on culture selection. Water Res. 44, 3419–3433. https://doi.org/10.1016/j.watres.2010.03.021

Arcos-Hernández, M. V., Laycock, B., Donose, B.C., Pratt, S., Halley, P., Al-Luaibi, S., Werker, A., Lant, P.A., 2013. Physicochemical and mechanical properties of mixed culture polyhydroxyalkanoate (PHBV). Eur. Polym. J. 49, 904–913. https://doi.org/10.1016/j.eurpolymj.2012.10.025

Argiz, L., González-Cabaleiro, R., Val del Río, Á., González-López, J., Mosquera-Corral, A., 2021. A novel strategy for triacylglycerides and polyhydroxyalkanoates production using waste lipids. Sci. Total Environ. 763, 142944. https://doi.org/10.1016/j.scitotenv.2020.142944

Bengtsson, S., Hallquist, J., Werker, A., Welander, T., 2008. Acidogenic fermentation of industrial wastewaters: Effects of chemostat retention time and pH on volatile fatty acids production. Biochem. Eng. J. 40, 492–499. https://doi.org/10.1016/j.bej.2008.02.004

Bengtsson, S., Karlsson, A., Alexandersson, T., Quadri, L., Hjort, M., Johansson, P., Morgan-Sagastume, F., Anterrieu, S., Arcos-Hernandez, M., Karabegovic, L., Magnusson, P., Werker, A., 2017. A process for polyhydroxyalkanoate (PHA) production from municipal wastewater treatment with biological carbon and nitrogen removal demonstrated at pilot-scale. N. Biotechnol. 35, 42–53. https://doi.org/10.1016/j.nbt.2016.11.005

Bossu, J., Angellier-Coussy, H., Totee, C., Matos, M., Reis, M., Guillard, V., 2020. Effect of the Molecular Structure of Poly(3-hydroxybutyrate- co -3-hydroxyvalerate) (P(3HB-3HV)) Produced from Mixed Bacterial Cultures on Its Crystallization and Mechanical Properties. Biomacromolecules 21, 4709–4723. https://doi.org/10.1021/acs.biomac.0c00826

Brandrup, J.; Immergut, E. H.; Grulke, E.A.., 2003. Polymer Handbook. John Wiley & Sons, Ltd.

Campanari, S., Augelletti, F., Rossetti, S., Sciubba, F., Villano, M., Majone, M., 2017. Enhancing a multi-stage process for olive oil mill wastewater valorization towards polyhydroxyalkanoates and biogas production. Chem. Eng. J. 317, 280–289. https://doi.org/10.1016/j.cej.2017.02.094

Carvalheira, M., Cassidy, J., Ribeiro, J.M., Oliveira, B.A., Freitas, E.B., Roca, C., Carvalho, G., Oehmen, A., Reis, M.A.M., 2018. Performance of a two-stage anaerobic digestion system treating fruit pulp waste: The impact of substrate shift and operational conditions. Waste Manag. 78, 434–445. https://doi.org/10.1016/j.wasman.2018.06.013

Carvalheira, M., Duque, A., 2021. From Food Waste to Volatile Fatty Acids towards a Circular Economy, in: Fermentation - Processes, Benefits and Risks [Working Title]. IntechOpen, p. 13. https://doi.org/10.5772/intechopen.96542

Chen, G.-Q., 2009. A microbial polyhydroxyalkanoates (PHA) based bio- and materials industry. Chem. Soc. Rev. 38, 2434. https://doi.org/10.1039/b812677c

Chen, Z., Huang, L., Wen, Q., Guo, Z., 2015. Efficient polyhydroxyalkanoate (PHA) accumulation by a new continuous feeding mode in three-stage mixed microbial culture (MMC) PHA production process. J. Biotechnol. 209, 68–75. https://doi.org/10.1016/j.jbiotec.2015.06.382

Chen, Z., Huang, L., Wen, Q., Zhang, H., Guo, Z., 2017. Effects of sludge retention time, carbon and initial biomass concentrations on selection process: From activated sludge to polyhydroxyalkanoate accumulating cultures. J. Environ. Sci. (China) 52, 76–84. https://doi.org/10.1016/j.jes.2016.03.014

Chua, A.S.M., Takabatake, H., Satoh, H., Mino, T., 2003. Production of polyhydroxyalkanoates (PHA) by activated sludge treating municipal wastewater: Effect of pH, sludge retention time (SRT), and acetate concentration in influent. Water Res. https://doi.org/10.1016/S0043-1354(03)00252-5

Conca, V., da Ros, C., Valentino, F., Eusebi, A.L., Frison, N., Fatone, F., 2020. Long-term validation of polyhydroxyalkanoates production potential from the sidestream of municipal wastewater treatment plant at pilot scale. Chem. Eng. J. https://doi.org/10.1016/j.cej.2020.124627

Cooper, T.A., 2013. Developments in bioplastic materials for packaging food, beverages and other fast-moving consumer goods, in: Trends in Packaging of Food, Beverages and Other Fast-Moving Consumer Goods (FMCG). Elsevier, pp. 108–152. https://doi.org/10.1533/9780857098979.108

Crank, M.; Patel, M., 2005. Techno-economic Feasibility of Largescale Production of Bio-based Polymers in Europe.

De Donno Novelli, L., Moreno Sayavedra, S., Rene, E.R., 2021. Polyhydroxyalkanoate (PHA) production via resource recovery from industrial waste streams: A review of techniques and perspectives. Bioresour. Technol. 331, 124985. https://doi.org/10.1016/j.biortech.2021.124985

Dias, J.M., Oehmen, A., Serafim, L.S., Lemos, P.C., Reis, M.A., Oliveira, R., 2008. Metabolic modelling of polyhydroxyalkanoate copolymers production by mixed microbial cultures. BMC Syst. Biol. 2, 59. https://doi.org/10.1186/1752-0509-2-59

Dionisi, D., Beccari, M., Gregorio, S.D., Majone, M., Papini, M.P., Vallini, G., 2005. Storage of biodegradable polymers by an enriched microbial community in a sequencing batch reactor operated at high organic load rate. J. Chem. Technol. Biotechnol. https://doi.org/10.1002/jctb.1331

Dionisi, D., Majone, M., Vallini, G., Di Gregorio, S., Beccari, M., 2006. Effect of the applied organic load rate on biodegradable polymer production by mixed microbial cultures in a sequencing batch reactor. Biotechnol. Bioeng. 93, 76–88. https://doi.org/10.1002/bit.20683

Duque, A.F., Oliveira, C.S.S., Carmo, I.T.D., Gouveia, A.R., Pardelha, F., Ramos, A.M., Reis, M.A.M., 2014. Response of a three-stage process for PHA production by mixed microbial cultures to feedstock shift: Impact on polymer composition. N. Biotechnol. 31, 276–288. https://doi.org/10.1016/j.nbt.2013.10.010

Ellen MacArthur Foundation, 2016. The New Plastics Economy: Rethinking the future of plastics, Ellen

MacArthur Foundation.

Estévez-Alonso, Á., Pei, R., van Loosdrecht, M.C.M., Kleerebezem, R., Werker, A., 2021. Scaling-up microbial community-based polyhydroxyalkanoate production: status and challenges. Bioresour. Technol. 327, 124790. https://doi.org/10.1016/j.biortech.2021.124790

European Bioplastics, 2020. Bioplastics market data 2020 [WWW Document]. URL https://www.european-bioplastics.org/market/ (accessed 8.5.21).

European Bioplastics, 2019. Bioplastics market data 2019. https://doi.org/docs.european-bioplastics.org/publications/market_data/Report_Bioplastics_Market_Data_2019.pdf

Fra-Vázquez, A., Palmeiro-Sánchez, T., del Río, Á.V., Mosquera-Corral, A., 2020. Transformation of organic contamination from wastewater into bioplastics (polyhydroxyalkanoate) by microorganisms. Wastewater Treat. Residues as Resour. Biorefinery Prod. Biofuels 2015, 415–433. https://doi.org/10.1016/b978-0-12-816204-0.00018-7

Geyer, R., Jambeck, J.R., Law, K.L., 2017. Production, use, and fate of all plastics ever made. Sci. Adv. 3, e1700782. https://doi.org/10.1126/sciadv.1700782

Gouveia, A.R., Freitas, E.B., Galinha, C.F., Carvalho, G., Duque, A.F., Reis, M.A.M., 2017. Dynamic change of pH in acidogenic fermentation of cheese whey towards polyhydroxyalkanoates production: Impact on performance and microbial population. N. Biotechnol. 37, 108–116. https://doi.org/10.1016/j.nbt.2016.07.001

Gurieff, N., Lant, P., 2007. Comparative life cycle assessment and financial analysis of mixed culture polyhydroxyalkanoate production. Bioresour. Technol. https://doi.org/10.1016/j.biortech.2006.10.046

Jambeck, J.R., Geyer, R., Wilcox, C., Siegler, T.R., Perryman, M., Andrady, A., Narayan, R., Law, K.L., 2015. Plastic waste inputs from land into the ocean. Science (80-.). 347, 768–771. https://doi.org/10.1126/science.1260352

Jiang, J., Zhang, Y., Li, K., Wang, Q., Gong, C., Li, M., 2013. Volatile fatty acids production from food waste: Effects of pH, temperature, and organic loading rate. Bioresour. Technol. 143, 525–530. https://doi.org/10.1016/j.biortech.2013.06.025

Jiang, Y., Marang, L., Kleerebezem, R., Muyzer, G., Van Loosdrecht, M.C.M., 2011. Effect of temperature and cycle length on microbial competition in PHB-producing sequencing batch reactor. ISME J. https://doi.org/10.1038/ismej.2010.174

Jiang, Y., Marang, L., Tamis, J., van Loosdrecht, M.C.M., Dijkman, H., Kleerebezem, R., 2012. Waste to resource: Converting paper mill wastewater to bioplastic. Water Res. https://doi.org/10.1016/j.watres.2012.07.028

Johnson, K., Kleerebezem, R., van Loosdrecht, M.C.M., 2010. Influence of the C/N ratio on the performance of polyhydroxybutyrate (PHB) producing sequencing batch reactors at short SRTs. Water Res. https://doi.org/10.1016/j.watres.2009.12.031

Keshavarz, T., Roy, I., 2010. Polyhydroxyalkanoates: bioplastics with a green agenda. Curr. Opin.

Microbiol. 13, 321–326. https://doi.org/10.1016/j.mib.2010.02.006

Kim, D.Y., Kim, H.W., Chung, M.G., Rhee, Y.H., 2007. Biosynthesis, modification, and biodegradation of bacterial medium-chain-length polyhydroxyalkanoates. J. Microbiol. https://doi.org/1

Klemeš, J.J., Fan, Y. Van, Jiang, P., 2021. Plastics: friends or foes? The circularity and plastic waste footprint. Energy Sources, Part A Recover. Util. Environ. Eff. 43, 1549–1565. https://doi.org/10.1080/15567036.2020.1801906

Koller, M., Braunegg, G., 2018. Advanced approaches to produce polyhydroxyalkanoate (PHA) biopolyesters in a sustainable and economic fashion. EuroBiotech J. 2, 89–103. https://doi.org/10.2478/ebtj-2018-0013

Koller, M., Maršálek, L., de Sousa Dias, M.M., Braunegg, G., 2017. Producing microbial polyhydroxyalkanoate (PHA) biopolyesters in a sustainable manner. N. Biotechnol. 37, 24–38. https://doi.org/10.1016/j.nbt.2016.05.001

Kourmentza, C., Kornaros, M., 2016. Biotransformation of volatile fatty acids to polyhydroxyalkanoates by employing mixed microbial consortia: The effect of pH and carbon source. Bioresour. Technol. https://doi.org/10.1016/j.biortech.2016.10.014

Kourmentza, C., Plácido, J., Venetsaneas, N., Burniol-Figols, A., Varrone, C., Gavala, H.N., Reis, M.A.M., 2017. Recent advances and challenges towards sustainable polyhydroxyalkanoate (PHA) production. Bioengineering. https://doi.org/10.3390/bioengineering4020055

Kumar, A., K. Srivastava, J., Mallick, N., K. Singh, A., 2015. Commercialization of Bacterial Cell Factories for the Sustainable Production of Polyhydroxyalkanoate Thermoplastics: Progress and Prospects. Recent Pat. Biotechnol. 9, 4–21. https://doi.org/10.2174/2211550104666150615211414

Lambert, S., Wagner, M., 2017. Environmental performance of bio-based and biodegradable plastics: the road ahead. Chem. Soc. Rev. 46, 6855–6871. https://doi.org/10.1039/C7CS00149E

Lebreton, L., Andrady, A., 2019. Future scenarios of global plastic waste generation and disposal. Palgrave Commun. 5, 6. https://doi.org/10.1057/s41599-018-0212-7

Lee, S.Y., 1996. Bacterial polyhydroxyalkanoates. Biotechnol. Bioeng. 49, 1–14. https://doi.org/10.1002/(SICI)1097-0290(19960105)49:1<1::AID-BIT1>3.0.CO;2-P

Lemoigne, M., 1926. Produits de déshydration et de polymerisation de l'acide boxybutyrique. Bull. Soc. Chim. Biol 8, 770–782.

Lemos, P.C., Levantesi, C., Serafim, L.S., Rossetti, S., Reis, M.A.M., Tandoi, V., 2008. Microbial characterisation of polyhydroxyalkanoates storing populations selected under different operating conditions using a cell-sorting RT-PCR approach. Appl. Microbiol. Biotechnol. https://doi.org/10.1007/s00253-007-1301-5

Lorini, L., di Re, F., Majone, M., Valentino, F., 2020a. High rate selection of PHA accumulating mixed cultures in Sequencing Batch Reactors with uncoupled carbon and nitrogen feeding. N. Biotechnol. https://doi.org/10.1016/j.nbt.2020.01.006

Lorini, L., Martinelli, A., Pavan, P., Majone, M., Valentino, F., 2020b. Downstream processing and characterization of polyhydroxyalkanoates (PHAs) produced by mixed microbial culture (MMC) and organic urban waste as substrate. Biomass Convers. Biorefinery. https://doi.org/10.1007/s13399-020-00788-w

Lu, J., Tappel, R.C., Nomura, C.T., 2009. Mini-Review: Biosynthesis of Poly(hydroxyalkanoates). Polym. Rev. 49, 226–248. https://doi.org/10.1080/15583720903048243

Mannina, G., Presti, D., Montiel-Jarillo, G., Carrera, J., Suárez-Ojeda, M.E., 2020. Recovery of polyhydroxyalkanoates (PHAs) from wastewater: A review. Bioresour. Technol. 297, 122478. https://doi.org/10.1016/j.biortech.2019.122478

Marang, L., Jiang, Y., van Loosdrecht, M.C.M., Kleerebezem, R., 2013. Butyrate as preferred substrate for polyhydroxybutyrate production. Bioresour. Technol. https://doi.org/10.1016/j.biortech.2013.05.031

Mathuriya, A.S., Yakhmi, J. V, 2017. Polyhydroxyalkanoates: Biodegradable Plastics and Their Applications, in: Handbook of Ecomaterials. Springer International Publishing, Cham, pp. 1–29. https://doi.org/10.1007/978-3-319-48281-1_84-1

Meikle, J.L., 1995. American Plastic: A Cultural History. Rutgers University Press.

Moretto, G., Lorini, L., Pavan, P., Crognale, S., Tonanzi, B., Rossetti, S., Majone, M., Valentino, F., 2020. Biopolymers from urban organic waste: Influence of the solid retention time to cycle length ratio in the enrichment of a Mixed Microbial Culture (MMC). ACS Sustain. Chem. Eng. https://doi.org/10.1021/acssuschemeng.0c04980

Morgan-Sagastume, F., Bengtsson, S., De Grazia, G., Alexandersson, T., Quadri, L., Johansson, P., Magnusson, P., Werker, A., 2020. Mixed-culture polyhydroxyalkanoate (PHA) production integrated into a food-industry effluent biological treatment: A pilot-scale evaluation. J. Environ. Chem. Eng. https://doi.org/10.1016/j.jece.2020.104469

Nielsen, C., Rahman, A., Rehman, A.U., Walsh, M.K., Miller, C.D., 2017. Food waste conversion to microbial polyhydroxyalkanoates. Microb. Biotechnol. 10, 1338–1352. https://doi.org/10.1111/1751-7915.12776

OECD, 2018. Improving Markets for Recycled Plastics. OECD Publishing. https://doi.org/10.1787/9789264301016-en

Oliveira, C.S.S., Silva, C.E., Carvalho, G., Reis, M.A., 2017. Strategies for efficiently selecting PHA producing mixed microbial cultures using complex feedstocks: Feast and famine regime and uncoupled carbon and nitrogen availabilities. N. Biotechnol. 37, 69–79. https://doi.org/10.1016/j.nbt.2016.10.008

Parawira, W., Murto, M., Zvauya, R., Mattiasson, B., 2006. Comparative performance of a UASB reactor and an anaerobic packed-bed reactor when treating potato waste leachate. Renew. Energy 31, 893–903. https://doi.org/10.1016/j.renene.2005.05.013

Philip, S., Keshavarz, T., Roy, I., 2007. Polyhydroxyalkanoates: Biodegradable polymers with a range

of applications. J. Chem. Technol. Biotechnol. https://doi.org/10.1002/jctb.1667

Plastics Europe, 2020. Plastics – the Facts 2020 [WWW Document]. URL https://www.plasticseurope.org/en/resources/publications/4312-plastics-facts-2020 (accessed 5.7.21).

Reis, M., Albuquerque, M., Villano, M., Majone, M., 2011. Mixed Culture Processes for Polyhydroxyalkanoate Production from Agro-Industrial Surplus/Wastes as Feedstocks, Second Edi. ed, Comprehensive Biotechnology, Second Edition. Elsevier B.V. https://doi.org/10.1016/B978-0-08-088504-9.00464-5

Sabapathy, P.C., Devaraj, S., Meixner, K., Anburajan, P., Kathirvel, P., Ravikumar, Y., Zabed, H.M., Qi, X., 2020. Recent developments in Polyhydroxyalkanoates (PHAs) production – A review. Bioresour. Technol. 306, 123132. https://doi.org/10.1016/j.biortech.2020.123132

Serafim, L.S., Lemos, P.C., Albuquerque, M.G.E., Reis, M.A.M., 2008. Strategies for PHA production by mixed cultures and renewable waste materials. Appl. Microbiol. Biotechnol. 81, 615–628. https://doi.org/10.1007/s00253-008-1757-y

Silva, F., Campanari, S., Matteo, S., Valentino, F., Majone, M., Villano, M., 2017. Impact of nitrogen feeding regulation on polyhydroxyalkanoates production by mixed microbial cultures. N. Biotechnol. https://doi.org/10.1016/j.nbt.2016.07.013

Singh, A.K., Mallick, N., 2009. SCL-LCL-PHA copolymer production by a local isolate, Pseudomonas aeruginosa MTCC 7925. Biotechnol. J. 4, 703–711. https://doi.org/10.1002/biot.200800307

Steinbüchel, A., Lütke-Eversloh, T., 2003. Metabolic engineering and pathway construction for biotechnological production of relevant polyhydroxyalkanoates in microorganisms. Biochem. Eng. J. 16, 81–96. https://doi.org/https://doi.org/10.1016/S1369-703X(03)00036-6

Sudesh, K., Abe, H., Doi, Y., 2000. Synthesis, structure and properties of polyhydroxyalkanoates: biological polyesters. Prog. Polym. Sci. 25, 1503–1555. https://doi.org/10.1016/S0079-6700(00)00035-6

Tamis, J., Lužkov, K., Jiang, Y., Loosdrecht, M.C.M. va., Kleerebezem, R., 2014. Enrichment of Plasticicumulans acidivorans at pilot-scale for PHA production on industrial wastewater. J. Biotechnol. https://doi.org/10.1016/j.jbiotec.2014.10.022

Tamis, J., Mulders, M., Dijkman, H., Rozendal, R., van Loosdrecht, M.C.M.M., Kleerebezem, R., 2018. Pilot-Scale Polyhydroxyalkanoate Production from Paper Mill Wastewater: Process Characteristics and Identification of Bottlenecks for Full-Scale Implementation. J. Environ. Eng. (United States). https://doi.org/10.1061/(ASCE)EE.1943-7870.0001444

Valentino, F., Lorini, L., Pavan, P., Bolzonella, D., Majone, M., 2019. Organic fraction of municipal solid waste conversion into polyhydroxyalkanoates (PHA) in a pilot scale anaerobic/aerobic process. Chem. Eng. Trans. 74, 265–270. https://doi.org/10.3303/CET1974045

Valentino, F., Morgan-Sagastume, F., Campanari, S., Villano, M., Werker, A., Majone, M., 2017. Carbon recovery from wastewater through bioconversion into biodegradable polymers. N.

Biotechnol. 37, 9–23. https://doi.org/10.1016/j.nbt.2016.05.007

Villano, M., Beccari, M., Dionisi, D., Lampis, S., Miccheli, A., Vallini, G., Majone, M., 2010. Effect of pH on the production of bacterial polyhydroxyalkanoates by mixed cultures enriched under periodic feeding. Process Biochem. 45, 714–723. https://doi.org/10.1016/j.procbio.2010.01.008

Wang, X., Oehmen, A., Freitas, E.B., Carvalho, G., Reis, M.A.M., 2017. The link of feast-phase dissolved oxygen (DO) with substrate competition and microbial selection in PHA production. Water Res. 112, 269–278. https://doi.org/10.1016/j.watres.2017.01.064

2

SLUDGE RETENTION TIME IMPACTS ON POLYHYDROXYALKANOATE PRODUCTIVITY IN UNCOUPLED STORAGE/GROWTH PROCESSES

SUMMARY:

The process involving mixed microbial cultures (MMCs) and waste-based substrates emerged as an alternative solution to reduce the market price of polyhydroxyalkanoates (PHAs). The selection of an efficient MMC that displays a significant PHA accumulation potential and a high growth rate is considered a key factor for the MMC PHA production feasibility. This study used a pilot plant to investigate the dynamics of growth vs storage in a mixed culture fed with fermented fruit waste under uncoupled carbon and nitrogen feeding. Varying sludge retention times (SRTs) (2 and 4 d) and organic loading rates (OLRs) (from 2.6 to 14.5 $gCOD.L^{-1}.d^{-1}$) were imposed for this purpose. Results showed that, regardless of the OLR imposed, cultures selected at lower SRT grew faster and more efficiently using stored PHA. However, they had inferior specific storage rates and accumulation capacity, resulting in lower PHA productivity. Additionally, the polymer storage yield was independent of the SRT, and was directly linked with the abundance of putative PHA-storers in the MMC. The high PHA productivity (4.6 ± 0.3 $g.L^{-1}.d^{-1}$) obtained for the culture selected at 4 d of SRT was 80% above that obtained for the lower SRT tested, underlining the importance of achieving a good balance between culture growth and accumulation capacity to increase the viability of the PHA-producing process from wastes.

KEYWORDS:

Polyhydroxyalkanoates (PHAs); Mixed microbial cultures (MMCs); Pilot-scale; Fruit waste; Sludge retention time (SRT); Organic loading rate (OLR).

PUBLISHED AS: Matos, M., Cruz, R.A.P., Cardoso, P., Silva, F., Freitas, E.B., Carvalho, G., Reis, M.A.M., 2021. Sludge retention time impacts on polyhydroxyalkanoate productivity in uncoupled storage/growth processes. Sci. Total Environ. 799, 149363. https://doi.org/10.1016/j.scitotenv.2021.149363

2.1 Introduction

The production of plastics emerged in the 1950s and exponentially increased in the following decades, attaining a massive amount of 368 million metric tons in 2019 (Plastics Europe, 2020). Currently, more than 60% of all produced plastics end up in landfills or in the natural environment, causing serious threats to several ecosystems (Geyer et al., 2017). Polyhydroxyalkanoates (PHAs) are an innovative material with great potential to replace the petroleum-derived plastics due to its biodegradable and thermoplastics properties (Kumar et al., 2020; Mannina et al., 2020). The PHA market size is estimated to increase from 62 million USD in 2020 to 121 million USD by 2025 (Markets and Markets, 2021), being a key polymer in the biodegradable plastic market (European Bioplastics, 2020).

A promising PHA production strategy consists in using open mixed microbial cultures (MMCs) and waste-based feedstocks. This approach effectively reduces both the cost and environmental impact associated to PHA obtained from pure cultures and first-generation biomass (Kumar et al., 2018). The MMC process typically consists of a three-stage process: (1) fermentation of the carbon feedstock into a mixture of soluble fermentation products (SFP) that are precursors for PHA biosynthesis; (2) selection of an aerobic community highly enriched in PHA-storing bacteria; and (3) production of PHA using the previously selected culture which is fed with the SFP under growth limiting conditions to reach its maximum PHA capacity (Sabapathy et al., 2020).

The selection of a robust culture with a significant PHA accumulation potential and a high growth rate are considered key factors for the MMC PHA production success. Indeed, these two parameters have a direct impact on the global PHA productivity of the process (Reis et al., 2011; Valentino et al., 2017), so culture selection is a critical step of the three-stage process. A high selective pressure towards the enrichment of PHA-storers can be achieved by applying an aerobic dynamic feeding (ADF) strategy, where alternating periods of feast (carbon excess) and famine (carbon absence) are cyclically established in a sequencing batch reactor (SBR) (De Donno Novelli et al., 2021; Sabapathy et al., 2020). Some waste-based feedstocks contain both carbon (C) and nitrogen (N) sources in sufficient amounts for PHA production and bacterial growth. If the substrate contains both a N source and an external C, culture growth usually starts at the beginning of the feast phase, and can be extended into the famine phase depending on the C/N ratio (Albuquerque et al., 2007; Johnson et al., 2010; Serafim et al., 2004). In this situation, storage and growth occur simultaneously during feast, with competition between the two metabolisms. The long famine phase acts then as a physiological selective pressure, inducing the microbial culture to promote storage rather than growth in the following feast phase (Reis et al., 2011).

More recently, Oliveira et al. (2017) and Silva et al. (2017) proposed to uncouple the availability of C and N while maintaining the feast/famine regime during the selection process. This strategy creates a high selective pressure by separating the storage and growth metabolisms. Under these conditions, PHA is stored during feast and the growth of PHA-storers is favoured over other organisms during famine,

due to their ability to grow using the previously stored PHA, in the absence of external C source. While the uncoupled feeding strategy can only be used with feedstocks that are poor in nutrients, this approach was shown to be particularly interesting when operating the process at high organic loading rates (OLRs), since it effectively enhanced the PHA storage response by significantly limiting the growth of flanking populations (Argiz et al., 2021; Campanari et al., 2017; Oliveira et al., 2017).

In addition to the OLR and the feeding strategy, the operational sludge retention time (SRT) is also tightly bound to the competition between storage and growth. The SRT theoretically regulates the age of microbial consortia. It can be assumed that, when feeding the C source coupled to the N source, a lower SRT selects a population with increased specific growth rate and growth yield, thus driving a higher amount of C for growth, and less for PHA storage. Lemos et al. (2008) confirmed this hypothesis, using acetate as the sole C source, obtaining lower storage yields and specific PHA storage rates in the selection reactor for lower sludge ages. However, Johnson et al. (2010), observed that the selection and growth/storage dynamics of a culture fed under coupled C and N and operated at different SRTs was also highly dependent on the kind of limitation the culture is experiencing, i.e., if it selected under nitrogen limiting (N is depleted before C) or carbon limited (N is available during all cycle) conditions. These results do not allow to conclude if the lower storage response usually observed for lower SRTs in the SBR is a result of the higher C demand needed for growth (consequence of metabolism), or if it is actually a limitation of the culture that intrinsically has a lower storage ability (consequence of competitive selection). On the other hand, the impact of SRT on culture selection and on PHA production performance was never assessed with the uncoupled strategy. By uncoupling the two processes, the actual mechanisms driving competition between storage and growth could be clarified.

This work aims to elucidate, for the first time, how the dynamics between growth and storage mechanisms change with the SRT when those two metabolic processes are not competing for the same C source (PHA storage from external C in the feast and growth on internal PHA during famine). This strategy was imposed in two pilot-scale SBRs fed with a real nutrient-deficient feedstock – fruit waste (FW) – which were operated at different SRTs. In addition to the highly selective uncoupled C and N regime, the OLR was increased step-wisely in both SBRs up to levels rarely considered in literature (maximum 14.5 $gCOD.L^{-1}.d^{-1}$) and maximum PHA content on biomass was envisaged to enhance the global PHA productivity. This performance parameter has a strong impact in the design of the PHA production process, therefore it is a good indicator to compare the culture efficiency and the process viability under different conditions.

2.2 Materials and methods

2.2.1 Experimental set-up and operation of the reactors

A three-stage pilot scale was operated for PHA production using MMCs. The experimental setup used is schematically represented in Figure 2.1. The FW was fed to an acidogenic fermenter (step 1), where its organic carbon was converted into a mixture of SFP. This step was followed by a decanting stage, where the resulting SFP stream was clarified to remove the coarse solids facilitating the operation of the subsequent reactors. The refined SFP stream was then fed to the selection reactor (step 2), for the enrichment of a PHA-producing MMC and to a PHA accumulation reactor (step 3), where the previously selected culture was inoculated and fed with the fermented FW until attaining its maximum PHA storage capacity. More details about the individual reactor's design can be found in Appendix A.

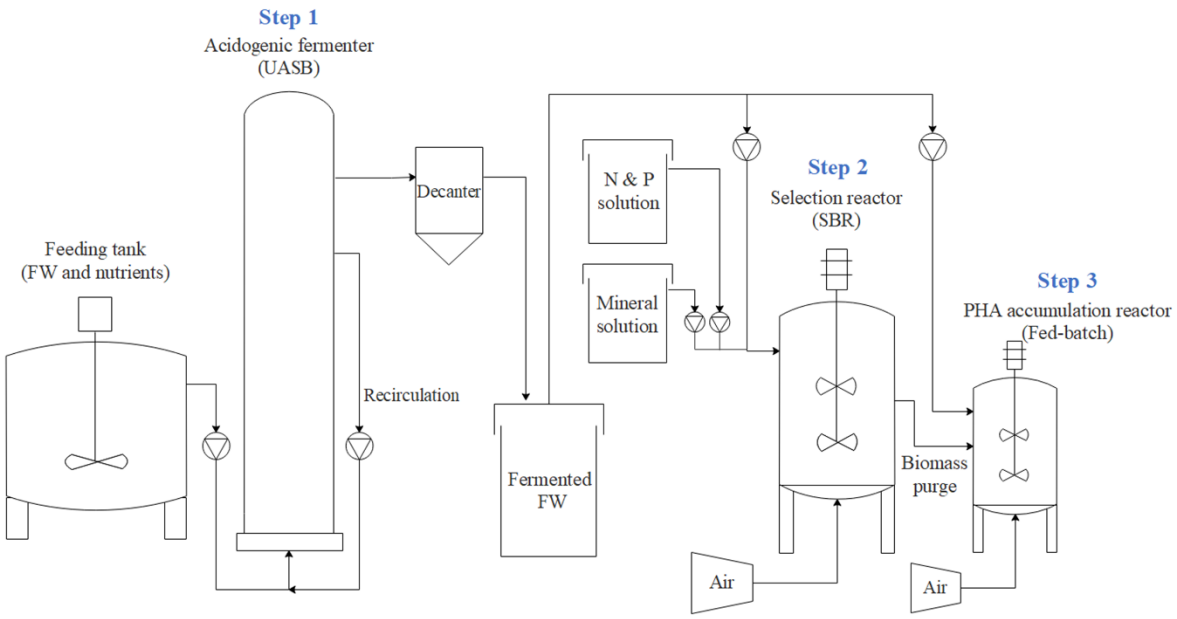

Figure 2.1 - Configuration of the pilot plant unit adopted in this study.

2.2.1.1 Acidogenic fermentation

An upflow anaerobic sludge blanket (UASB) reactor with a working volume of 60 L was operated in continuous mode. For the specific period in which the SFP were collected, the operating conditions were set as follows: temperature of 29.7 ± 0.7 °C, pH 5.0 ± 0.1, HRT of 24 h and OLR of 30 ± 2 $gCOD.L^{-1}.d^{-1}$.

The FW feedstock (Sumol+Compal S.A., Portugal) had a high total chemical oxygen demand (175 ± 13 $gCOD.L^{-1}$) which was adjusted with tap water to achieve the desired OLR. The feedstock was

comprised of 85% ± 1% (gCOD basis) of soluble biodegradable compounds prior to fermentation, which were fully exhausted.

The characteristics of the clarified fermented stream used as feedstock for the selection and accumulation reactors are listed in Table 2.1.. The stream was largely comprised of PHA bioprecursors, namely volatile fatty acids (VFAs)– acetate (HAce), propionate (HPro), butyrate (HBut) and valerate (HVal) – lactate (HLac) and ethanol (EtOH) (Reis et al., 2011). Additionally, it was nutrient-deficient (low ammonium and phosphate concentrations) enabling the implementation of an uncoupled C-N feeding strategy in the selection reactor.

Table 2.1 - Characteristics of the clarified fermented feedstock. Ranges of the key parameters are presented as minimum/maximum values detected in the feedstock.

Parameter	**Min/max values**					
Ammonium ($mg\text{-}N.L^{-1}$)	0/9					
Phosphate ($mg\text{-}P.L^{-1}$)	11/32					
SFP concentration ($gCOD.L^{-1}$)	22/26					
SFP composition (%, gCOD-basis)	HLac	HAce	HPro	EtOH	HBut	HVal
	0/2	15/31	3/13	0/9	51/68	2/12

2.2.1.2 Culture selection reactor

Two 100 L SBRs were inoculated with fresh activated sludge (Mutela WWTP, Portugal) and operated with a HRT of 1 d, at room temperature and under uncontrolled pH. The two SBRs were operated with different SRTs: 4 d in SBR 4d and 2 d in SBR 2d. Air was provided at 60 $L_{air}.L_{reactor}^{-1}.h^{-1}$, which was sufficient to ensure a dissolved oxygen (DO) above 2 $mg\text{-}O_2.L^{-1}$ throughout the cycle, to guarantee non-limiting conditions.

The SBR cycles had a length of 12 h, comprising: influent feeding (0.20 h), aerated feast/famine period (10.88 h), biomass withdrawal (0.20 h, only once a day in the case of SBR 4d), settling (0.75h) and withdrawal of exhausted effluent (0.17h). A solution containing ammonium and phosphate (N & P solution) was fed after 3 h or 4 h (SBR 4d or SBR 2d, respectively) of the beginning of the cycle in order to keep the N feeding uncoupled from the C. The C:N:P ratio was adjusted to 100:7:1 (mol-basis) (Silva et al., 2017).

The OLR was increased in four steps for both SBRs: 2.6, 5.4, 6.6, 9.3 and 12.3 $gCOD.L^{-1}.d^{-1}$ for the SBR 4d, and 2.7, 6.3, 10.6, 12.9 and 14.5 $gCOD.L^{-1}.d^{-1}$ for the SBR 2d. The clarified SFP stream was diluted using a mineral solution to adjust the reactor OLR to the desired values, as described by Serafim et al. (2004).

The SBRs working sequence (pump filling, aeration, mixing and withdrawal) was automatically controlled by a software developed within the research group, which also recorded in real time the values of DO and pH. The DO trends allowed to identify the length of the feast phase, which is a parameter used to easily assess the performance of the feast-famine regime. During the feast phase, the DO is low due to microbial consumption for substrate oxidation. At the end of the feast phase, a sharp increase in the DO concentration profile occurs indicating the depletion of the organic carbon thus corresponding to the start of the famine phase.

The profiles of total suspended solids (TSS), PHA content on biomass and available SFP, nitrogen and phosphorus were assessed for each OLR tested.

2.2.1.3 PHA accumulation fed-batch assays

The maximum storage capacity of the MMCs selected at the highest OLR values was assessed in fed-batch accumulation assays carried out in a 60 L reactor. The assays (performed in duplicate) consisted on feeding the SFP without nutrient supplementation to 25 L of biomass collected from each one of the SBRs at the end of famine phase. The reactor was operated at room temperature, oxygen was supplied by sparging air at 60 $L_{air}.L_{reactor}^{-1}.h^{-1}$, and the pH was controlled at 8.5 by automatically adding the acid SFP stream (pH-stat mode).

2.2.2 Analytical methods

LCK 914 Hach Lange kits (Hach-Lange, Germany) were used to determine chemical oxygen demand (COD) following the manufacturer's instructions.

TSS and volatile suspended solids (VSS) were determined using the protocol described in Standard Methods (APHA, 1998).

SFP concentrations of filtered samples were determined through high performance liquid chromatography (HPLC) using a VWR Hitachi Chromaster chromatographer as described by Oliveira et al. (2017).

Ammonium and phosphate concentrations were determined using a colorimetric method implemented in a segmented flow analyser (Skalar San++ system, Skalar Analytical).

Lyophilised biomass pellets were processed using the method described by Lanham et al. (2013) to quantify 3-hydroxybutyrate (3-HB) and 3-hydroxyvalerate (3-HV) monomer concentrations by gas chromatography (GC) using a Bruker 430-GC gas chromatographer.

Molecular mass distribution (M_w) and polydispersity indices (PDI) of the produced PHA were determined by size exclusion chromatography (SEC) (Waters Millennium system) as described by Pereira et al. (2019).

A detailed description of these methodologies can be found in Appendix A.

2.2.3 Microbiological analyses

Biomass samples were collected in both SBR 4d and SBR 2d throughout the operational period and were phylogenetically characterised based on high throughput sequencing of the 16S rRNA gene. DNA was extracted with the FastDNA Spin kit for soil (MP Biomedicals, USA), using the standard protocol with a few exceptions: sample of 500 µL, 480 µL of Sodium Phosphate Buffer and 120 µL of MT Buffer were added to a tube of Lysing Matrix. 16S rRNA gene amplicon sequencing and bioinformatic processing was carried out using Illumina technology by DNASense (Aalborg, Denmark).

Principal component analysis (PCA) was performed to visually detect the dynamics of the microbial communities throughout the study. Prior to the analysis, operational taxonomic units (OTUs) that are not present in more than 0.1% relative abundance were removed. The data was transformed by applying the Hellinger transformation (Legendre and Gallagher, 2001). The distance between the data points plotted is indicative of the similarity of the microbial composition of the samples.

Putative PHA-storers were identified using the references reported in Appendix A (Table A3).

2.2.4 Calculations

Feast to famine length ratio (FF ratio, $h.h^{-1}$) was calculated as the fraction between the time lengths of the feast and the famine phases.

The percentages of PHA content in biomass (%, w/w) were assessed by dividing the PHA content by the measured VSS determined at the same time of the assay. The active biomass (X_a, $g.L^{-1}$) concentrations were calculated by the difference between VSS concentration ($g.L^{-1}$) and PHA concentration ($g.L^{-1}$) (at the same reaction time).

Biomass volumetric productivity (P_X) was calculated by the fraction between X_a concentration ($g\text{-}X_a.L^{-1}$) and the SRT (d).

Specific substrate uptake rates ($-q_{SFP}$, $gCOD\text{-}SFP.gCOD\text{-}X_a^{-1}.L^{-1}$), specific PHA storage (q_{PHA}, $gCOD\text{-}PHA.gCOD\text{-}X_a^{-1}.h^{-1}$) and consumption ($-q_{PHA}^{famine}$, $gCOD\text{-}PHA.gCOD\text{-}X_a^{-1}.h^{-1}$) rates, and maximum specific growth rates (μ_{max}, h^{-1}) were calculated from the slope of the linear regression of total SFP, PHA and X_a specific concentrations, respectively, over time. The goodness-of-fit of each linear regression was assessed by the R^2 ($R^2 > 0.80$).

Storage yields ($Y_{PHA/SFP}$, gCOD-PHA.gCOD-SFP^{-1}) were calculated by dividing the q_{PHA} by the $-q_{SFP}$. Growth yields on PHA ($Y_{X/PHA}$, gCOD-X_a.gCOD-PHA^{-1}) were determined as the ratio between μ_{max} and $-q_{PHA}^{famine}$.

Concentrations of all carbon compounds (3-HB, 3-HV, SFP and X_a) were converted into COD units in accordance with the oxidation stoichiometry presented in Appendix A.

2.3 Results

Two PHA-storing cultures were selected with SRT of either 4 d or 2 d and gradually increased OLR. The performance and population dynamics were evaluated in the SBR and through assays in the accumulation fed-batch reactor to characterise and compare the two cultures.

2.3.1 Culture selection

2.3.1.1 SRT of 4 d

For the SBR operated at 4d of SRT (SBR 4d), the OLR was initially set to 2.60 gCOD.L^{-1}.d^{-1}, then increased in four steps up to 12.3 gCOD.L^{-1}.d^{-1} (see Figure A1 A in Appendix A for more details). The performance of the culture was assessed for each OLR tested, and the results are summarised in Table 2.2.

The observed FF ratio did not increase significantly along the operation period despite the increase in OLR (Figure A1 A in Appendix A). In fact, the FF decreased after an initial value of 0.16 during start-up, and remained consistently below 0.1 during the rest of the operation period (Table 2.2). On the other hand, the increase of OLR had a high impact on the active biomass (X_a) concentration, which raised from 1.75 to 7.9 g-X_a.L^{-1}.

The specific substrate uptake ($-q_{SFP}$) and storage (q_{PHA}) rates showed an unexpected trend. Both rates increased sharply with the OLR up to maximum values of 1.1 gCOD.gCOD-X_a^{-1}.h^{-1} and 1.01 gCOD.gCOD-X_a^{-1}.h$^{-1,}$ respectively, for an OLR of 6.6 gCOD.L^{-1}.d^{-1}, while further increase of OLR to 12.3 gCOD.L^{-1}.d^{-1} caused a decrease to 0.55 gCOD.gCOD-X_a^{-1}.h^{-1} and 0.41 gCOD.gCOD-X_a^{-1}.h^{-1}, respectively (Table 2.2). The same trend was observed for the storage yield ($Y_{PHA/SFP}$), which attained maximum values of 0.90 gCOD.gCOD^{-1} at the middle-range OLRs (5.4 - 6.6 gCOD.L^{-1}.d^{-1}) and tended to decrease for higher OLR values (Table 2.2).

The performance parameters relative to the famine period (e.g. maximum specific PHA consumption ($-q_{PHA}^{famine}$), maximum growth rates (μ_{max}) and growth yield on PHA ($Y_{X/PHA}$)) were relatively stable despite the increase in OLR, excluding the first OLR period which coincided with the acclimation period (Table 2.2).

The PHA obtained in the process throughout this experiment was a copolymer of 3-HB and 3-HV monomers, with a 3-HV content that varied between 14.0% and 24.6% on a Cmol-basis.

2.3.1.2 SRT of 2 d

Similarly to the SBR 4d, in the reactor operated at SRT of 2 d (SBR 2d) the OLR was initially set to 2.7 $gCOD.L^{-1}.d^{-1}$ and increased in four steps up to 14.5 $gCOD.L^{-1}.d^{-1}$ (see Figure A1 B in Appendix A for more details). The results are summarised in Table 2.2.

The FF ratio varied slightly with the OLR increments, ranging between 0.24 and 0.39 in the stable periods (Table 2.2).

The X_a concentration increased linearly with the increasing OLR up to a value of 4.67 $g\text{-}X_a.L^{-1}$ at the maximum OLR tested (14.5 $gCOD.L^{-1}.d^{-1}$) (Table 2.2).

The performance of this culture was quite different from that of the culture selected in SBR 4d. The $-q_{SFP}$ and q_{PHA} increased with the OLR reaching maximum values of 0.65 $gCOD.gCOD\text{-}X_a^{-1}.h^{-1}$ and 0.50 $gCOD.gCOD\text{-}X_a^{-1}.h^{-1,}$ respectively, at OLR 14.5 $gCOD.L^{-1}.d^{-1}$. Also, the $Y_{PHA/SFP}$ increased from 0.41 $gCOD.gCOD^{-1}$ to 0.77 $gCOD.gCOD^{-1}$. After the initial variations observed during the first OLR step, which were likely due to acclimatisation, no significant fluctuations were observed for the parameters determined during the famine period, such as the $-q_{PHA}^{famine}$, the μ_{max} and the $Y_{X/PHA}$ (Table 2.2).

The copolymer produced had a 3-HV content ranging between 10.8% and 23.2% (Cmol-basis) in this experiment.

Table 2.2 – Main parameters monitored and determined for SBR operation at SBR 4d and SBR 2d for each OLR tested. Values presented are mean (standard deviation).

	SBR 4d					**SBR 2d**				
OLR	**2.60**	**5.4**	**6.6**	**9.3**	**12.3**	**2.7**	**6**	**10.6**	**12.9**	**14.5**
(gCOD.L^{-1}.d^{-1})	(0.01)	(0.1)	(0.5)	(0.1**)**	(0.1)	(0.2)	(1)	(0.5)	(0.2)	(0.6)
FF ratio	**0.16**	**0.056**	**0.035**	**0.056**	**0.09**	**0.30**	**0.24**	**0.35**	**0.39**	**0.27**
(h.h^{-1})	(0.02)	(0.009)	(0.005)	(0.006)	(0.01)	(0.03)	(0.01)	(0.02)	(0.03)	(0.03)
X_a	**1.75**	**4.84**	**5.09**	**6.97**	**7.9**	**1.24**	**2.5**	**3.6**	**4.2**	**4.67**
(g.L^{-1})	(0.05)	(0.02)	(0.09)	(0.06)	(0.3)	(0.05)	(0.3)	(0.2)	(0.6)	(0.06)
Δ PHA feast	**22.4**	**18.2**	**19.6**	**18.9**	**22**	**32**	**24.2**	**22.6**	**27**	**26**
(%, w/w)	(0.02)	(0.3)	(0.7)	(0.1)	(1)	(3)	(0.9)	(0.5)	(1)	(3)
$-q_{SFP}$	**0.44**	**1.04**	**1.1**	**0.75**	**0.55**	**0.45**	**0.47**	**0.52**	**0.58**	**0.65**
(gCOD.gCOD-X_a^{-1}.h^{-1})	(0.01)	(0.04)	(0.1)	(0.05)	(0.07)	(0.03)	(0.05)	(0.03)	(0.03)	(0.03)
q_{PHA}	**0.209**	**0.93**	**1.01**	**0.61**	**0.41**	**0.18**	**0.29**	**0.34**	**0.40**	**0.50**
(gCOD.gCOD-X_a^{-1}.h^{-1})	(0.005)	(0.03)	(0.05)	(0.04)	(0.07)	(0.02)	(0.01)	(0.04)	(0.02)	(0.01)
$Y_{PHA/SFP}$	**0.47**	**0.90**	**0.90**	**0.81**	**0.74**	**0.41**	**0.62**	**0.66**	**0.69**	**0.77**
(gCOD.gCOD^{-1})	(0.02)	(0.04)	(0.09)	(0.08)	(0.02)	(0.05)	(0.04)	(0.08)	(0.06)	(0.02)
$-q_{PHA}^{famine}$	**0.128**	**0.07**	**0.083**	**0.063**	**0.068**	**0.122**	**0.145**	**0.12**	**0.12**	**0.141**
(gCOD.gCOD-X_a^{-1}.h^{-1})	(0.006)	(0.01)	(0.002)	(0.001)	(0.006)	(0.003)	(0.003)	(0.01)	(0.01)	(0.006)
μ_{max}	**0.10**	**0.047**	**0.054**	**0.042**	**0.044**	**0.103**	**0.109**	**0.087**	**0.08**	**0.103**
(h^{-1})	(0.01)	(0.004)	(0.008)	(0.003)	(0.003)	(0.008)	(0.004)	(0.006)	(0.01)	(0.006)
$Y_{X/PHA}$	**0.80**	**0.7**	**0.7**	**0.67**	**0.66**	**0.84**	**0.75**	**0.74**	**0.76**	**0.73**
(gCOD.gCOD^{-1})	(0.06)	(0.1)	(0.1)	(0.05)	(0.05)	(0.07)	(0.01)	(0.08)	(0.01)	(0.07)

2.3.2 PHA accumulation assays

The storage response of the cultures selected at the highest OLRs in each one of the SBRs was evaluated in two fed-batch accumulation assays performed in duplicate in the accumulation reactor: the Acc 4d (inoculated with SBR 4d biomass) and the Acc 2d (with biomass from SBR 2d). The assays were performed with no N addition, thus no microbial growth was enabled. The concentration of SFP in the reactor (C_{SFP}) was quite stable in the period when the specific rates and yields were calculated (3.80 ± 0.04 gCOD.L^{-1} and 4.43 ± 0.07 gCOD.L^{-1} for Acc 4d and Acc 2d, respectively (Table 2.3)). The supply of external carbon was practically continuous due to the operation with pH-stat control using the SFP solution to correct the pH. Due to this, no polymer was consumed during the accumulation assays. Both cultures were fed and aerated until a stable PHA content was attained, corresponding to their maximum PHA accumulation capacity.

Table 2.3 summarises the average maximum specific substrate uptake ($-q_{SFP}$) and storage (q_{PHA}) rates, storage yields ($Y_{PHA/SFP}$) and PHA content on biomass and the PHA characteristics obtained for the different assays.

In general, the storage response of the Acc 2d was lower than that observed in the Acc 4d. Despite the similar $Y_{PHA/SFP}$, the culture selected at the lower SRT was only capable to accumulate a maximum amount of 49.2 ± 0.4 % (w/w) of PHA, contrasting with the 69 ± 2 % (w/w) obtained for SBR 4d biomass. In addition, the specific storage rate in Acc 2d (0.53 gCOD.gCOD-X_a^{-1}.h^{-1}) was nearly half of that observed in Acc 4d (0.97 gCOD.gCOD-X_a^{-1}.h^{-1}) (Table 2.3). This difference in performance by the two cultures contrasted with the behaviour observed in the SBRs (in the phase of maximum OLR), where the cultures had similar q_{PHA} (0.41 and 0.50 gCOD.gCOD-X_a^{-1}.h^{-1} respectively for SBR 4d and SBR 2d) and $Y_{PHA/SFP}$ (0.74 and 0.76 gCOD.$gCOD^{-1}$ respectively for SBR 4d and SBR 2d).

The polymer produced during the accumulation assays had a 3-HV fraction of 16.8 ± 0.8% and 13.21 ± 0.02% (w/w), for the cultures enriched with SRT of 4d and 2d, respectively, both of them displaying similar molecular weights (M_w) and polydispersity indices (PDI) (Table 2.3).

Table 2.3 - Main parameters determined in the accumulation reactor inoculated with culture selected at the maximum OLR tested in SBR 4d (Acc 4d) and SBR 2d (Acc 2d). Values presented are mean (standard deviation).

Reactor	Acc 4d	Acc 2d
Inoculum source	SBR 4d	SBR 2d
Culture selected at OLR	**12.3**	**14.5**
($gCOD.L^{-1}.d^{-1}$)	(0.1)	(0.6)
C_{SFP} [a]	**3.80**	**4.43**
($gCOD.L^{-1}$)	(0.04)	(0.07)
SFP composition [HLac/HAce/HPro/EtOH/HBut/HVal] (%, gCOD-basis)	**0/23.7/8.4/6/57.6/4.0** (0/0.2/0.2/1/0.2/0.7)	**0/19/3.9/7.8/67/2.2** (0/2/0.3/0.4/1/0.6)
$-q_{SFP}$ [b]	**1.31**	**0.6939**
($gCOD.gCOD\text{-}X_a^{-1}.h^{-1}$)	(0.09)	(0.0004)
q_{PHA} [b]	**0.97**	**0.53**
($gCOD.gCOD\text{-}X_a^{-1}.h^{-1}$)	(0.04)	(0.03)
$Y_{PHA/SFP}$ [b]	**0.74**	**0.76**
($gCOD.gCOD^{-1}$)	(0.02)	(0.05)
Max. PHA content	**69**	**49.2**
(%, w/w)	(2)	(0.4)
Polymer 3-HV content	**16.8**	**13.21**
(%, w/w)	(0.8)	(0.02)
Polymer M_w (kDa)	451	453
Polymer PDI	2.38	2.47

[a]average SFP concentration on reactor at the period where the specific rates and yield were calculated

[b]maximum values

2.3.3 Microbial community analysis

Biomass samples collected at different OLRs (6.6 and 12.3 $gCOD.L^{-1}.d^{-1}$ from SBR 4d and 6.3, 12.9 and 14.5 $gCOD.L^{-1}.d^{-1}$ from SBR 2d) were analysed through high throughput sequencing of the 16S rRNA gene, and compared with the profile of the full-scale activated sludge used as inoculum.

Despite the similarly of the inoculum, the community enriched in the SBR 2d highly diverged from the one obtained in the SBR 4d, as evidenced by their distance in the PCA plot (Figure 2.2). Additionally, the microbial profile clearly changed with the increase in OLRs in each of the reactors, as can be observed by the distances of the corresponding points in the PCA results (Figure 2.2). Detailed high throughput sequencing results obtained for the SBR 4d and SBR 2d are presented, respectively, in Tables A1 and A2 in Appendix A. In the SBR 2d culture, the putative PHA-accumulating organisms

consistently increased with the OLR, achieving 71.8% for the highest OLR. In contrast, a maximum relative abundance of putative PHA-storers of 93.0% was detected for the SBR 4d enrichment when operated at 6.6 $gCOD.L^{-1}.d^{-1}$. This value decreased to 60.2% at the maximum OLR but the putative PHA-storers concentration remained stable thereafter (Table 2.4), suggesting that above 6.6 $gCOD.L^{-1}.d^{-1}$ the increase of X_a reflected growth of flanking microorganisms.

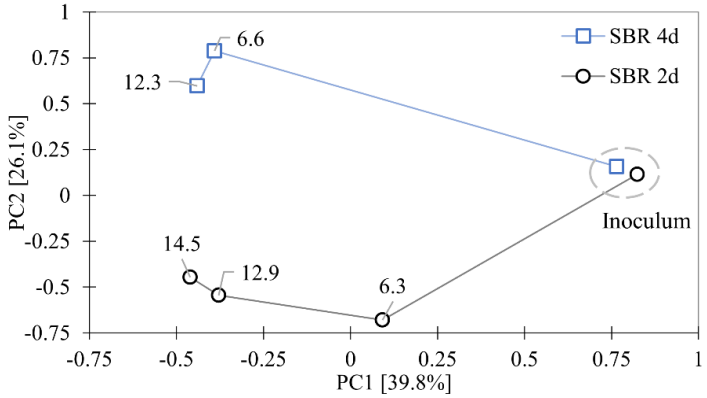

Figure 2.2 - PCA ordination highlighting the differences in OTUs abundance between the microbial communities selected in SBR 4d and SBR 2d (data labels correspond to the operational OLR). The relative contribution (eigenvalue) of each axis to the total inertia in the data is indicated in percent at the axis titles.

Table 2.4 - Relative abundance (% of total reads) and concentration of putative PHA-storers calculated for the cultures present in SBR 4d and SBR 2d. Values of putative PHA-storers concentration are mean (standard deviation).

Reactor	OLR ($gCOD.L^{-1}.d^{-1}$)	Relative abundance of putative PHA-storers (% of total reads)[a]	Concentration of putative PHA-storers ($g.L^{-1}$)[b]
SBR 4d	Inoculum	18.9	
	6.6	93.3	4.8 (0.1)
	12.3	60.2	4.8 (0.2)
SBR 2d	Inoculum	12.3	
	6.3	21.9	0.55 (0.07)
	12.9	47.4	2.0 (0.3)
	14.5	71.8	3.36 (0.04)

[a]according to the relative abundance of sequences affiliated with known putative PHA-storers (more details can be found in Appendix A)

[b]estimated using the corresponding X_a presented in Table 2.

2.4 Discussion

2.4.1 Growth vs storage response

The determined specific rates and yields were very similar between the two SBRs for the first OLR tested (Table 2.2). This similarity in the culture response can be attributed to the short period of acclimatisation time at this point (Figure A1 in Appendix A), which is unlikely to be enough to enrich a PHA-storing community. For this reason, and considering that both reactors showed distinct yields and kinetic profiles throughout the rest of the study (Table 2.2), the parameters calculated for this initial operational period were not used as a mean of comparison between the assays.

The maximum specific growth rate (μ_{max}), calculated during famine, was not affected by the OLR. As expected, the μ_{max} was driven by the SRT, being 2.1 times higher, on average, for SBR 2d than for SBR 4d (Table 2.2). The same trend was observed for the $-q_{PHA}^{famine}$, which was the double for the SBR 2d than for the SBR 4d. The similar proportion in μ_{max} and $-q_{PHA}^{famine}$ for SRT 4d and SRT 2d confirms that, in the famine phase, PHA and growth are fully correlated. The $Y_{X/PHA}$ were also not significantly different between OLR values for each SBR. However, these values were on average 15% higher for the SBR 2d than for the SBR 4d (see Table 2.2), indicating that when the uncoupled strategy is used, cultures selected at a lower SRT can use the accumulated PHA for growth more efficiently, independently of the OLR applied. Contrasting to what happens when using the traditional coupled feeding approach, the OLR did not affect the culture growth performance. In fact, in the traditional approach, growth and storage metabolisms compete with each other for the external substrate concentration (which is usually directly linked to the OLR) while in the uncoupled feeding the biomass grows from the stored PHA. Thus, in this case, if the culture is able to accumulate enough polymer to ensure unlimiting conditions, the OLR will have a low impact on the growth rate. The fact that, for the same SRT, the $-q_{PHA}^{famine}$ was constant for all the OLR tested, confirms that assumption.

The $Y_{PHA/SFP}$ followed different trends in the two SBRs as the OLR was increased, tending to decrease in SBR 4d and to increase in SBR 2d (Figure 2.3 A). It was hypothesised that those differences in the $Y_{PHA/SFP}$ could be related with the abundance of PHA-storing bacteria selected at each condition. In fact, as shown in Figure 2.3 B, the $Y_{PHA/SFP}$ trends seem to be directly related with the enrichment of the culture in putative PHA-storers indicating that, independently of the OLR and SRT, an efficient microbial selection seems to be the driving force to obtain a high storage yield. If a deeper characterization of the microbial population is required, it is recommended to analyse the PHA synthase gene to effectively determine the abundance of PHA-storing organisms and validate this hypothesis.

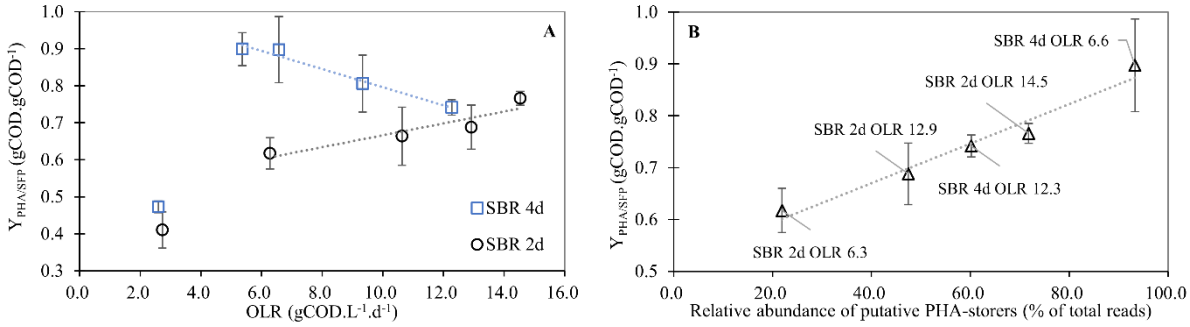

Figure 2.3 – Storage yields ($Y_{PHA/SFP}$) as a function of (A) the different OLR values applied and (B) the relative abundance of known putative PHA-storers, determined in the SBR 4d and SBR 2d.

The genus *Paracoccus* significantly dominated the MMC at SBR 4d (see Table A1 in Appendix A), however as the OLR increased beyond 6.6 $gCOD.L^{-1}.d^{-1}$ a sudden decrease in the abundance of *Paracoccus* was observed. *Paracoccus* growth has previously been reported to be potential inhibited by high OLR values (Wen et al., 2018), which may have happened in this case. Additionally, a substrate inhibition period observed at this phase (as further discussed below) may have given the opportunity of flanking populations to thrive, making the relative abundance of putative PHA-storers to significantly decrease from the 93.3% to 60.2% at the maximum OLR (Table 2.4). For the SBR 2d the increasing OLR favoured the growth of other putative PHA-storers, which may not have been as susceptible to substrate inhibition (Table 2.4).

The highest relative abundance of putative PHA-storers (93.3%) and high storage yield (0.90 $gCOD.gCOD^{-1}$) were observed for the SBR 4d operated at 6.6 $gCOD.L^{-1}.d^{-1}$ (Figure 2.3 B). This value was quite high when compared with studies where the coupled feeding approach was used. For example, Moretto et al. (2020), who studied the effect of SRT using the coupled strategy, obtained a maximum abundance of putative PHA-storers of only 64% using an SRT of 1 d and an OLR of 4.0 $gCOD.L^{-1}.d^{-1}$. This demonstrates that, as expected, the uncoupled strategy in this study worked as an effective measure to increase the selective pressure to enrich for PHA-accumulating organisms.

In the current work, the two C-uptake mechanisms (storage and growth) are separated and use different carbon sources (SFP and stored PHA, respectively), thus the $Y_{PHA/SFP}$ was maximal for each operating condition and was only dependent on the relative abundance of putative PHA-storers. This response differs from the cultures fed with the coupled strategy in which $Y_{PHA/SFP}$ is conditioned by either the PHA-storers abundance or the growth kinetics. For instance, in SBR 4d at OLR 12.3 $gCOD.L^{-1}.h^{-1}$, 60.2% of the enriched community was comprised of putative PHA-storers (Table 2.4), a value that was very similar to that obtained by Moretto et al. (2020) for their best-case scenario (64% of putative PHA-storers for an SRT of 1 d and OLR of 4.0 $gCOD.L^{-1}.d^{-1}$). However, the $Y_{PHA/SFP}$ obtained in the current study was substantially higher (0.74 $gCOD.gCOD^{-1}$, Table 2.2, vs 0.46 $gCOD.gCOD^{-1}$, Moretto et al. (2020)), likely because in the latter study, growth and storage occurred simultaneously at the expense of the external carbon feed, decreasing its availability for storage.

The storage rates trends were also highly affected by the OLR (Figure 2.4 A). The q_{PHA} in SBR 4d were initially more than 3-fold higher than in SBR 2d, although from OLR 6.6 gCOD.L^{-1}.d^{-1} onwards the q_{PHA} tended to decrease in the SBR 4d and to increase in SBR 2d, converging to similar values (Figure 2.4 A).

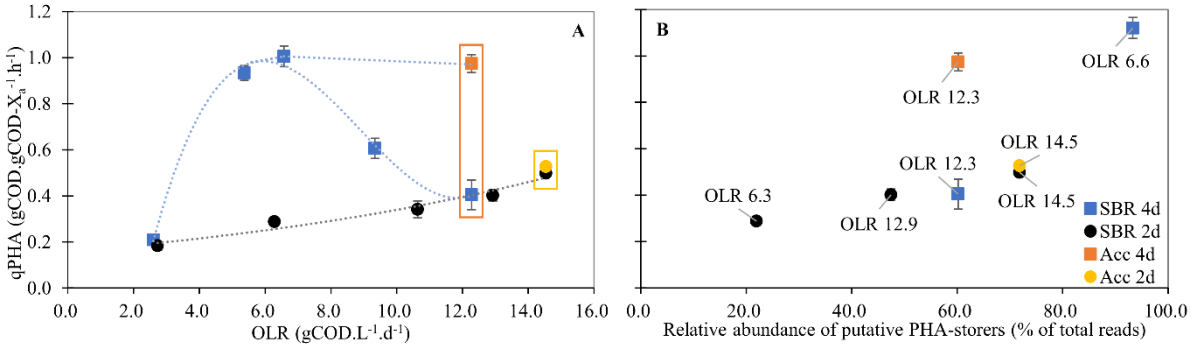

Figure 2.4 - Specific storage rates (q_{PHA}) obtained in the SBRs and accumulation assays as a function of (A) the different OLR values applied in SBRs and (B) the relative abundance of known putative PHA-storers of the cultures selected at the different OLRs in SBR 4d and SBR 2d. The orange and yellow rectangles highlight q_{PHA} obtained for the same culture inoculated in the SBR and Acc reactors.

The decreased q_{PHA} observed in SBR 4d seemed to be a clear consequence of substrate inhibition rather than the result of culture selection. This hypothesis is validated by the results obtained in the accumulation reactor Acc 4d (Figure 2.4 B), in which a lower SFP concentration was applied (SFP in the reactor of 3.80 gCOD.L^{-1}, Table 2.3), similar to the one imposed when the maximum q_{PHA} was observed (OLR 6.6 gCOD.L^{-1}.d^{-1}, which corresponds to a SFP concentration in the reactor of 3.3 gCOD.L^{-1}). It was found that the SBR 4d culture selected at OLR 12.3 gCOD.L^{-1}.d^{-1}, and then used as inoculum in Acc 4d, showed a q_{PHA} value similar to that maximum obtained for the OLR 6.6 gCOD.L^{-1}.d^{-1} (Figure 2.4 A – orange rectangle). This result indicates that higher q_{PHA} could also be achieved by the culture selected at the maximum OLR when no substrate inhibition conditions are applied, as occurred in Acc 4d.

Interestingly, the inhibition effect was not observed for the SBR 2d. As shown in Figure 2.4 A (yellow rectangle) the culture selected at the maximum OLR in SBR 2d showed similar q_{PHA} values when inoculated in Acc 2d at a lower SFP concentrations (7.25 gCOD.L^{-1} in SBR 2d and 4.43 gCOD.L^{-1} in Acc 2d – Table 2.3). Additionally, the q_{PHA} increased with the OLR throughout the whole experiment, suggesting that, when using the uncoupled strategy, cultures selected at lower SRT are less sensitive to high SFP concentrations. In sum, comparing the real q_{PHA} (i.e., when no substrate inhibition is observed) of the cultures selected at the different SRTs it is possible to conclude that, regardless of the amount of putative PHA-accumulators, the cultures selected at the highest SRT (SBR 4d) had faster intrinsic storage kinetics at all OLRs tested (Figure 2.4 B).

When the coupled feeding strategy is used, the growth kinetics of a PHA-producing MMC is favoured at lower SRT for both carbon and nitrogen limited cultures. However, the cultures selected

under nitrogen limited conditions always showed higher ammonia uptake rates than the carbon limited ones, independently on the SRT used (Johnson et al., 2010). Regarding the storage mechanism, Johnson et al. (2010) did not report detailed measurements on the specific storage rates obtained in the accumulation assays. Thus, no clear correlation was made between the operating condition imposed in the SBR (different SRT and/or type of limitation) and the intrinsic storage kinetics of the culture (i.e., when the selected MMC is subjected to C excess under nutrient-limiting conditions to ensure no competition between growth and storage). From the best of the authors knowledge, there are no other studies in the literature that allow to infer about the relationship between the culture intrinsic growth and storage behaviour and the selection SRT. Lemos et al. (2008) studied the SRT on nitrogen-limited cultures but also did not report detailed data of accumulation assays. On the other hand, Chen et al. (2017) reported the accumulation measurements, but did not specify the type of limitation at which the cultures were being selected, making impossible to compare their growth behaviour. Lastly, Moretto et al. (2020) also did not show the type of selection limitation and neither kinetic results obtained in accumulation assays under nutrient-limiting conditions.

When operating under the uncoupled feeding approach, there is no competition between the growth and storage mechanism. Thus, it can be assumed that the culture growth and storage intrinsic responses are driven only by the applied SRT, which physically selects PHA-storers with distinct abilities. Higher SRTs favoured the growth of organisms that have a high affinity towards the external substrate and faster storage kinetics. In contrast, applying a lower SRT favoured the selection of populations which are characterised by having higher maximum specific growth rates and lower storage rates.

2.4.2 Impact of the operational conditions on PHA production process

The physiochemical properties of PHA are highly influenced by the monomeric composition and M_w (Lorini et al., 2020b; Philip et al., 2007). In current work, the polymer 3-HV monomeric production varied linearly with the fraction of 3-HV precursors (propionate and valerate) in the feed, for all the SBR and accumulation assays (see Figure A2 in Appendix A). Additionally, no significant differences were observed within the linear correlations obtained for the two cultures selected at the different SRTs (Figure A2 in Appendix A), and the polymers obtained in the accumulation assays had similar M_w and PDI (Table 2.3) indicating that similar polymers can be produced with different selected cultures. The M_w observed (451 and 453 kDa, respectively for the polymers produced in Acc 4d and Acc 2d) was in the same order of magnitude than those reported in previous studies for commercial PHA produced from pure cultures (200 – 660 kDa) and for PHA produced from MMCs and waste-based feedstocks (220 – 650 kDa) (Albuquerque et al., 2011; Duque et al., 2014; Lorini et al., 2020b). A polymer with a M_w higher than 400 KDa and with a 3-HV monomeric composition between 7% and 20% (w/w), which was the case of the polymers obtained within this work, is considered to have good mechanical properties, lower melting temperature, increased flexibility and enhanced gas barrier properties when compared

with pure PHB, making it suitable e.g., for food packaging applications (Lorini et al., 2020b; Philip et al., 2007).

The global productivity of the PHA process can be used as indicator of overall performance. It can be calculated considering the biomass volumetric productivity (P_X) in the SBR and the maximum culture accumulation capacity in accumulation assays, thus reflecting the balance achieved between the growth and storage response. As expected, the P_X evolution was very responsive to the OLR in both SBR 4d and SBR 2d. For each OLR, the SRT did not impact the biomass productivity (Figure 2.5).

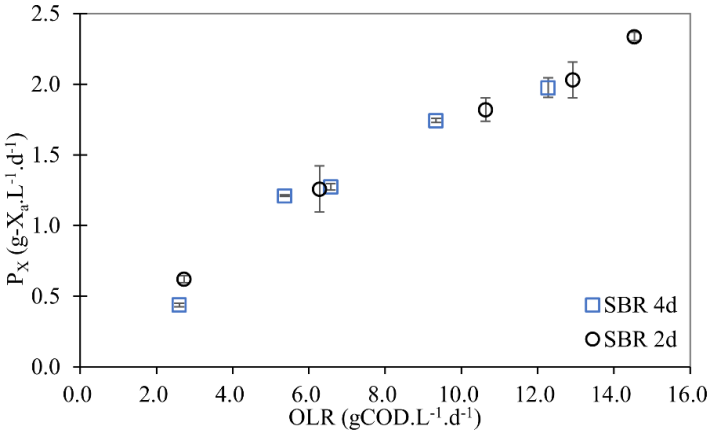

Figure 2.5 – Influence of the OLR values in the biomass volumetric productivity (P_X) obtained for the SBR 4d and SBR 2d.

On the other hand, despite the higher relative abundance of putative PHA-storers in SBR 2d at the maximum OLR tested (Table 2.4), this culture had inferior PHA accumulation capacity. At the end of the Acc 2d, the MMC was only capable to accumulate a maximum amount of 49.2% ± 0.4% (w/w) of PHA, contrasting with the 69% ± 2% (w/w) obtained for Acc 4d (Table 2.3). This behaviour seemed to be an intrinsic limitation associated to the microbial composition, confirming that in fact the culture selected in SBR 2d had a lower storage capability than the one selected at 4 d of SRT. Although the P_X was similar for both cultures, the superior accumulation capability of the culture selected at SRT 4 d greatly increased the global PHA productivity, which was almost 80% higher for the SBR 4d culture (4.6 ± 0.3 $g.L^{-1}.d^{-1}$) than for SBR 2d (2.6 ± 0.2 $g.L^{-1}.d^{-1}$). The process productivity has a high impact on the operating and investment costs, therefore it can be anticipated that the final PHA manufacturing cost will be lower for the higher SRT, demonstrating the potential of using the SRT in combination with OLR as tuning design parameters to increase the MMC PHA-process viability. Lorini et al. (2020a) operated a SBR system similar to the SBR 4d in this study in terms of OLR (12.725 gCOD. $L^{-1}.d^{-1}$) and C, N feeding strategy, although at different SRT (1 d). This study reported a PHA productivity of 2.4 ± 0.1 $g.L^{-1}.d^{-1}$ as a result of the lower PHA accumulation capacity of the culture (53% ± 3%, w/w), which may have been a consequence of the low SRT imposed.

It should also be noted that a period of substrate inhibition in SBR 4d may have affected the selection of PHA-storers. So, it can be hypothesised that, if this substrate inhibition could have been avoided, thus maintaining the PHA-storers relative abundance, an even higher global PHA productivity could have been reached using the SRT of 4d and the high OLR tested. To avoid this substrate inhibition, continuous or fed batch SBR feeding should be studied in order to assess the consequent impact on the overall process performance (maximum accumulation capacity and global storage yield and productivity).

The work herein discussed underlines the importance of in-depth understanding the impact of the SRT and OLR on the culture performance (growth/storage kinetics and accumulation capacity) to further optimising the PHA production process increasing its viability.

2.5 Conclusions and prospects

This work assesses, for the first time, the impact of the SRT and the OLR on the growth and storage dynamics of PHA-storers selected under uncoupled C and N availabilities.

The OLR works essentially as a means to increase the biomass productivity, which is similar for each OLR regardless the SRT. A maximum biomass productivity of 2.3 $g\text{-}X_a.L^{-1}.d^{-1}$ was achieved in this study. Both tested SRTs seemed to result in highly enriched PHA-accumulating cultures but the higher-SRT culture was more easily inhibited by high substrate concentrations. However, this culture had faster storage kinetics (83% faster) and enhanced accumulation capacity (40% higher), resulting in a global PHA productivity almost 80% above that observed for the lower-SRT community.

The study herein presented opens the possibility of, when using a nutrient-deficient substrate that allows the implementation of an uncoupled feeding strategy, maximising the process performance by tuning the SRT of the selection reactor in combination with the OLR applied.

2.6 References

Albuquerque, M.G.E., Eiroa, M., Torres, C., Nunes, B.R., Reis, M.A.M., 2007. Strategies for the development of a side stream process for polyhydroxyalkanoate (PHA) production from sugar cane molasses. J. Biotechnol. 130, 411–421. https://doi.org/10.1016/j.jbiotec.2007.05.011

Albuquerque, M.G.E., Martino, V., Pollet, E., Avérous, L., Reis, M.A.M., 2011. Mixed culture polyhydroxyalkanoate (PHA) production from volatile fatty acid (VFA)-rich streams: Effect of substrate composition and feeding regime on PHA productivity, composition and properties. J. Biotechnol. https://doi.org/10.1016/j.jbiotec.2010.10.070

APHA, 1998. Standard Methods for Examination of Water and Wastewater, 20th ed, American Public Health Association, Washington, DC.

Argiz, L., González-Cabaleiro, R., Val del Río, Á., González-López, J., Mosquera-Corral, A., 2021. A

novel strategy for triacylglycerides and polyhydroxyalkanoates production using waste lipids. Sci. Total Environ. 763, 142944. https://doi.org/10.1016/j.scitotenv.2020.142944

Campanari, S., Augelletti, F., Rossetti, S., Sciubba, F., Villano, M., Majone, M., 2017. Enhancing a multi-stage process for olive oil mill wastewater valorization towards polyhydroxyalkanoates and biogas production. Chem. Eng. J. 317, 280–289. https://doi.org/10.1016/j.cej.2017.02.094

Chen, Z., Huang, L., Wen, Q., Zhang, H., Guo, Z., 2017. Effects of sludge retention time, carbon and initial biomass concentrations on selection process: From activated sludge to polyhydroxyalkanoate accumulating cultures. J. Environ. Sci. (China) 52, 76–84. https://doi.org/10.1016/j.jes.2016.03.014

De Donno Novelli, L., Moreno Sayavedra, S., Rene, E.R., 2021. Polyhydroxyalkanoate (PHA) production via resource recovery from industrial waste streams: A review of techniques and perspectives. Bioresour. Technol. 331, 124985. https://doi.org/10.1016/j.biortech.2021.124985

Duque, A.F., Oliveira, C.S.S., Carmo, I.T.D., Gouveia, A.R., Pardelha, F., Ramos, A.M., Reis, M.A.M., 2014. Response of a three-stage process for PHA production by mixed microbial cultures to feedstock shift: Impact on polymer composition. N. Biotechnol. 31, 276–288. https://doi.org/10.1016/j.nbt.2013.10.010

European Bioplastics, 2020. Bioplastics market data [WWW Document]. URL https://www.european-bioplastics.org/market/ (accessed 5.7.21).

Geyer, R., Jambeck, J.R., Law, K.L., 2017. Production, use, and fate of all plastics ever made. Sci. Adv. 3, e1700782. https://doi.org/10.1126/sciadv.1700782

Johnson, K., Kleerebezem, R., van Loosdrecht, M.C.M., 2010. Influence of the C/N ratio on the performance of polyhydroxybutyrate (PHB) producing sequencing batch reactors at short SRTs. Water Res. https://doi.org/10.1016/j.watres.2009.12.031

Kumar, M., Ghosh, P., Khosla, K., Thakur, I.S., 2018. Recovery of polyhydroxyalkanoates from municipal secondary wastewater sludge. Bioresour. Technol. 255, 111–115. https://doi.org/10.1016/j.biortech.2018.01.031

Kumar, M., Rathour, R., Singh, R., Sun, Y., Pandey, A., Gnansounou, E., Andrew Lin, K.-Y., Tsang, D.C.W., Thakur, I.S., 2020. Bacterial polyhydroxyalkanoates: Opportunities, challenges, and prospects. J. Clean. Prod. 263, 121500. https://doi.org/10.1016/j.jclepro.2020.121500

Lanham, A.B., Ricardo, A.R., Albuquerque, M.G.E., Pardelha, F., Carvalheira, M., Coma, M., Fradinho, J., Carvalho, G., Oehmen, A., Reis, M.A.M., 2013. Determination of the extraction kinetics for the quantification of polyhydroxyalkanoate monomers in mixed microbial systems. Process Biochem. https://doi.org/10.1016/j.procbio.2013.07.023

Legendre, P., Gallagher, E.D., 2001. Ecologically meaningful transformations for ordination of species data. Oecologia. https://doi.org/10.1007/s004420100716

Lemos, P.C., Levantesi, C., Serafim, L.S., Rossetti, S., Reis, M.A.M., Tandoi, V., 2008. Microbial characterisation of polyhydroxyalkanoates storing populations selected under different operating

conditions using a cell-sorting RT-PCR approach. Appl. Microbiol. Biotechnol. https://doi.org/10.1007/s00253-007-1301-5

Lorini, L., di Re, F., Majone, M., Valentino, F., 2020a. High rate selection of PHA accumulating mixed cultures in Sequencing Batch Reactors with uncoupled carbon and nitrogen feeding. N. Biotechnol. https://doi.org/10.1016/j.nbt.2020.01.006

Lorini, L., Martinelli, A., Pavan, P., Majone, M., Valentino, F., 2020b. Downstream processing and characterization of polyhydroxyalkanoates (PHAs) produced by mixed microbial culture (MMC) and organic urban waste as substrate. Biomass Convers. Biorefinery. https://doi.org/10.1007/s13399-020-00788-w

Mannina, G., Presti, D., Montiel-Jarillo, G., Carrera, J., Suárez-Ojeda, M.E., 2020. Recovery of polyhydroxyalkanoates (PHAs) from wastewater: A review. Bioresour. Technol. 297, 122478. https://doi.org/10.1016/j.biortech.2019.122478

Markets and Markets, 2021. Polyhydroxyalkanoate (PHA) Market by Type (Short Chain Length, Medium Chain Length), Production Method (Sugar Fermentation, Vegetable Oil Fermentation, Methane Fermentation), Application, and Region - Global Forecast to 2025 [WWW Document]. URL https://www.marketsandmarkets.com/Market-Reports/pha-market-395.html (accessed 4.29.21).

Moretto, G., Lorini, L., Pavan, P., Crognale, S., Tonanzi, B., Rossetti, S., Majone, M., Valentino, F., 2020. Biopolymers from urban organic waste: Influence of the solid retention time to cycle length ratio in the enrichment of a Mixed Microbial Culture (MMC). ACS Sustain. Chem. Eng. https://doi.org/10.1021/acssuschemeng.0c04980

Oliveira, C.S.S., Silva, C.E., Carvalho, G., Reis, M.A., 2017. Strategies for efficiently selecting PHA producing mixed microbial cultures using complex feedstocks: Feast and famine regime and uncoupled carbon and nitrogen availabilities. N. Biotechnol. 37, 69–79. https://doi.org/10.1016/j.nbt.2016.10.008

Pereira, J.R., Araújo, D., Marques, A.C., Neves, L.A., Grandfils, C., Sevrin, C., Alves, V.D., Fortunato, E., Reis, M.A.M., Freitas, F., 2019. Demonstration of the adhesive properties of the medium-chain-length polyhydroxyalkanoate produced by Pseudomonas chlororaphis subsp. aurantiaca from glycerol. Int. J. Biol. Macromol. https://doi.org/10.1016/j.ijbiomac.2018.09.064

Philip, S., Keshavarz, T., Roy, I., 2007. Polyhydroxyalkanoates: Biodegradable polymers with a range of applications. J. Chem. Technol. Biotechnol. https://doi.org/10.1002/jctb.1667

Plastics Europe, 2020. Plastics – the Facts 2020 [WWW Document]. URL https://www.plasticseurope.org/en/resources/publications/4312-plastics-facts-2020 (accessed 5.7.21).

Reis, M., Albuquerque, M., Villano, M., Majone, M., 2011. Mixed Culture Processes for Polyhydroxyalkanoate Production from Agro-Industrial Surplus/Wastes as Feedstocks, Second Edi. ed, Comprehensive Biotechnology, Second Edition. Elsevier B.V.

https://doi.org/10.1016/B978-0-08-088504-9.00464-5

Sabapathy, P.C., Devaraj, S., Meixner, K., Anburajan, P., Kathirvel, P., Ravikumar, Y., Zabed, H.M., Qi, X., 2020. Recent developments in Polyhydroxyalkanoates (PHAs) production – A review. Bioresour. Technol. 306, 123132. https://doi.org/10.1016/j.biortech.2020.123132

Serafim, L.S., Lemos, P.C., Oliveira, R., Reis, M.A.M., 2004. Optimization of polyhydroxybutyrate production by mixed cultures submitted to aerobic dynamic feeding conditions. Biotechnol. Bioeng. 87, 145–160. https://doi.org/10.1002/bit.20085

Silva, F., Campanari, S., Matteo, S., Valentino, F., Majone, M., Villano, M., 2017. Impact of nitrogen feeding regulation on polyhydroxyalkanoates production by mixed microbial cultures. N. Biotechnol. https://doi.org/10.1016/j.nbt.2016.07.013

Valentino, F., Morgan-Sagastume, F., Campanari, S., Villano, M., Werker, A., Majone, M., 2017. Carbon recovery from wastewater through bioconversion into biodegradable polymers. N. Biotechnol. 37, 9–23. https://doi.org/10.1016/j.nbt.2016.05.007

Wen, Q., Ji, Y., Hao, Y., Huang, L., Chen, Z., Sposob, M., 2018. Effect of sodium chloride on polyhydroxyalkanoate production from food waste fermentation leachate under different organic loading rate. Bioresour. Technol. https://doi.org/10.1016/j.biortech.2018.07.036

3

COMBINED STRATEGIES TO BOOST POLYHYDROXYALKANOATE PRODUCTION FROM FRUIT WASTE IN A 3-STAGE PILOT PLANT

SUMMARY:

The full-scale implementation of polyhydroxyalkanoates (PHA) production using mixed microbial cultures (MMC) has been limited by the low PHA global productivity and overall process yield. This work aimed to demonstrate, at pilot scale, that combining different effective operating conditions it is possible to boost the PHA production performance when using fruit waste as substrate. The organic loading rate (OLR) and pH of the acidogenic reactor were successfully used as tuning parameters to obtain a high fermentation yield (0.74 gCOD.gCOD^{-1}) and a fermentate rich in butyrate, resulting in enhanced PHA production steps. A biomass highly enriched in PHA-storing microorganisms was selected as a result of uncoupling the carbon to the nitrogen feeding. The biomass concentration attained a notable value (7.83 g.L^{-1}) as a response to the high OLR (8.7 gCOD.L^{-1}.d^{-1}) imposed. In the PHA accumulation assays, the culture selected at the optimal OLR in the selection reactor achieved a high storage yield (0.98 gCOD.gCOD^{-1}), and the continuous feeding strategy led to a maximum PHA content of 80.5% (g-basis). The high global productivity (8.1 g-PHA.L^{-1}.d^{-1}) and overall process yield (0.45 gCOD.gCOD^{-1}) are, to the best of authors knowledge, the highest values reported for MMC using a real feedstocks at pilot scale. These results demonstrate the importance of combining different effective strategies to maximise the process performance, a promising result towards the full-scale implementation of PHA production from wastes and MMC.

KEYWORDS:

Polyhydroxyalkanoate (PHA); Mixed microbial cultures (MMC); Fruit waste (FW); Pilot plant; Acidogenic fermentation; Butyrate.

PUBLISHED AS: Matos, M., Cruz, R.A.P., Cardoso, P., Silva, F., Freitas, E.B., Carvalho, G., Reis, M.A.M., 2021. Combined Strategies to Boost Polyhydroxyalkanoate Production from Fruit Waste in a Three-Stage Pilot Plant. ACS Sustain. Chem. Eng. acssuschemeng.1c02432. https://doi.org/10.1021/acssuschemeng.1c02432

3.1 Introduction

The search for novel materials to replace synthetic petroleum-based polymers has been encouraged by a growing environmental awareness and the adoption of stricter legislation measures on plastic usage, fostering a transition towards a circular economy. Polyhydroxyalkanoates (PHA) have drawn significant attention as one of the most promising biopolymers. In particular, the copolymer poly(3-hydroxybutyrate-co-3-hydroxyvalerate) – P(3HB-co-3HV) – is very interesting not only due to its biocompatible and biodegradable character (Dietrich et al., 2017), but also to its exceptional thermal and mechanical properties, which are similar to synthetic polyesters (Reis et al., 2011).

Up to date, PHA exploitation has been limited by high manufacturing costs and consequent uncompetitive market price (2.2 to 5.0 €/Kg) when compared with the petroleum-based plastic (less than 1.0 €/Kg) (Valentino et al., 2017). Commercial PHA is produced using pure cultures of wild or engineered strains usually fed with defined substrates which account for 30-50% of the total production costs (Pérez et al., 2020). Over the past 20 years, an alternative process has been developed based on mixed microbial cultures (MMC) and carbon-rich wastes/by-products, providing simultaneously a means of reducing the overall operational costs and contributing to the implementation of a circular economy approach (Mannina et al., 2020; Valentino et al., 2017). The MMC process usually comprises three stages: (1) the acidogenic fermentation, to convert organic carbon into soluble fermentation products (SFP) that are precursors for PHA biosynthesis; (2) the selection of a PHA-producing enriched culture; and (3) the PHA accumulation, where the previously selected culture is fed with the SFP and accumulate PHA up to its maximum capacity (Reis et al., 2011).

The PHA producing process using MMC was recently implemented at pilot-scale (Moretto et al., 2020; Tamis et al., 2018; Valentino et al., 2019, 2018). However, the low global volumetric productivity obtained is considered as one of the major constraints for full-scale application, given the great impact of the capital costs on the polymer end-price (Valentino et al., 2017). Techno-economic analyses have indicated that other critical parameters to be maximised in order to increase the viability of the process are the overall PHA yield, to minimise the waste of resources, and the PHA content on biomass at the end of production, to reduce extraction costs (Moretto et al., 2020; Valentino et al., 2017). Lastly, the recovery and purification of the polymer is a time-consuming process, known to require large amounts of chemicals that also contribute significantly to increase the overall manufacturing costs of the product (Pérez-Rivero et al., 2019).

Several individual factors have been found to contribute to improve the global process performance. First, it is important to maximise the fermentation yield and to obtain a highly concentrated SFP stream, to reduce the reactor volumes and energy requirements associated with pumping and mixing needed in the subsequent steps. Previous research has also indicated that it is beneficial to direct the acidogenic fermentation towards a bioprecursors profile that enhances the PHA producing rate and yield. For

example, butyrate (HBut) has been indicated as a preferred substrate for PHA production since it is more energetically favourable at a metabolic level than other SFP (Kourmentza and Kornaros, 2016; Marang et al., 2013).

Regarding the culture selection stage, optimal performance encompasses an adequate selection of microorganisms with high storage capability and high growth rate, as both contribute to increase the global PHA volumetric productivity (Dionisi et al., 2006; Fra-Vázquez et al., 2020). It is well known that a PHA-storing bacterial enrichment can be achieved using alternating feast and famine operation conditions (Reis et al., 2011). High values of biomass productivity are usually obtained for higher organic loading rates (OLR), but increasing the OLR above a certain threshold extends the feast phase to a point where flanking, non-storing populations, overcome their internal metabolic limitations and start to grow. Therefore, high OLR may result in a reduction of specific storage rates and storage yields, particularly when using complex feedstocks as substrate (Albuquerque et al., 2010b; Campanari et al., 2014). The strategy of uncoupling the carbon to the nitrogen feeding was demonstrated to enhance the selective pressure, as well as culture performance and stability when using high OLR values (Carvalho et al., 2018; Lorini et al., 2020a). Moreover, this strategy is useful to ensure that the biomass uses stored PHA as carbon source for growth instead of external SFP, increasing the PHA storage yield obtained in the selection reactor (Oliveira et al., 2017).

As for the accumulation reactor, a key opportunity lays on the feeding strategy, as the conventional pulse-wise method usually leads to polymer consumption in between pulses, decreasing the final PHA content on cells (Albuquerque et al., 2011).

Significant efforts have been done to determine the operational conditions that contribute to achieve each one of the individual objectives above. However, the development of an integrated methodology incorporating those optimal individual conditions has not been attempted before and yet, may be a missing step to make PHA from MMC economically competitive.

This work investigated the combined effect of different effective strategies towards maximising the overall PHA production efficiency from fruit waste (FW) in a pilot plant. FW is globally produced in large quantities by the agro-food and urban sectors. The annual losses of fruits and vegetables are the highest among all types of food (up to 60% of production), contributing to several environmental problems (Riccardi et al., 2020; Sagar et al., 2018). The acidogenic reactor operating conditions were manipulated to obtain a high fermentation yield and to produce a highly concentrated SFP stream. Additionally, the PHA bioprecursors' profile was fine-tunned triggering to increase the HBut production (preferred substrate for PHA production) while maintaining a 3-hydroxyvalerate (3-HV) precursors' fraction above 10 % (gCOD-basis). FW is a nitrogen-deficient feedstock which enabled to implement an uncoupled carbon and nitrogen feeding strategy in the selection reactor, and the maximisation of the OLR in this stage. Finally, the accumulation reactor was fed in a continuous mode to make advantage of the maximum accumulation potential of the culture. The impact of this multi-strategy approach was evaluated using as indicators the overall process yield and global productivity obtained.

3.2 Materials and methods

3.2.1 Waste feedstock for PHA production

FW (Sumol+Compal S.A., Portugal) is a carbon-rich residue, that usually ends up being disposed of. The feedstock had low pH (3.9) and high total chemical oxygen demand content (175 ± 13 $gCOD.L^{-1}$), essentially comprised by easily biodegradable compounds (85 % of soluble COD), which are important factors to increase the acidogenic potential. Additionally, it had low ammonia (1.26 ± 0.07 $mg\text{-}N.L^{-1}$) and phosphorus (2.4 ± 0.7 $mg\text{-}P.L^{-1}$) concentrations.

3.2.2 Set-up and operation of the reactors

The FW was fed to an acidogenic reactor (stage 1) that was carried out in a 100 L upflow anaerobic sludge blanket (UASB) reactor. The clarified SFP end-stream was subsequently fed to a 100 L aerobic sequential batch reactor (SBR) for the selection of the PHA-producing culture (stage 2) and to a 60 L aerobic accumulation reactor, where PHA storage was maximised (stage 3). More details about the experimental setup and individual reactor's design can be found in Appendix B.

3.2.2.1 Acidogenic fermentation

The UASB reactor was operated using a working volume of 60 L. The superficial velocity was set at 2.88 $m.h^{-1}$ by means of an internal recirculation, promoting contact between granules and available carbon source. The temperature was kept at 30.0 ± 0.5 °C using an external jacket for cooling water circulation.

Twenty litres of anaerobic granules from a full-scale anaerobic expanded granular sludge bed bioreactor treating brewery wastewater (Leça do Balio, Portugal) were used to inoculate the reactor. After an initial 4-day period, at which the reactor was operated in batch mode, the FW started to be fed continuously at an OLR of 5 $gCOD.L^{-1}.d^{-1}$. The OLR was then gradually increased by reducing the dilution factor (i.e., reducing the amount of tap water added) and the hydraulic retention time (HRT) was set at 1 day. Nitrogen (as NH_4Cl) and Phosphorus (as KH_2PO_4) were added together with the feedstock to maintain the COD:N:P ratio (g-basis) at 100:0.5:0.1, also other minerals were supplied as follow: 120 $mg.L^{-1}$ of $MgSO_4.7H_2O$, 480 $mg.L^{-1}$ of $CaCl_2$ and 0.8 $mg.d^{-1}$ of $FeCl_3.6H_2O$.

The reactor pH was continuously monitored using a pH probe inserted on the reactor lid and manually controlled by adjusting the influent alkalinity through dosing $NaHCO_3$.

The effluent was decanted before being fed to the subsequent reactors to remove the coarse solids which will facilitate the PHA production reactors operation and the polymer extraction/purification.

3.2.2.2 Culture selection reactor

The SBR was inoculated with activated sludge from Mutela WWTP (Almada, Portugal) and operated with an HRT of 1 day and a sludge retention time (SRT) of 4 days, in 12-h cycles. From these 12 h, 0.20 h were used for feeding, 10.88 h for aerated feast and famine (out of which 0.20 h were used once a day for biomass withdrawal at the end of famine), 0.75 h for settling and 0.17 h for withdrawal.

The clarified fermented feedstock from UASB was diluted using a mineral nutrient solution as described by Serafim et al. 2004 to adjust the reactor OLR at final targeted values (1.7, 2.4, 3.4, 5.4 and 8.7 $gCOD.L^{-1}.d^{-1}$). The dilution ratio of the fermentation liquid was on average 1:11.6, 1:7.9, 1:5.3, 1:3 and 1:1.4, respectively for each tested OLR. The OLR increments were imposed whenever the feast to famine length (FF) ratio was steady for at least 3 SRT, this 3 SRT period corresponds to the pseudo steady state for each OLR tested.

A solution containing Nitrogen and Phosphorus was fed after 2 h of cycle starting. The C:N:P ratio was kept at 100:7:1(mol-basis) (Silva et al., 2017).

The reactor was operated at room temperature, stirred at 400 rpm and aeration was provided to keep the dissolved oxygen (DO) above non-oxygen-limiting conditions ($DO>2\ mg\text{-}O_2.L^{-1}$). The SBR working sequence was automatically controlled by DO.

The sharp increase in DO profile allowed to identify the end of feast phase.

3.2.2.3 Maximum accumulation potential (MAP) tests

The culture MAP was assessed in fed-batch accumulation assays (in duplicate) operated at room temperature. Aeration was provided at 60 $L_{air}.L_{reactor}^{-1}.h^{-1}$, agitation speed was set at 600 rpm. pH and DO were controlled through on-line sensors.

Reactor containing 25 L of biomass purged from SBR at the end of famine phase was fed with SFP without nutrient supplementation. The reactors were operated under pH-stat mode, where the SFP stream was continuously supplied as acid solution to control the reactor-set pH at 8.5. The MAP test was finalised after 5 h of experiment.

3.2.3 Analytical methods

The COD was assessed using LCK 914 Hach Lange kits (Hach-Lange, Germany).

The concentration of the SFP, ammonium and phosphate, active biomass and PHA were determined as described by Oliveira et al. 2017.

The biogas composition (H_2, N_2, O_2, CH_4 and CO_2) was determined as described by Carvalheira et al. 2018.

The molecular mass distribution of the produced polymer was characterized by size exclusion chromatography (SEC) as described by Pereira et al. 2019.

A detailed explanation of the methods is given in Appendix B.

3.2.4 Microbiological analyses

Microbiological analyses were conducted as described by Wang et al. 2017. More details can be found in Appendix B.

3.2.5 Calculations

The fermentation yield ($Y_{SFP/FW}$, gCOD-SFP.gCOD-FW^{-1}) was calculated by dividing the SFP concentration observed in the reactor end-stream by the difference between the total chemical oxygen demand and the SFP concentration measured in the influent FW.

Parameters from SBR and accumulation reactors were calculated as indicated by Oliveira et al. 2017. Exception was made for the growth yields on PHA ($Y_{X/PHA}$, gCOD-X_a.gCOD-PHA^{-1}) which were calculated by dividing active biomass formed by total amount of PHA consumed. Detailed explanations can be found in Appendix B.

The assumed COD conversion factors are detailed in Appendix B.

3.3 Results and discussion

3.3.1 Acidogenic reactor performance: impact of OLR and pH

The UASB reactor was operated in continuous mode for more than 250 days. The operating conditions of the reactor were adjusted along operation to: i) obtain a high yield of SFP on substrate, minimising fermentable carbon losses through the effluent; ii) obtain a highly concentrated SFP end-stream, reducing reactor volumes and energy requirements related with pumping and mixing needed in the PHA production steps; iii) direct the fermentation towards obtaining majorly HBut, since HBut is known to require less energy per carbon-mole for transmembrane transport than smaller SFP, thus conducing to higher PHA conversion yields (Kourmentza and Kornaros, 2016; Marang et al., 2013).

Simultaneously, fermentation targeted a 3-HV precursors (propionate, HPro, and valerate, HVal) (Reis et al., 2011) concentration above 10 % (gCOD-basis) to ensure a desired level of elasticity to the final product. OLR together with pH were used as tuning parameters to achieve the above objectives (Lee et al., 2014).

The reactor was inoculated with granules from a methanogenic reactor aiming at minimizing the long start-up periods associated to granulation processes (Lee et al., 2014). In order to inhibit the methanogenic activity and enrich the biomass in acidogenic bacteria, the reactor was initially operated at low pH (below 4.40) (Figure 3.1 A). No methane was detected in the gas outflow from day 41 of operation onwards, the first 37 days of reactor operation (start-up phase) were considered a period of instability and should not be used as comparison with the following days of operation.

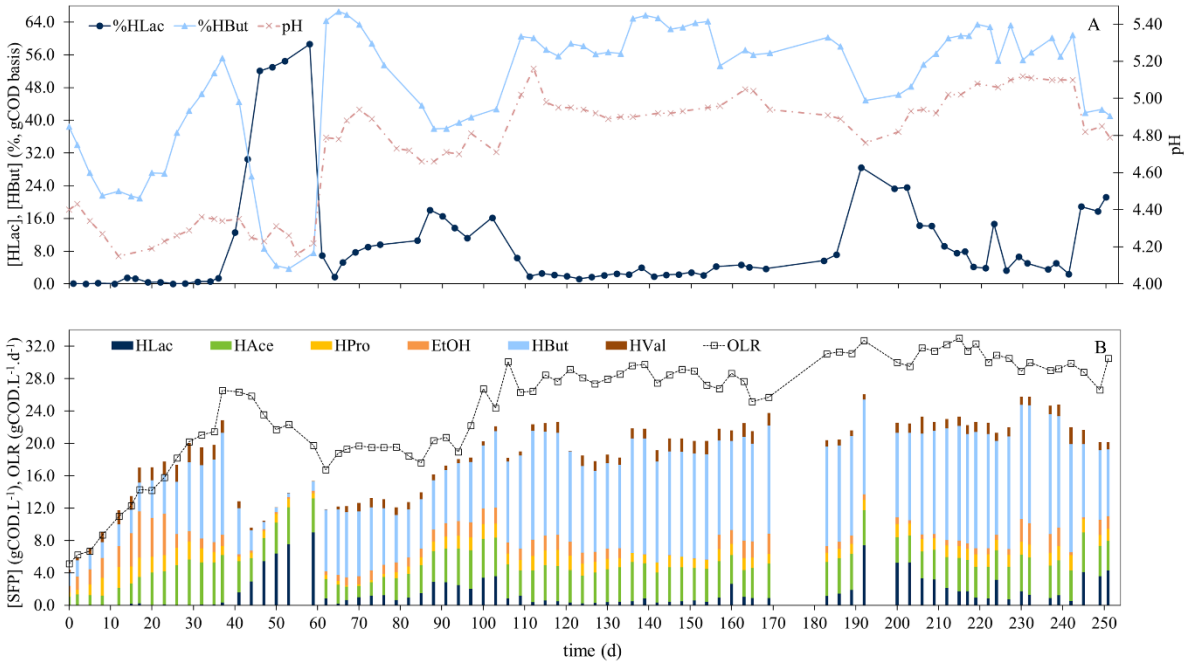

Figure 3.1 – Profiles of OLR, pH and SFP in the UASB reactor using fruit waste as feedstock. (A) pH conditions applied and fraction of produced HLac and HBut, (B) Imposed OLR and effluent SFP profiles.

The OLR was initially set to 5 $gCOD.L^{-1}.d^{-1}$ to avoid substrate inhibition, then it was gradually increased between days 0 - 37 and 86 - 107 at an average rate of 0.5 $gCOD.\ L^{-1}.d^{-1}$ until being stabilised at 29 ± 2 $gCOD.L^{-1}.d^{-1}$ from108 onwards (Figure 3.1 B), this pseudo steady state period was considered in the calculations. The OLR was not further increased due to excessive gas (mostly CO_2 and H_2) production which disturbed the sludge blanket, resulting in deterioration of the granules' integrity and subsequent pipe clogging. Despite this limitation, the maximum OLR imposed was high when compared to maximal values reported with other residues, such as 13.7 $gCOD.L^{-1}.d^{-1}$ for cheese whey (Duque et al., 2014) or 25.7 $gCOD.L^{-1}.d^{-1}$ for fruit pulp waste (Mateus et al., 2020).

During the whole operation period, the acidified end-stream was largely comprised of volatile fatty acids – acetate (HAce), HPro, HBut and HVal – lactate (HLac) and ethanol (EtOH) (Figure 3.1 B). All of the produced SFP have been described in the literature as PHA bioprecursors (Reis et al., 2011).

The initial rapid increase of OLR resulted in a sharp drop of the fermentation yield and a shift between HBut and HLac production (Figure 3.1 A and B, day 41). OLR was decreased in an attempt to stabilise the reactor. Although the acidification degree responded positively, HLac continued to increase up to becoming the dominant SFP (58.6%, gCOD-basis) (Figure 3.1 A, day 60). HLac production is usually described as a consequence of low pH conditions or process disturbances (Duque et al., 2014; Temudo et al., 2007). In fact, during this phase the pH had been set in low values (4.22) to inhibit methanogenic bacteria. The pH was then increased to 4.79 which resulted in the re-establishment of HBut production in detriment of HLac.

Similar disturbances in SFP production were observed in two other periods (from day 88 to 108 and 191 to 203). In both cases, the pH was slightly adjusted resulting in the rapid recovery of the HBut production as major SFP (Figure 3.1 A)

Figure 3.2 shows a linear correlation between the reactor pH (in the range of 4.04 and 4.88) and the fraction of HBut in the total fermented products. pH between 4.88 and 5.18 did not significantly impact on HBut production, which stabilised at 57% ± 4% (gCOD-basis). In another study (data not shown), pH values between 4.70 and 6.30 were tested using the same feedstock, it was observed that above pH 5.20 the HBut fraction tended to decrease reaching a minimum of 42% ± 4% (gCOD-basis).

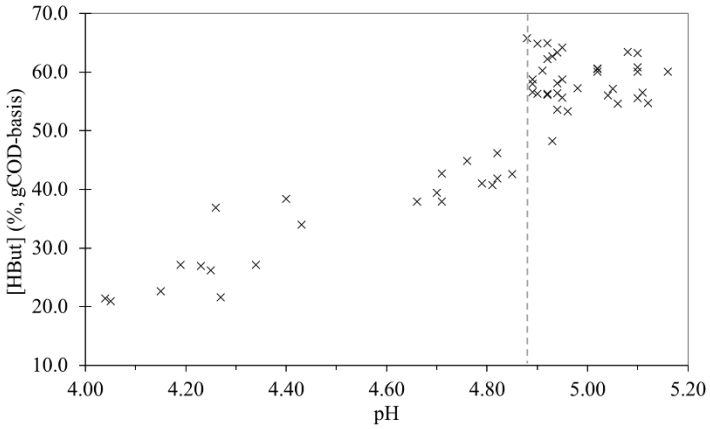

Figure 3.2 – Correlation between pH in the UASB reactor and the fraction of HBut produced (excludes the values obtained for the initial start-up period of 37 days)**.**

During the pseudo steady state periods, the 3-HV precursors fraction was 12% ± 3% (gCOD-basis), meeting the target value (> 10% 3-HV precursors) and, therefore, not compromising the possibility of obtaining a copolymer enriched in 3-HV monomers.

It is evident from Figure 3.1 A that there was a dynamic relationship between HBut and HLac production: when HLac decreases, HBut production increases and vice versa. This suggests that the

acidogenic culture enriched in this study predominantly performed two metabolic pathways: HLac fermentation and HBut fermentation. For the latter it is possible that, besides the direct conversion of sugars to HBut, the HLac is also decomposed to HBut, with simultaneous hydrogen (H_2) and carbon dioxide (CO_2) production (i.e., 2 moles of HLac are converted into 1 mol of HBut, 2 moles of CO_2 and 2 moles of H_2) (Asunis et al., 2019). Similar behaviour was previously observed using other complex feedstock such as maize silage (Sträuber et al., 2012).

For the period of stable performance (between days 108 and 251), the fermentation yield ($Y_{SFP/FW}$) was on average 0.74 ± 0.09 ($gCOD.gCOD^{-1}$). This value is in the same range of those reported for other residues, such as cheese whey (Duque et al., 2014) or fruit pulp waste (Mateus et al., 2020) (0.65-0.74 and 0.54-0.76 on gCOD-basis, respectively). During this period, the SFP profile was largely dominated by HBut (56.8%), followed by HAce (18.4%) and HLac (7.5%) (% gCOD-basis) (Figure 3.1 B and more details in Table B1 in Appendix B). As intended, the SFP concentration was increased up to 22 ± 2 $gCOD.L^{-1}$, which was higher than in other reported acidogenic reactors fed with waste substrates (10.6 $gCOD.L^{-1}$ for cheese whey (Duque et al., 2014), 18.1 $gCOD.L^{-1}$ for fruit pulp waste (Mateus et al., 2020)). This is a big step towards decreasing the capital costs associated with high reactor volumes and the operational costs related with pumping and mixing in the subsequent steps of the process.

The gas outlet had H_2 (77% ± 3%) and CO_2 (16% ± 3%) (% molar-basis) as main constituents (more information of gas composition and productivity in Table B1 in Appendix B).

Results from UASB reactor indicate that the high OLR worked as a means to obtain a highly concentrated SFP stream and that pH adjustments successfully resulted in tailoring the end-stream PHA precursors' profile dominated by HBut while maintaining the target fraction of 3-HV precursors.

3.3.2 Selection reactor

In order to determine the conditions that maximise the enrichment of a PHA-producing culture and biomass volumetric productivity, the selection reactor was operated with different substrate compositions and concentrations.

The applied OLR was initially set at 1.7 $gCOD.L^{-1}.d^{-1}$, then subsequent increased up to 8.7 $gCOD.L^{-1}.d^{-1}$. The performance of the PHA-storing community was characterised before shifting to the following OLR. The composition of the fed SFP varied throughout the operation time (Table 3.1), reflecting the fluctuations observed in the UASB effluent, mainly variation in HLac (0 - 52 %), HAce (21 – 30 %) and HBut (14 - 63%) fractions (% in gCOD-basis).

3.3.2.1 Impact of loading rate in biomass concentration and productivity

It is expected that operation of the selection SBR at higher OLRs conduce to higher biomass concentrations and thus to maximum biomass productivities. However, high OLRs has been previously

reported to cause insufficient selection efficiency and performance instability when using real wastes as feedstock (Albuquerque et al., 2010b; Campanari et al., 2014; Oliveira et al., 2017). In this study, the OLR was increased using an uncoupled carbon and nitrogen feeding strategy, which limits the growth of non-storing organisms until nutrients are externally added, despite the length of feast phase (Oliveira et al., 2017). Results show that FF ratio was consistently below 0.1 throughout the study (Table 3.1), even in periods of instability associated to variations in the feed composition or changes in OLR, indicating a good enrichment in PHA storing organisms (Reis et al., 2011), thus confirming that using the uncoupled carbon and nitrogen feeding strategy, higher OLR can be applied without disturbing the selective pressure of the culture.

The increase in OLR resulted in a remarkable value of active biomass (X_a) concentration (7.8 g-X_a.L^{-1}, Table 3.1) achieved for the highest OLR (8.7 gCOD.L^{-1}.d^{-1}), which, to the best of our knowledge, was the highest value so far obtained in a PHA selection reactor using MMC and waste feedstocks. The biomass volumetric productivity (P_X) (Table 3.1) gradually increased with increasing OLR up to a maximum of 2.0 ± 0.1 g-X_a.L^{-1}.d^{-1}. Other authors (Lorini et al., 2020a; Oliveira et al., 2017) have used uncoupled feeding strategy and high OLR values with the objective of increasing X_a. For example, Lorini et al. 2020a, operated a SBR with a mixture of synthetic HAce and HPro at similar OLR (8.5 gCOD.L^{-1}.d^{-1}) but lower SRT (1 d), which resulted in a very low biomass concentration (1.6 g-X_a.L^{-1}). However, due to the lower SRT used, the biomass productivity (1.6 g-X_a.L^{-1}.d^{-1}) was only slightly lower than that obtained in our study (2.0 ± 0.1 g-X_a.L^{-1}.d^{-1}) with a higher SRT. Though the higher complex composition of FW relatively to the synthetic feedstocks, the current study demonstrated that high biomass productivity values are also possible. This is an impactful result, which brings this process closer to real full-scale implementation.

For the highest OLR, the dilution ratio of the fermentation liquid was substantially decreased from 1:11.6 to 1:1.4 (see section 3.2.2 - Set-up and operation of the reactors). However, the fermented stream still had to be diluted to maintain the HRT of 1 day. Ideally, higher HRT should be further evaluated to decrease as much as possible the working volume of the reactor and consequently the capital and operational costs associated.

Table 3.1 – Operating conditions and performance parameters of the PHA-accumulating mixed culture subjected to different OLR values. Parameters determined for pseudo steady state phases. Values presented are **mean** (standard deviation).

Operating conditions			**Value**		
OLR ($gCOD.L^{-1}.d^{-1}$)	**1.7** (0.2)	**2.4** (0.2)	**3.4** (0.1)	**5.4** (0.2)	**8.7** (0.1)
SFP profile [HLac/HAce/HPro/EtOH/HBut/HVal] (% gCOD-basis)	10/25/9/16/31/8	52/30/8/2/14/1	16/29/8/5/41/4	0/21/8/4/60/6	0/23/5/3/63/5
Operating time (d)	0 – 20	21 – 83	84 – 101	102 – 135	136 – 202
Reactor performance			**Value**		
FF ratio ($h.h^{-1}$)	**0.062** (0.008)	**0.040** (0.007)	**0.039** (0.004)	**0.031** (0.004)	**0.055** (0.006)
X_a ($g.L^{-1}$)	**1.4** (0.1)	**3.1** (0.4)	**4.58** (0.07)	**6.87** (0.09)	**7.8** (0.4)
P_X ($g.L^{-1}.d^{-1}$)	**0.35** (0.04)	**0.8** (0.1)	**1.14** (0.02)	**1.72** (0.02)	**2.0** (0.1)
Δ PHA (%, w/w)	**10.0** (0.4)	**11.1** (0.8)	**12** (3)	**15.4** (0.5)	**19.2** (0.8)
3-HV content (end feast, w/w)	**0.314** (0.001)	**0.17** (0.04)	**0.21** (0.02)	**0.23** (0.01)	**0.19** (0.02)
$-q_{SFP}$ ($gCOD.gCOD\text{-}X_a^{-1}.h^{-1}$)	**0.6** (0.1)	**0.68** (0.02)	**0.8** (0.1)	**1.0** (0.1)	**1.167** (0.005)
q_{PHA} ($gCOD.gCOD\text{-}X_a^{-1}.h^{-1}$)	**0.31** (0.07)	**0.452** (0.007)	**0.648** (0.002)	**0.92** (0.05)	**1.10** (0.01)
$Y_{PHA/SFP}$ ($gCOD.gCOD^{-1}$)	**0.53** (0.01)	**0.70** (0.03)	**0.8** (0.1)	**0.93** (0.04)	**0.95** (0.06)
$Y_{X/PHA}$ ($gCOD.gCOD^{-1}$)	**0.68** (0.06)	**0.76** (0.04)	**0.78** (0.09)	**0.774** (0.003)	**0.79** (0.2)

3.3.2.2 Impact of substrate concentration and profile on substrate uptake and polymer storage

Substrate preferences and culture kinetics are highly dependent on the selected microbial community structure (Albuquerque et al., 2013). Since each MMC obtained is unique, it is of high importance to evaluate how the fed SFP concentration and composition affected the culture performance in each particular case.

Data points were collected from different OLR applied to the SBR reactor, corresponding to a wide range SFP concentrations (total and individual) inside the reactor. The values considered for this analysis corresponded to points where the PHA content on biomass was well below saturation, avoiding any influence of product inhibition on the specific uptake and storage rates.

The effect of total SFP, HAce, HLac and HBut concentration on specific uptake rates can be mathematically described using the Michaelis-Menten (M-M) model (Figure 3.3). HPro, EtOH and HVal were not considered in the individual analysis due to the low concentrations observed for these SFP during the whole operation.

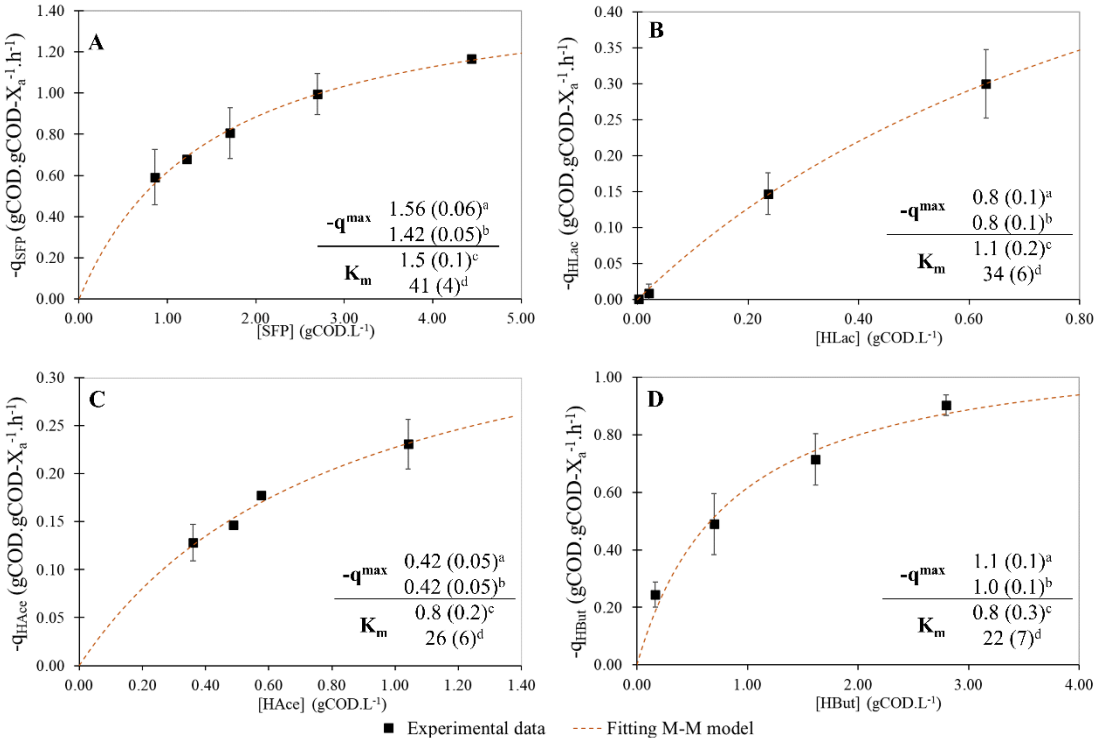

Figure 3.3 – Specific uptake rates of total SFP (A), HLac (B), HAce (C) and HBut (D) as a function of their concentrations in SBR. Estimated mean (standard deviation) values of $-q_{max}$ and K_m for each corresponding substrate are also represented. [a] in gCOD.gCOD-Xa^{-1}.h^{-1}; [b] in Cmol.Cmol-Xa^{-1}.h^{-1}; [c] in gCOD.L^{-1}; [d] in Cmmol.L^{-1}

The specific uptake rate of total SFP and of HBut tended to a maximum at concentrations higher than 2.7 and 1.6 gCOD.L^{-1}, respectively (which correspond to an OLR of 5.4 gCOD.L^{-1}.d^{-1}) (Figure 3.3 A and D). This means that at this OLR the substate concentration in the reactor is not limiting the specific substrate uptake rate (zero order kinetics). The same trend was followed by the specific storage rate (q_{PHA}), which increased from 0.31 gCOD.gCOD-X_a^{-1}.h^{-1} (OLR of 1.7 gCOD.L^{-1}.d^{-1}) to a maximum value of 1.10 gCOD.gCOD-X_a^{-1}.h^{-1} (OLR of 8.7 gCOD.L^{-1}.d^{-1}) (Table 3.1), indicating that OLR above 5.4 gCOD.L^{-1}.d^{-1} (SFP concentration of 2.7 gCOD.L^{-1}) do not result in significant higher q_{PHA}.

From the fitting of the M-M model to the experimental data, the affinity constant (K_m) and maximum specific uptake rates ($-q^{max}$) for total SFP, HLac, HAce and HBut were calculated (Figure 3.3 A - D). The K_m for both total and individual SFP (ranged between 23 and 41 Cmmol.L^{-1}, Figure 3.3 A - D) were significantly higher than typical values used for PHA production modelling, where acetate was used as sole carbon source (varied between 0.0083 and 0.2 Cmmol.L^{-1}) (Dias et al., 2005; Johnson et al., 2009). This may be related with the use of a complex mixture of SFP in this study. The K_m for total SFP (41 Cmmol.L^{-1}) obtained in the current study was also higher than that obtained by Albuquerque et al. 2010a (18 Cmmol.L^{-1}) for fermented molasses. This can be explained by the fact that those authors used the same SFP relative composition during all the experiments contrasting with our case where both SFP relative compositions and concentration changed along operation. Nevertheless, HBut showed the lowest affinity constant among the other SFP (23 Cmmol.L^{-1}).

The highest value of $-q^{max}$ was observed for HBut, followed by HLac and HAce, showing that HBut is the preferred substrate for the selected culture (Figure 3.3 B – D). The value for acetate (0.42 Cmol.Cmol-X_a^{-1}.h^{-1}) was similar to that of Albuquerque et al. 2010a (0.31 Cmol.Cmol-X_a^{-1}.h^{-1}), which may be explained by the fact that the fermented feedstock used in their study was mainly composed by HAce (60% Cmol-basis).

The composition of SFP (namely, the presence of HBut) also impacted on the storage yield ($Y_{PHA/SFP}$). A plot of $Y_{PHA/SFP}$ in function of the HBut fraction show that they are linearly correlated, raising from 0.70 ± 0.03 to 0.95 ± 0.06 (gCOD.$gCOD^{-1}$) when the fraction of HBut increased from 8% to 63% (gCOD-basis) (Figure 3.4). The data used in this correlation were collected from day 42 onwards (2.4 gCOD.L^{-1}.d^{-1} OLR tested) when the community composition was stable and fully enriched in PHA accumulating bacteria (as detailed in Appendix B).

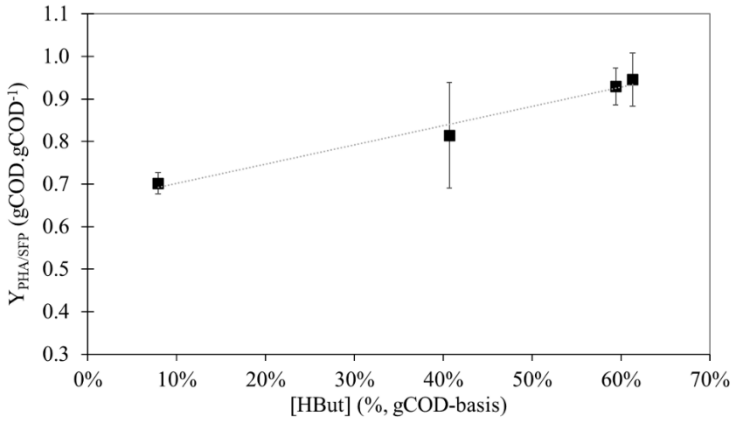

Figure 3.4 – Correlation between butyrate (HBut) fraction observed in SBR and storage yield ($Y_{PHA/SFP}$).

This result can be explained by the fact that HBut consumption is more energetically efficient than other SFP for PHA production (Marang et al., 2013; Wang et al., 2018). The theoretical amount of ATP required for the uptake of 1 Cmol of HBut is 1/2 mol, which is lower than that required for uptake of HAce (1 mol) or HLac (2/3 mol) (Jiang et al., 2011; Wang et al., 2018).

Even though the literature is rich in studies where the strategies used in the current work (uncoupled feeding strategy, high/ideal OLR and high HBut fraction) were tested individually, there is no examples where they were implemented together. Lorini et al. 2020a, Oliveira et al. 2017 and Campanari et al. 2017 used the uncoupled feeding strategy and high OLR values to produce PHA using either synthetic or fermented waste feedstocks. In none of the cases the HBut fraction was greater than 20 % (gCOD-basis). Consequently, the storage rates (0.481 gCOD.gCOD-X_a^{-1}.h^{-1}, 0.24 Cmol.Cmol-X_a^{-1}.h^{-1} and 0.496 gCOD.gCOD-X_a^{-1}.h^{-1}, respectively) and the storage yields (0.57 gCOD.gCOD^{-1}, 0.72 Cmol.Cmol^{-1} and 0.46 gCOD.gCOD^{-1}, respectively) were lower than in our study (0.92 gCOD.gCOD-X_a^{-1}.h^{-1} and 0.93 gCOD.gCOD^{-1} for the ideal OLR 5.4 gCOD.L^{-1}.d^{-1}, Table 3.1). On the other hand, Jiang et al. 2012, which used a real feedstock with 90% (mol-basis) of HBut and applied the coupled feeding approach, selected a biomass with a maximum specific storage rate of 2 Cmol.Cmol-X_a^{-1}.h^{-1} (determined in an accumulation assay) and a storage yield of 0.73 gCOD.gCOD^{-1}. Nonetheless, in that study the storage rate was very high, possible resulting from the high HBut fraction, the storage yield was constrained by the use of the coupled feeding strategy, which allowed the biomass to use the supplied SFP for growth.

The percentage of 3-HV monomers in the stored polymer was linearly correlated with the fraction of HPro and HVal in the feed and ranged within 0.17 and 0.314 (w/w) (Table 3.1). Thus, this confirms that by controlling the profile of SFP in the acidogenic reactor, by applying specific conditions, the monomeric polymer composition produced by a well selected PHA accumulating bacteria can be anticipated.

3.3.3 Accumulation step: maximum accumulation potential (MAP)

The MAP was evaluated for the culture selected at ideal OLR value of 5.4 $gCOD.L^{-1}.d^{-1}$. The fermented stream used in these assays was highly enriched in HBut and had the following composition: 21.3% HAce, 8.7% HPro, 5.4% EtOH, 58.0% HBut and 6.7% HVal (% in gCOD-basis).

The average kinetic performance of the MAP assays is summarised in Table 3.2. It is worth noting that the average maximum PHA content (80.5% ± 0.3%) and the storage yield (0.98 ± 0.01 $gCOD.gCOD^{-1}$) obtained in these assays are the highest values reported for MMC using complex/real feedstocks. The fact the storage yield obtained was even higher than the stoichiometric yield of PHA on pure butyrate (0.85 $gCOD.gCOD^{-1}$) (Marang et al., 2013) suggests that other carbon sources present in the complex feedstock matrix (not identified in the performed analysis) were being converted into PHA which could have contributed to the high storage yield. Similar behaviour was previously observed when using other real waste feedstocks as carbon source, such as cheese whey or olive oil mill wastewater (Campanari et al., 2017; Oliveira et al., 2017).

Table 3.2 – Calculated kinetic parameters of the maximum accumulation potential test and comparison with literature studies. Values presented are mean (standard deviation).

		References		
Parameter	**This study**	**Jiang et al. 2012**	**Lorini et al. 2020a**	**Oliveira et al. 2017**
OLR ($gCOD.L^{-1}.d^{-1}$)[a]	5.4	2.25	8.5	8.5
C, N feeding[a]	uncoupled	coupled	uncoupled	uncoupled
Carbon source	Fermented FW	f-PMW[b]	Synthetic HAce + HPro	f-CW[c]
$-q_{SFP}$[d] ($gCOD.gCOD\text{-}X_a^{-1}.h^{-1}$)	1.03 (0.02)	-	-	-
q_{PHA}[d] ($gCOD.gCOD\text{-}X_a^{-1}.h^{-1}$)	1.01 (0.01)	2.0[e]	0.241 (0.02)	0.40 (0.03)[e]
$Y_{PHA/SFP}$ ($gCOD.gCOD^{-1}$)	0.98 (0.01)	0.80	0.74 (0.02)	0.96 (0.07)[f]
Max. PHA content (%,w/w)	80.5 (0.3)	76.8	70 (3)	< 35
Global PHA productivity ($g.L^{-1}.d^{-1}$)	8.1 (0.1)	2.0	2.89 (0.05)	6.09

[a]related to SBR
[b]Fermented paper mill wastewater (f-PMW)
[c]Fermented cheese whey (f-CW)
[d]Maximum rates
[e]in $Cmol.Cmol\text{-}X_a^{-1}.h^{-1}$
[f]in $Cmol.Cmol^{-1}$

The specific PHA storage and SFP uptake rates were constant during the first hour, resulting in a linear increase of the PHA concentration. Both rates decreased along the assay due to the increasing PHA content in biomass. The continuous feeding strategy resulted in a steady increase in stored PHA concentration, where no polymer losses were observed during all the operation time as tends to happen with pulse-wise feeding (Oliveira et al., 2017).

Although slightly higher, the PHA content obtained in this study was comparable with those obtained by Jiang et al. 2012 (76.8%) and Lorini et al. 2020a (70%) (Table 3.2). Both studies used feeding regimes that maximised the PHA content. Jiang et al. 2012 operated the reactor in pH stat, as in our study. Lorini et al. 2020a fed the reactor every hour to guarantee carbon excess along operation. On the other hand, Oliveira et al. 2017 operated the in pulse-wise mode which resulted in a PHA content on biomass below 35% due to the loss of PHA in between pulses.

The global PHA productivity reflects the required process volumes and time to produce a given polymer amount. This parameter was calculated taking in consideration the culture's production capacity in the accumulation assays and the P_X of the selection reactor. The global PHA productivity obtained was 8.1 ± 0.1 $g.L^{-1}.d^{-1}$ (Table 3.2). This value was much higher than that reported by Jiang et al. 2012 (2 $g.L^{-1}.d^{-1}$) (Table 3.2). Although those authors obtained a high PHA content due to the continuous operation mode and fed the reactor with a fermentate reach in HBut (90% mol-basis), the P_X was constrained at 0.6 $g\text{-}X_a.L^{-1}.d^{-1}$ by the low OLR applied (2.25 $gCOD.L^{-1}.d^{-1}$) resulting in the lower PHA productivity. The global productivity obtained in the current study was also almost 3 times higher than that obtained by Lorini et al. 2020a. Those authors had a similar P_X than that in our study, although the culture had a lower storage performance (no HBut in the feed) resulting in a lower global productivity. The value reported by Oliveira et al. 2017 cannot be compared with other studies since those authors estimated the global productivity considering produced PHA that was consumed in between pulses, while in our case it corresponds to the real value.

The P(3HB-co-3HV) produced had a final 3-HV content of 0.24 ± 0.02 (w/w), which correlates well with the 3-HV precursors composition in the feed. The molecular weight (M_w) (311 kDa) was in the same order of magnitude than values reported in the literature for MMC fed with waste feedstocks (220 – 650 kDa) (Albuquerque et al., 2011; Duque et al., 2014). Accordingly to the literature, a polymer with a 3-HV content around 0.20 (w/w) has good stiffness, increased flexibility, lower melting temperature and improved gas barrier properties when compared with pure polyhydroxybutyrate (PHB), which makes it an ideal candidate to be used for packaging applications, the largest market for bioplastic usage (Lorini et al., 2020b).

3.3.4 Overall PHA yield

The overall PHA yield on FW is a crucial parameter that may be considered to evaluate the economic and technical feasibility of the PHA producing process.

A global COD mass balance was done considering as basis 1 Kg of P(3HB-co-3HV) with 0.24 (w/w) of 3-HV monomers and using the results obtained for the optimal conditions determined in each step (assumptions and a COD flow scheme are detailed in Appendix B). Based on this, the overall yield of the process ($Y_{PHA/FW}$) was 0.45 gCOD.gCOD^{-1}.

This analysis revealed that the overall yield obtained in this study was higher when compared to other MMC processes performed at pilot-scale. Tamis et al. 2014 used Mars candy factory wastewaters as carbon source and obtained an overall yield of 0.30 gCOD.gCOD^{-1}, and in another study using paper mill wastewater (Tamis et al., 2018), the overall yield was 0.34 gCOD.gCOD^{-1}. The observed $Y_{PHA/FW}$ was even slightly higher than that estimated by Valentino et al. 2017 (0.42 gCOD.gCOD^{-1}) as the theoretical value that may be achieved considering best laboratory scale results (at that time) using synthetic feedstock as substrate. The lower results obtained in these studies are related with the lower fermentation yield, growth yield on SFP and storage yield than obtained for FW, also with the inferior PHA accumulation capacity (more details about the individual parameters used in the overall yield calculation can be found in Table B4 in Appendix B).

Several factors contributed to the high overall yield: i) the operational conditions applied in the acidogenic reactor allowed to achieve a high fermentation yield (0.74 gCOD.gCOD^{-1}) that was only slightly below the theoretical yield of conversion of glucose in HBut (0.83 gCOD.gCOD^{-1}, assuming the stoichiometry described in Batstone et al. 2002). Since this parameter was calculated in relation to the total COD of the FW and this residue has about 15% of insoluble COD (which can be more difficult to hydrolyse) it can be assumed that the fermentation yield cannot be further improved; ii) the higher HBut fraction of the SFP stream was crucial to maximise yields on both selection and accumulation reactors; iii) the strategy of uncoupling the carbon to the nitrogen feeding ensured that the biomass does not use the available SFP for growth, which resulted in a high selection on PHA accumulating organisms, thus enhancing the storage yield obtained.

Lastly, achieving a high PHA on biomass content at the end of the accumulation step is essential to increase the PHA extraction yield, which impacts directly on extraction costs. Conventional extraction methods use large volumes of halogenated solvents, compromising the “environmentally-friendly” character of the bioplastic and accounting for 30-50% of the total production cost (Colombo et al., 2020). Multiple novel green solutions have been recently explored, however, despite the advantages of these methods, the polymer purity and yield achieved are usually lower than that obtained using the traditional approach.(Li and Wilkins, 2020). Thus, further studies are still required in order to design an efficient and cost-effective downstream process that does not jeopardize the positive environmental impact of PHA production from wastes.

The approach herein described highlights the importance of combining different optimal operational strategies to maximise each step performance to turn the MMC 3-stage a potential process for full-scale implementation.

3.4 Conclusions

This study demonstrated, at pilot scale, the possibility of significant enhancing PHA production performance from fruit waste by combining different effective operating strategies.

First, by fine-tuning the acidogenic pH it was possible to obtain a high fermentation yield and a stream highly enriched in HBut, which enhanced the PHA storing rate and yield. Combining uncoupling carbon and nitrogen addition with high OLR resulted in a culture highly enriched in PHA-accumulators with enhanced biomass productivity. Additionally, combining the previous operation conditions with the strategy of feeding the accumulation reactor in continuous mode led to a high PHA content at the end of the assay.

The global PHA productivity and overall yield obtained are, to the best of our knowledge, the highest values reported for MMC using complex feedstocks. These parameters have a direct impact on the investment and operational costs. Therefore, it can be anticipated that the conditions applied contribute for the reduction of the final PHA production costs as compared to values reported to date, demonstrating the potential for full-scale implementation of PHA production from fruit waste.

3.5 References

Albuquerque, M.G.E., Carvalho, G., Kragelund, C., Silva, A.F., Barreto Crespo, M.T., Reis, M.A.M., Nielsen, P.H., 2013. Link between microbial composition and carbon substrate-uptake preferences in a PHA-storing community. ISME J. 7, 1–12. https://doi.org/10.1038/ismej.2012.74

Albuquerque, M.G.E., Concas, S., Bengtsson, S., Reis, M.A.M., 2010a. Mixed culture polyhydroxyalkanoates production from sugar molasses: The use of a 2-stage CSTR system for culture selection. Bioresour. Technol. https://doi.org/10.1016/j.biortech.2010.04.019

Albuquerque, M.G.E., Martino, V., Pollet, E., Avérous, L., Reis, M.A.M., 2011. Mixed culture polyhydroxyalkanoate (PHA) production from volatile fatty acid (VFA)-rich streams: Effect of substrate composition and feeding regime on PHA productivity, composition and properties. J. Biotechnol. https://doi.org/10.1016/j.jbiotec.2010.10.070

Albuquerque, M.G.E., Torres, C.A.V., Reis, M.A.M., 2010b. Polyhydroxyalkanoate (PHA) production by a mixed microbial culture using sugar molasses: Effect of the influent substrate concentration on culture selection. Water Res. 44, 3419–3433. https://doi.org/10.1016/j.watres.2010.03.021

Asunis, F., De Gioannis, G., Isipato, M., Muntoni, A., Polettini, A., Pomi, R., Rossi, A., Spiga, D., 2019.

Control of fermentation duration and pH to orient biochemicals and biofuels production from cheese whey. Bioresour. Technol. https://doi.org/10.1016/j.biortech.2019.121722

Batstone, D.J., Keller, J., Angelidaki, I., Kalyuzhnyi, S. V., Pavlostathis, S.G., Rozzi, A., Sanders, W.T., Siegrist, H., Vavilin, V.A., 2002. The IWA Anaerobic Digestion Model No 1 (ADM1). Water Sci. Technol. https://doi.org/10.2166/wst.2002.0292

Campanari, S., Augelletti, F., Rossetti, S., Sciubba, F., Villano, M., Majone, M., 2017. Enhancing a multi-stage process for olive oil mill wastewater valorization towards polyhydroxyalkanoates and biogas production. Chem. Eng. J. 317, 280–289. https://doi.org/10.1016/j.cej.2017.02.094

Campanari, S., E Silva, F.A., Bertin, L., Villano, M., Majone, M., 2014. Effect of the organic loading rate on the production of polyhydroxyalkanoates in a multi-stage process aimed at the valorization of olive oil mill wastewater. Int. J. Biol. Macromol. 71, 34–41. https://doi.org/10.1016/j.ijbiomac.2014.06.006

Carvalheira, M., Cassidy, J., Ribeiro, J.M., Oliveira, B.A., Freitas, E.B., Roca, C., Carvalho, G., Oehmen, A., Reis, M.A.M., 2018. Performance of a two-stage anaerobic digestion system treating fruit pulp waste: The impact of substrate shift and operational conditions. Waste Manag. 78, 434–445. https://doi.org/10.1016/j.wasman.2018.06.013

Carvalho, G., Pedras, I., Karst, S.M., Oliveira, C.S.S., Duque, A.F., Nielsen, P.H., Reis, M.A.M., 2018. Functional redundancy ensures performance robustness in 3-stage PHA-producing mixed cultures under variable feed operation. N. Biotechnol. https://doi.org/10.1016/j.nbt.2017.08.007

Colombo, B., Pereira, J., Martins, M., Torres-Acosta, M.A., Dias, A.C.R.V., Lemos, P.C., Ventura, S.P.M., Eisele, G., Alekseeva, A., Adani, F., Serafim, L.S., 2020. Recovering PHA from mixed microbial biomass: Using non-ionic surfactants as a pretreatment step. Sep. Purif. Technol. 253, 117521. https://doi.org/10.1016/j.seppur.2020.117521

Dias, J.M.L., Serafim, L.S., Lemos, P.C., Reis, M.A.M., Oliveira, R., 2005. Mathematical modelling of a mixed culture cultivation process for the production of polyhydroxybutyrate. Biotechnol. Bioeng. https://doi.org/10.1002/bit.20598

Dietrich, K., Dumont, M.J., Del Rio, L.F., Orsat, V., 2017. Producing PHAs in the bioeconomy — Towards a sustainable bioplastic. Sustain. Prod. Consum. https://doi.org/10.1016/j.spc.2016.09.001

Dionisi, D., Majone, M., Vallini, G., Di Gregorio, S., Beccari, M., 2006. Effect of the applied organic load rate on biodegradable polymer production by mixed microbial cultures in a sequencing batch reactor. Biotechnol. Bioeng. 93, 76–88. https://doi.org/10.1002/bit.20683

Duque, A.F., Oliveira, C.S.S., Carmo, I.T.D., Gouveia, A.R., Pardelha, F., Ramos, A.M., Reis, M.A.M., 2014. Response of a three-stage process for PHA production by mixed microbial cultures to feedstock shift: Impact on polymer composition. N. Biotechnol. 31, 276–288. https://doi.org/10.1016/j.nbt.2013.10.010

Fra-Vázquez, A., Palmeiro-Sánchez, T., del Río, Á.V., Mosquera-Corral, A., 2020. Transformation of

organic contamination from wastewater into bioplastics (polyhydroxyalkanoate) by microorganisms. Wastewater Treat. Residues as Resour. Biorefinery Prod. Biofuels 2015, 415–433. https://doi.org/10.1016/b978-0-12-816204-0.00018-7

Jiang, Y., Marang, L., Kleerebezem, R., Muyzer, G., van Loosdrecht, M.C.M., 2011. Polyhydroxybutyrate production from lactate using a mixed microbial culture. Biotechnol. Bioeng. 108, 2022–2035. https://doi.org/10.1002/bit.23148

Jiang, Y., Marang, L., Tamis, J., van Loosdrecht, M.C.M., Dijkman, H., Kleerebezem, R., 2012. Waste to resource: Converting paper mill wastewater to bioplastic. Water Res. https://doi.org/10.1016/j.watres.2012.07.028

Johnson, K., Kleerebezem, R., Van Loosdrecht, M.C.M., 2009. Model-based data evaluation of polyhydroxybutyrate producing mixed microbial cultures in aerobic sequencing batch and fed-batch reactors. Biotechnol. Bioeng. https://doi.org/10.1002/bit.22380

Kourmentza, C., Kornaros, M., 2016. Biotransformation of volatile fatty acids to polyhydroxyalkanoates by employing mixed microbial consortia: The effect of pH and carbon source. Bioresour. Technol. https://doi.org/10.1016/j.biortech.2016.10.014

Lee, W.S., Chua, A.S.M., Yeoh, H.K., Ngoh, G.C., 2014. A review of the production and applications of waste-derived volatile fatty acids. Chem. Eng. J. https://doi.org/10.1016/j.cej.2013.09.002

Li, M., Wilkins, M.R., 2020. Recent advances in polyhydroxyalkanoate production: Feedstocks, strains and process developments. Int. J. Biol. Macromol. 156, 691–703. https://doi.org/10.1016/j.ijbiomac.2020.04.082

Lorini, L., di Re, F., Majone, M., Valentino, F., 2020a. High rate selection of PHA accumulating mixed cultures in Sequencing Batch Reactors with uncoupled carbon and nitrogen feeding. N. Biotechnol. https://doi.org/10.1016/j.nbt.2020.01.006

Lorini, L., Martinelli, A., Pavan, P., Majone, M., Valentino, F., 2020b. Downstream processing and characterization of polyhydroxyalkanoates (PHAs) produced by mixed microbial culture (MMC) and organic urban waste as substrate. Biomass Convers. Biorefinery. https://doi.org/10.1007/s13399-020-00788-w

Mannina, G., Presti, D., Montiel-Jarillo, G., Carrera, J., Suárez-Ojeda, M.E., 2020. Recovery of polyhydroxyalkanoates (PHAs) from wastewater: A review. Bioresour. Technol. 297, 122478. https://doi.org/10.1016/j.biortech.2019.122478

Marang, L., Jiang, Y., van Loosdrecht, M.C.M., Kleerebezem, R., 2013. Butyrate as preferred substrate for polyhydroxybutyrate production. Bioresour. Technol. https://doi.org/10.1016/j.biortech.2013.05.031

Mateus, S., Carvalheira, M., Cassidy, J., Freitas, E., Oehmen, A., Reis, M.A.M., 2020. Two-stage anaerobic digestion system treating different seasonal fruit pulp wastes: Impact on biogas and hydrogen production and total energy recovery potential. Biomass and Bioenergy 141.

https://doi.org/10.1016/j.biombioe.2020.105694

Moretto, G., Lorini, L., Pavan, P., Crognale, S., Tonanzi, B., Rossetti, S., Majone, M., Valentino, F., 2020. Biopolymers from urban organic waste: Influence of the solid retention time to cycle length ratio in the enrichment of a Mixed Microbial Culture (MMC). ACS Sustain. Chem. Eng. https://doi.org/10.1021/acssuschemeng.0c04980

Oliveira, C.S.S., Silva, C.E., Carvalho, G., Reis, M.A., 2017. Strategies for efficiently selecting PHA producing mixed microbial cultures using complex feedstocks: Feast and famine regime and uncoupled carbon and nitrogen availabilities. N. Biotechnol. 37, 69–79. https://doi.org/10.1016/j.nbt.2016.10.008

Pereira, J.R., Araújo, D., Marques, A.C., Neves, L.A., Grandfils, C., Sevrin, C., Alves, V.D., Fortunato, E., Reis, M.A.M., Freitas, F., 2019. Demonstration of the adhesive properties of the medium-chain-length polyhydroxyalkanoate produced by Pseudomonas chlororaphis subsp. aurantiaca from glycerol. Int. J. Biol. Macromol. https://doi.org/10.1016/j.ijbiomac.2018.09.064

Pérez-Rivero, C., López-Gómez, J.P., Roy, I., 2019. A sustainable approach for the downstream processing of bacterial polyhydroxyalkanoates: State-of-the-art and latest developments. Biochem. Eng. J. 150, 107283. https://doi.org/10.1016/j.bej.2019.107283

Pérez, V., Mota, C.R., Muñoz, R., Lebrero, R., 2020. Polyhydroxyalkanoates (PHA) production from biogas in waste treatment facilities: Assessing the potential impacts on economy, environment and society. Chemosphere 255, 126929. https://doi.org/10.1016/j.chemosphere.2020.126929

Reis, M., Albuquerque, M., Villano, M., Majone, M., 2011. Mixed Culture Processes for Polyhydroxyalkanoate Production from Agro-Industrial Surplus/Wastes as Feedstocks, Second Edi. ed, Comprehensive Biotechnology, Second Edition. Elsevier B.V. https://doi.org/10.1016/B978-0-08-088504-9.00464-5

Riccardi, C., Buiarelli, F., Castellani, F., Di Filippo, P., Lorini, L., Majone, M., Matos, M., Pomata, D., Simonetti, G., Sommer Ferreira, B., Valentino, F., 2020. Polychlorinated Biphenyl Profile in Polyhydroxy-alkanoates Synthetized from Urban Organic Wastes. Polymers (Basel). 12, 659. https://doi.org/10.3390/polym12030659

Sagar, N.A., Pareek, S., Sharma, S., Yahia, E.M., Lobo, M.G., 2018. Fruit and Vegetable Waste: Bioactive Compounds, Their Extraction, and Possible Utilization. Compr. Rev. Food Sci. Food Saf. 17, 512–531. https://doi.org/10.1111/1541-4337.12330

Serafim, L.S., Lemos, P.C., Oliveira, R., Reis, M.A.M., 2004. Optimization of polyhydroxybutyrate production by mixed cultures submitted to aerobic dynamic feeding conditions. Biotechnol. Bioeng. 87, 145–160. https://doi.org/10.1002/bit.20085

Silva, F., Campanari, S., Matteo, S., Valentino, F., Majone, M., Villano, M., 2017. Impact of nitrogen feeding regulation on polyhydroxyalkanoates production by mixed microbial cultures. N. Biotechnol. https://doi.org/10.1016/j.nbt.2016.07.013

Sträuber, H., Schröder, M., Kleinsteuber, S., 2012. Metabolic and microbial community dynamics

during the hydrolytic and acidogenic fermentation in a leach-bed process. Energy. Sustain. Soc. https://doi.org/10.1186/2192-0567-2-13

Tamis, J., Lužkov, K., Jiang, Y., Loosdrecht, M.C.M. va., Kleerebezem, R., 2014. Enrichment of Plasticicumulans acidivorans at pilot-scale for PHA production on industrial wastewater. J. Biotechnol. https://doi.org/10.1016/j.jbiotec.2014.10.022

Tamis, J., Mulders, M., Dijkman, H., Rozendal, R., van Loosdrecht, M.C.M.M., Kleerebezem, R., 2018. Pilot-Scale Polyhydroxyalkanoate Production from Paper Mill Wastewater: Process Characteristics and Identification of Bottlenecks for Full-Scale Implementation. J. Environ. Eng. (United States). https://doi.org/10.1061/(ASCE)EE.1943-7870.0001444

Temudo, M.F., Kleerebezem, R., Van Loosdrecht, M., 2007. Influence of the pH on (Open) mixed culture fermentation of glucose: A chemostat study. Biotechnol. Bioeng. https://doi.org/10.1002/bit.21412

Valentino, F., Gottardo, M., Micolucci, F., Pavan, P., Bolzonella, D., Rossetti, S., Majone, M., 2018. Organic Fraction of Municipal Solid Waste Recovery by Conversion into Added-Value Polyhydroxyalkanoates and Biogas. ACS Sustain. Chem. Eng. 6, 16375–16385. https://doi.org/10.1021/acssuschemeng.8b03454

Valentino, F., Moretto, G., Lorini, L., Bolzonella, D., Pavan, P., Majone, M., 2019. Pilot-Scale Polyhydroxyalkanoate Production from Combined Treatment of Organic Fraction of Municipal Solid Waste and Sewage Sludge. Ind. Eng. Chem. Res. 58, 12149–12158. https://doi.org/10.1021/acs.iecr.9b01831

Valentino, F., Morgan-Sagastume, F., Campanari, S., Villano, M., Werker, A., Majone, M., 2017. Carbon recovery from wastewater through bioconversion into biodegradable polymers. N. Biotechnol. 37, 9–23. https://doi.org/10.1016/j.nbt.2016.05.007

Wang, X., Carvalho, G., Reis, M.A.M., Oehmen, A., 2018. Metabolic modeling of the substrate competition among multiple VFAs for PHA production by mixed microbial cultures. J. Biotechnol. https://doi.org/10.1016/j.jbiotec.2018.06.342

Wang, X., Oehmen, A., Freitas, E.B., Carvalho, G., Reis, M.A.M., 2017. The link of feast-phase dissolved oxygen (DO) with substrate competition and microbial selection in PHA production. Water Res. 112, 269–278. https://doi.org/10.1016/j.watres.2017.01.064

4

UNDERSTANDING THE POLYHYDROXYALKANOATE (PHA) BIOPRECURSORS PRODUCTION FROM FRUIT WASTE BY MIXED MICROBIAL CULTURES THROUGH PILOT SCALE EXPERIMENTS AND METABOLIC MODELLING

SUMMARY:

Polyhydroxyalkanoates (PHAs) are biodegradable plastics that represent a sustainable alternative to the commonly used petroleum derived polyolefins. An effective method for PHAs production is the 3-stage process involving mixed microbial cultures (MMCs) as waste-based feedstocks, which has the potential for lowering the costs associated to the typical pure cultures production process. The copolymer poly(3-hydroxybutyrate-*co*-3-hydroxyvalerate) – P(3HB-*co*-3HV) – is the most common copolymer found in the MMC PHA production process from wastes. This is a very versatile copolymer since its properties can be manipulated by varying the 3-HV monomeric composition, making it suitable for a wide range of applications. This study was focused on studying the possibility of tailoring the P(3HB-*co*-3HV) composition by controlling the operating pH (between 4.69 and 6.34) of a pilot-scale upflow anaerobic sludge blanket (UASB) acidogenic reactor fed with fruit waste. The different fermentation products profiles produced were then fed to a pilot-scale accumulation reactor to evaluate their impact on polymer composition. The results showed that the fermentation yield of the UASB was maintained quite stable between 0.72 and 0.79 $gCOD.gCOD^{-1}$ during the entire operational period, while the 3-HV bioprecursors fraction in the effluent was highly affected by the reactor pH. Overall, it was possible to vary the 3-HV monomeric composition of the polymers produced from 0.16 (gCOD-basis),

when the pH of the UASB reactor was set at 4.69, to 0.44 (gCOD-basis), when the pH increased until 5.92. Moreover, the soluble fermentation product (SFP) profiles were similar for identical pH values tested in different periods of operation, showing the resilience of the selected MMC, which can produce a consistent SFP stream, further resulting in the same target PHA monomeric composition. Additionally, the IWA Anaerobic Digestion Model No. 1 (ADM1) was expanded to include the pathway for valerate production from lactate, which was found to be important within the UASB. The developed model was able to dynamically predict the production of the different PHA bioprecursors (3-HB and 3-HV) in the UASB reactor as a function of organic loading rate and pH (over the operating range of 4.20-5.16), providing a tool for process optimisation and tailoring the final PHA monomeric composition.

KEYWORDS:

Polyhydroxyalkanoate monomeric composition; Mixed microbial cultures (MMC); Fruit waste; Acidogenic fermentation; IWA Anaerobic Digestion Model No. 1 (ADM1)

TO BE PUBLISHED AS: Matos, M.; Uçar, N., Cardoso, P., Carvalho, G., Reis, M.A.M.,. Santos, J.; Oehmen, A., Understanding the Polyhydroxyalkanoate (PHA) Bioprecursors Production from Fruit Waste by mixed Microbial Cultures through Pilot Scale Experiments And Metabolic Modelling .

4.1 Introduction

Polyhydroxyalkanoates (PHAs) are a group of biobased and biodegradable polyesters which have been recognised as one of the key polymers to drive the bioplastic market (European Bioplastics, 2020). However, even though PHA usage can effectively contribute to decrease the dependence on non-renewable plastics, its market share is still constrained by comparatively high manufacturing costs. Therefore, promising PHA production approaches, based on the usage of mixed microbial cultures (MMCs) and waste-based resources, have appeared as a means of reducing the production costs and the environmental concerns associated to the current commercial PHA products, which are majorly obtained using pure cultures and defined substrates (Montiel-Jarillo et al., 2017).

A few recent studies performed at pilot-scale have focused on the usage of urban waste and agri-food residues as feedstocks for PHA production from MMCs, such as organic fraction of municipal solid waste (Moretto et al., 2020), candy factory wastewater (Tamis et al., 2014a), tomato waste centrate (Bengtsson et al., 2017), and fruit waste (FW) (Matos et al., 2021). In particular, FW is one of the major categories among all types of food waste (representing up to 60% of total fruit production), contributing to numerous problems of sustainability (Sagar et al., 2018; Tedesco et al., 2019). FW is considered a carbon-rich residue (175 $gCOD.L^{-1}$) essentially comprised of easily biodegradable compounds (85% of soluble chemical oxygen demand – COD). This feedstock was recently used to demonstrate the operation of a pilot plant for production of PHA using MMC with unprecedented volumetric productivity and yield (Matos et al., 2021).

The PHAs obtained from MMCs and complex feedstocks are usually produced in a three-stage process: (1) an acidogenic fermentation to convert the organic carbon of the feedstock into a mixture of soluble fermentation products (SFP) that are bioprecursors for PHA production; (2) the selection of an aerobic MMC highly enriched in PHA-storers through cyclically applying periods of carbon excess (feast) and carbon absence (famine); and finally (3) the PHA production, where the previously selected culture is fed with the SFP until attaining its maximum PHA capacity (Sabapathy et al., 2020).

The PHA monomeric composition directly influences its thermo-mechanical properties, e.g. polyhydroxybutyrate (PHB) is a stiff and brittle polymer with limited applications, while the incorporation of 3-hydroxyvalerate (3-HV) leads to the production of the copolymer poly(3-hydroxybutyrate-*co*-3-hydroxyvalerate) – P(3HB-*co*-3HV) – which is more elastic and flexible (Lorini et al., 2020). The properties of P(3HB-*co*-3HV) are very versatile and can be manipulated by varying its 3-HV monomeric content, a fact that makes this material suitable for a wide range of applications (Lorini et al., 2020).

Within the PHA production involving MMCs, it is possible to control the polymer composition, and thus its properties, by varying the SFP profile fed into the PHA-production reactor. For instance, acetate

(HAce) and butyrate (HBut) tend to yield 3-hydroxybutyrate (3-HB) monomers, while the presence of propionate (HPro) and valerate (HVal) increases the final proportion of 3-HV in the polymer chains (Jiang et al., 2011; Lemos et al., 2006; Zhang, 2015). The operating pH of the acidogenic reactor was found to be crucial on the manipulation of the SFP profile by selecting different species composition and/or bacterial groups dominance that display distinct SFP metabolic pathways (Gouveia et al., 2017; Hassan and Nelson, 2012; Horiuchi et al., 2002; Pittmann and Steinmetz, 2013). However, the relationships found between pH and SFP production performance and profile seem to be highly dependent on the type of feedstock used (Carvalheira and Duque, 2021).

Continuous stirred tank reactors (CSTRs) are usually used to perform the acidogenic fermentation step. This stage is followed by intensive solid/liquid separation procedures (e.g. centrifugation or ultra-filtration) to separate the anaerobic biomass from the liquid fermentate that will be used in the subsequent PHA production steps (Albuquerque et al., 2007; Campanari et al., 2017; Duque et al., 2014; Jiang et al., 2012; Moretto et al., 2020). Although not frequently used in the PHA production process, the upflow anaerobic sludge blanket (UASB) reactor is the most common and suitable configuration to treat food industry residues due to the ability to support high organic loading rates (OLRs) and short hydraulic retention times (HRTs), while keeping the sludge retention time (SRT) at high values (Demirel et al., 2005). Indeed, UASBs are an ideal reactor design for the first stage of the PHA-production using MMC because granular sludge is more easily retained inside the reactor, which reduces the amount of biomass in the liquid effluent, and thus the necessity of applying such exhaustive and costly solid/liquid separation processes is avoided (Hassan and Nelson, 2012; Parawira et al., 2006). A retained microbial consortium also leads to increased reactor stability and performance (Parawira et al., 2006). Nevertheless, a more stable granular biomass may be disadvantageous when trying to manipulate the SFP profile through varying the operating pH, as shifts in the microbial composition are likely to occur more slowly as compared with suspended biomass (Atasoy et al., 2019). Thus far, the impact of the acidogenic reactor pH on PHA monomeric composition was never assessed when using an UASB reactor configuration.

Predicting acidogenic fermentation and PHA production metabolisms is a critical factor to promote the desired PHA monomeric composition production. There are several mathematical models already developed that successfully describe PHA composition production as a function of the SFP profile (Tamis et al., 2014b; Wang et al., 2018). On the other hand, a modelling approach describing 3-HB and 3-HV bioprecursors production has never been reported as a predictive tool to customise the PHA monomeric composition. IWA Anaerobic Digestion Model No. 1 (ADM1) is the most widely used model to describe anaerobic fermentation reactors as it is general and expandable (Girault et al., 2011), making it an ideal starting point to describe the variation of SFP with pH . However, ADM1 needs some adjustments when applied to non-methanogenic systems, since it does not account for some important metabolic pathways, e.g., lactate (HLac), ethanol (EtOH) and HVal formation from sugars.

This work aimed to investigate, at pilot-scale, the possibility of tailoring the precursors that influence P(3HB-*co*-3HV) monomeric composition by dynamically changing the operating pH of a continuous UASB reactor fed with FW. The impact of the operating conditions imposed was assessed by evaluating the acidogenic community composition, its performance and the impact of SFP profile on PHA composition. Additionally, an extension of the ADM1 model was developed to dynamically predict PHA bioprecursors production from FW, in order to build a powerful tool for process optimisation and PHA composition prediction. Calibration and validation of the model were performed using data from two distinct pilot-scale UASB reactors fed with FW where different OLRs were applied and pH and SFP performance dynamics were assessed.

4.2 Materials and methods

4.2.1 Acidogenic reactor setup

A 60 L UASB reactor was operated in continuous mode under anaerobic conditions using FW as carbon source. The FW residue was supplied by a Portuguese fruit juice company (Sumol+Compal S.A., Almeirim), more details of the influent characteristics were previously reported by Matos et al. (2021). The feed solution was prepared in a 200 L refrigerated tank (4ºC) where the FW was diluted with tap water to achieve the desired organic loading rate (OLR). The residue contained very low ammonia (1.26 ± 0.07 mg-N.L^{-1}) and phosphorus (2.39 ± 0.7 mg-P.L^{-1}) concentrations, so those elements were supplemented as NH_4Cl and KH_2PO_4 together with the feedstock maintaining the COD:N:P ratio at 100:0.5:0.1 (g-basis). Other minerals were also supplied, as follows: 480 mg.L^{-1} of $CaCl_2$, 120 mg.L^{-1} of $MgSO_4.7H_2O$, and 0.8 mg.d^{-1} of $FeCl_3.6H_2O$.

The reactor was inoculated with twenty litres of anaerobic granules from a previous UASB treating FW and operated as described by Matos et al. (2021).

At start-up, the OLR was 7.5 gCOD.L^{-1}.d^{-1}, then it was increased at an average rate of 0.37 gCOD. L^{-1}.d^{-1} until stabilising at 28 ± 2 gCOD.L^{-1}.d^{-1}. The reactor superficial velocity was set to 2.88 m.h^{-1}, by means of an internal recirculation pump, to promote contact between biomass and the substrate. The hydraulic retention time (HRT) was set to 1 d and the temperature was kept at 29.9 ± 0.7 °C. Flow rates were monitored 3 times a week.

After the OLR increasing period (first 56 d of operation), the culture was maintained for 100 d at an average pH of 4.88 ± 0.03, corresponding to phase 0 (Table 4.1). After this period, the pH was changed dynamically as described in Table 4.1. The culture was subjected to sequential pH values of 4.69, 5.22, 5.92 and 6.34 (phases I to IV respectively, Table 4.1), and then reduced back to 5.89 and 5.18 (phase V and VI respectively, Table 4.1). Changes in pH were performed after reaching pseudo-steady state, i.e.,

stable SFP profile. The operating pH was monitored using a probe inserted on the reactor lid and it was controlled through dosing NaHCO3 to adjust the influent alkalinity.

The fermented end-stream was decanted before being fed to the PHA production reactor.

Both influent and effluent streams of the acidogenic reactor were regularly monitored (at least 3 times a week) through assessment of the concentrations of SFP, total COD, ammonium and phosphate. The gas outlet flowrate, the profile of gaseous fermentation products and reactor pressure were also monitored.

Table 4.1 – Performance of the UASB reactor fed with FW and operated under dynamic operating pH. The values listed are **average** (standard deviation).

Period	Days (d)	pH	OLR ($g.L^{-1}.d^{-1}$)	Total SFP ($gCOD.L^{-1}$)	$Y_{SFP/FW}$ ($gCOD.gCOD^{-1}$)	r_{SFP} ($mgCOD.L^{-1}.h^{-1}$)
0	56-156	**4.88** (0.03)	**29** (1)	**21** (2)	**0.72** (0.06)	**884** (88)
I	157-171	**4.69** (0.02)	**31** (3)	**22** (1)	**0.73** (0.06)	**922** (59)
II	172-187	**5.22** (0.06)	**27.3** (0.9)	**22** (1)	**0.79** (0.03)	**900** (61)
III	188-208	**5.92** (0.04)	**25.9** (0.6)	**19.8** (0.2)	**0.75** (0.01)	**825** (7)
IV	209-236	**6.34** (0.06)	**26** (1)	**19.5** (0.3)	**0.75** (0.03)	**811** (14)
V	237-277	**5.89** (0.08)	**27.1** (0.6)	**21.1** (0.7)	**0.78** (0.02)	**878** (29)
VI	278-318	**5.19** (0.04)	**30** (2)	**22.2** (0.3)	**0.76** (0.02)	**922** (10)

4.2.2 PHA production assays

Duplicated PHA production assays were conducted in fed-batch mode using SFP streams collected along UASB operation at pH 4.69, 5.22 and 5.92 (Table 4.2). The SFP composition profiles fed into the PHA production reactor had distinct relative abundance of 3-HV precursors (between 10% and 34%, gCOD-basis), as can be observed in Table 4.2. Different SFP profiles were observed due to the high environmental temperature which caused some SFP alterations during storage. The major difference was in the amount of HAce which increased in some of the cases, however the 3-HB/3-HV precursors fraction was not highly affected (Table 4.2).

The experiments were carried out in a stirred 60 L reactor operated at room temperature, under controlled pH (8.5) and continuously sparged with air at 60 $L_{air}.L_{reactor}^{-1}.h^{-1}$. The accumulation tests consisted of feeding the fermented feedstock to 25 L of a PHA-storing culture previously enriched in the selection reactor and collected at the end of the famine phase. The selection reactor consisted of a

100 L sequential batch reactor (SBR) fed with fermented FW and operated as described by Matos et al. (2021) (HRT of 1 d, SRT of 4 d, OLR of 5.4 $gCOD.L^{-1}.d^{-1}$, room T).

All assays were fed in a pulse-wise mode controlled as a function of the dissolved oxygen (DO), i.e., the substrate was fed manually when the DO increased abruptly. DO was continuously acquired over time.

Table 4.2 – SFP profiles used for the PHA production assays.

UASB pH	SFP profile [HLac/HAce/HPro/EtOH/HBut/HVal] (%, gCOD-basis)	Fraction of 3-HV precursors (%, in gCOD-basis)
4.69	26/19/7/0/44/3	10
	2/16/7/2/70/3	10
5.22	0/28/8/5/48/11	22
	0/42/14/8/27/9	23
5.92	1/40/15/0/29/15	33
	1/26/14/0/40/19	34

4.2.3 Analytical methods

Chemical oxygen demand (COD), total suspended solids (TSS), volatile suspended solids (VSS), SFP, ammonium, phosphate and PHA concentrations were determined as described by Matos et al. (2021b).

Briefly, COD was measured using Hach Lange kits (Hach-Lange, Germany) following the manufacturer's instructions.

TSS and VSS were determined using the procedure described in Standard Methods (APHA, 1998).

SFP profile of filtered samples were determined through high performance liquid chromatography (HPLC) on a VWR Hitachi Chromaster chromatographer.

Ammonium and phosphate concentrations were measured by colorimetry in a segmented flow analyser (Skalar San++ system, Skalar Analytical).

3-HB and 3-HV monomer concentrations were determined by gas chromatography (GC) on a Bruker 430-GC gas chromatographer.

4.2.4 Microbiological analyses

Samples of sludge were collected from the UASB reactor at the end of each pH period. The samples were phylogenetically characterised through high throughput sequencing of the 16S rRNA gene. Total

DNA of the organisms was extracted using a FastDNA Spin kit for soil (MP Biomedicals, USA), following the manufacturer's protocol with a few exceptions: 500 µL of sample, 480 µL Sodium Phosphate Buffer and 120 µL MT Buffer were added to a tube of Lysing Matrix E. 16S rRNA gene amplicon sequencing was carried out using MiSeq Illumina technology by DNASense (Aalborg, Denmark).

The relative abundance of the archaeal versus bacterial populations was investigated on biomass samples taken throughout the operating period. Semi-qualitative fluorescence in situ hybridization (FISH) was carried out according to Amann, 1995. Fluorescein isothiocyanate (FITC)-labelled EUBmix probe was applied for all Bacteria (mixture of EUB338, EUB338-II and EUB338-III) mixed with the Cyanine 3 (Cy3)-labelled ARC915 probe targeting Archaea (Crocetti et al., 2006). More details about the fluorescently labelled oligonucleotide probes are available in the database probeBase 2016 (Greuter et al., 2016).

Hybridised samples were observed with an epifluorescence microscope Zeiss Imager D2 at 1000X.

Principal component analysis (PCA) was applied to the analysis of microbial communities. The scores obtained for the first two principal components (PCs) were analysed to visually detect differences and similarities on the cultures' composition. Prior to the implementation, operational taxonomic units (OTUs) that were not present in more than 0.1% (% of total reads) were not considered. Hellinger transformation (Legendre and Gallagher, 2001) was applied to transform the data.

4.2.5 Calculations

The fermentation yield ($Y_{SFP/FW}$, gCOD-SFP.gCOD-FW^{-1}) was calculated as follows:

$$Y_{SFP/FW} = \frac{SFP_{out} - SFP_{in}}{(TCOD_{in} - SFP_{in}) - (TCOD_{out} - SFP_{out})}$$

where SFP_{in} and SFP_{out} (gCOD.L^{-1}) are the SFP quantified in the reactor influent and end-stream, respectively, and $TCOD_{in}$ and $TCOD_{out}$ (gCOD.L^{-1}) are the measured total COD of the influent FW and end-stream, respectively.

SFP volumetric productivity (r_{SFP}, mgCOD.L^{-1}.h^{-1}) was calculated by dividing the produced SFP, converted to COD units, by the HRT (h).

Concentrations of the carbon compounds (SFP, 3-HB and 3-HV) were converted into COD units according with the following oxidation stoichiometry: 1.07 gCOD.g-HLac^{-1}, 1.07 gCOD.g-HAce^{-1}, 1.51 gCOD.g-HPro^{-1}, 2.08 gCOD.g-EtOH^{-1}, 1.82 gCOD.g-HBut^{-1}, 2.04 gCOD.g-HVal^{-1}, 1.67 gCOD.g-3-HB^{-1}, 1.92 gCOD.g-3-HV^{-1}.

4.3 Model description and development

Anaerobic processes, such as those occurring in UASB reactors, are most commonly described by the ADM1 model (Batstone et al., 2002). ADM1 incorporates many of the processes required to predict PHA bioprecursors production as well. However, two important PHA bioprecursors, lactate and ethanol, were excluded from ADM1 to simplify the model, as including these fermentation products has a low impact on methanogenic systems.

According to the experimental results obtained in this study (see section 4.4.1 – Impact of acidogenic pH on the PHA precursors composition), lactate, ethanol and valerate were detected as products of fermentation of carbohydrates present in FW in addition to the typically found organic acids (acetate, propionate, and butyrate). Moreover, since lactic acid has a strong effect on operating pH values (due to its low pK_a of 3.08), it should be considered in the ADM1 model in order to properly describe the acidogenic fermentation process (Batstone et al., 2002).

Lactate and ethanol were previously incorporated into an extended version of ADM1 by Peiris et al. 2006 and Antonopoulou et al. 2012. Peiris et al. 2006 defined lactate and ethanol as intermediate products of glucose fermentation and included their uptake processes into their model. On the other hand, Antonopoulou et al. 2012 described ethanol as a final product, and lactate as an intermediate product. Experimental data in this study showed that lactate is an intermediate product and ethanol is a final product, therefore the model published by Antonopoulou et al. 2012 was used as the base model in this study.

Nevertheless, the production of valeric acid from glucose fermentation has not previously been considered in any existing model. ADM1 based models follow a pathway that assumes the valeric acid is produced only from acidogenesis of amino acids. Yu et al. 2004 suggested that propionate could be converted to valeric acid by using hydrogen as an electron donor. This approach was implemented in our extended ADM1 model since the experimental data shows the existence of valerate in considerable amounts in the reactor (see section 4.4.1 – Impact of acidogenic pH on the PHA precursors composition) and amino acids were not identified in the feedstock. For consistency with the proposed propionate production pathway proposed by Peiris et al. 2006 and Antonopoulou et al. 2012 (from lactate uptake), valerate production was also considered in our model to be derived from lactate (via propionate).

All the stoichiometric reactions considered in the extended ADM1 developed in this study are summarised in Table 4.3.

Table 4.3 – Stoichiometric equations of monosaccharides and lactate fermentation implemented in the extended ADM1 model developed in this study.

Products	Reaction
monosaccharide fermentation	
1. Acetate	$C_6H_{12}O_6 + 2H_2O \longrightarrow 2CH_3COOH + 2CO_2 + 4H_2$
2. Ethanol	$C_6H_{12}O_6 \longrightarrow 2CH_3CH_2OH + 2CO_2$
3. Butyrate	$C_6H_{12}O_6 \longrightarrow CH_3(CH_2)_2COOH + 2CO_2 + 2H_2$
4. Lactate	$C_6H_{12}O_6 \longrightarrow 2CH_3CH(OH)COOH$
lactate fermentation	
1. Propionate	$CH_3CH(OH)COOH + H_2 \longrightarrow CH_3CH_2COOH + H_2O$
2. Valerate	$CH_3CH(OH)COOH + 7H_2{+}2CO_2 \longrightarrow CH_3(CH_2)_3COOH + 5H_2O$
3. Acetate	$CH_3CH(OH)COOH{+}H_2O \longrightarrow CH_3COOH + 2H_2 + CO_2$

4.3.1 Stoichiometric coefficients calculation

Yields from the uptake of monosaccharides and lactate were redefined by simply balancing the elements of the key reactions outlined in Table 4.3, following the method suggested by Batstone, 2002.

Briefly, the fraction of monosaccharides and lactate that degrades via each one of the stoichiometric reactions (Table 4.3) can be expressed as $\eta_{1,sug}$, $\eta_{2,sug}$, $\eta_{3,sug}$, $\eta_{4,sug}$ and $\eta_{1,lac}$, $\eta_{2,lac}$, $\eta_{3,lac}$, respectively for monosaccharides and lactate uptake (each fraction number identifies the reaction number represented in Table 4.3). Thus, the yields of each product can be calculated from these fractions, and the relative coefficient of each component for the different reactions (Table 4.3) is described on a COD basis in Table 4.4. Through the relationships described in Table 4.4., the nine stoichiometric coefficients can be estimated by only five independent parameters, while the carbon and redox balances are closed.

The Gujer matrix of the model with the suggested modifications and stoichiometric coefficients derived from the monosaccharide and lactate fermentation equations is presented in Table C1 of Appendix C.

Table 4.4 - Stoichiometric coefficients from monosaccharides and lactate uptake.

Products	**Yield**[a]
monosaccharide fermentation	
Acetate	$f_{AC,SUG} = 0.67\ \eta_{1,sug}$
Ethanol	$f_{ET,SUG} = \eta_{2,sug}$
Butyrate	$f_{BUT,SUG} = 0.83\ \eta_{3,sug}$
Lactate	$f_{LAC,SUG} = 1\ (1 - \eta_{1,sug} - \eta_{2,sug} - \eta_{3,sug})$
Hydrogen	$f_{H2,SUG} = 0.33\ \eta_{1,sug} + 0.17\ \eta_{3,sug}$
lactate fermentation	
Propionate	$f_{PROP,LAC} = 1.17\ \eta_{1,lac}$
Valerate	$f_{VAL,LAC} = 2.17\ \eta_{2,lac}$
Acetate	$f_{AC,LAC} = 0.67\ (1 - \eta_{1,lac} - \eta_{2,lac})$
Hydrogen	$f_{H2,LAC} = 0.33 - 0.50\ \eta_{1,lac} - 1.50\ \eta_{2,lac}$

[a] $f_{AC,SUG}$, $f_{ET,SUG}$, $f_{BUT,SUG}$, $f_{LAC,SUG}$ and $f_{H2,SUG}$ are the respective yields of acetate, ethanol, butyrate, lactate and hydrogen from monossacharides and $f_{PROP,LAC}$, $f_{VAL,LAC}$, $f_{AC,LAC}$ and $f_{H2,LAC}$ are the respective yields of acetate, propionate, valerate and hydrogen from lactate .

4.3.2 Plant model setup

The developed model was implemented in Dynamita's Sumo 21 software. An anaerobic digester with a cyclone was set up to simulate a UASB reactor. The cyclone was used to prevent sludge being washed out of the reactor, as the UASB retains the predominantly granular biomass of the process. A chemical ($NaHCO_3$) dosage pump and PID controller were used to set pH in the reactor correctly, simulating the implemented pH controller setup (see section 4.2.1 – Acidogenic reactor setup). The dynamic influent wastewater data and the reactor temperature served as inputs to the model.

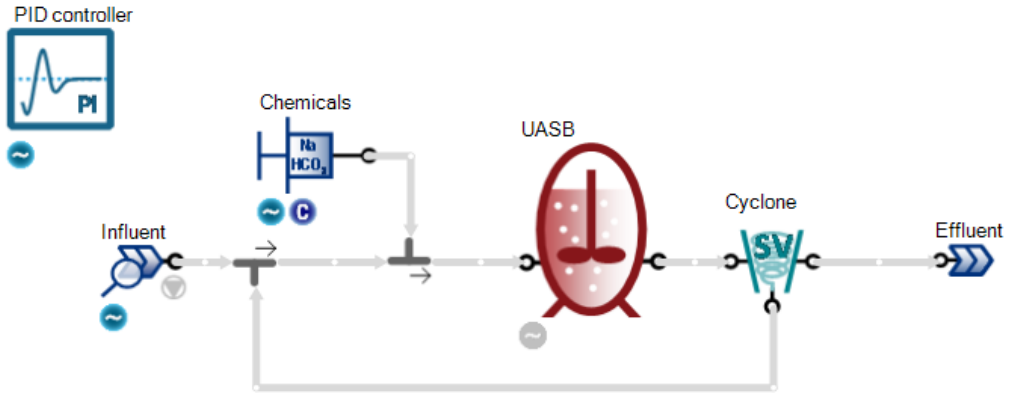

Figure 4.1 – Layout of the UASB system in the Sumo 21 software

4.3.3 Influent fractionation

An additional sampling campaign was performed to collect additional data (as identified in Table C4 in Appendix C) needed to complete the fractionation of the influent so that the measured data could be converted into model state variables. Additionally, the fractionation of carbohydrates, proteins, and lipids corresponded to the study of Galí et al. 2009, which characterised apple pulp waste, a residue that is similar to that used in this study. Table C4 of appendix C summarises the average values of the parameters used for the influent fractionation.

The influent fractionation was performed by closing the mass balances of total COD, total nitrogen and total phosphorous as described in Table C5 in Appendix C. The mass balances were closed with absolute percent errors of 0%, 1% and 8%, respectively for total carbon, total nitrogen and total phosphorus.

The conversion of the measured/estimated parameters into state variables is summarised in Table C6 in appendix C and resulted in the fractions presented in Table 4.5.

Table 4.5 - Estimated fractions per total COD, total nitrogen and total phosphorous.

Fraction	Description	Value
fr_S_{SUG}	Soluble monosaccharides	82.4%
fr_S_{VAL}	Soluble total Valerate	0.0%
fr_S_{BUT}	Soluble total Butyrate	0.0%
fr_S_{PROP}	Soluble total Propionate	0.1%
fr_S_{AC}	Soluble total Acetate	0.1%
fr_S_{LAC}	Soluble total Lactate	0.2%
fr_S_{ET}	Soluble total Ethanol	0.0%
fr_X_{CH}	Particulate carbohydrates	13.2%
fr_X_{PROT}	Particulate proteins	1.8%
fr_X_{LIP}	Particulate lipids	1.9%
fr_X_{U}	Particulate Inerts	0.3%
fr_NH,TN	Ammonia	73%
fr_PO4,TP	Orthophosphate	84%

4.3.4 Model calibration and validation

The extended ADM1 model was calibrated and validated to accurately derive a reliable set of parameters capable of predicting the UASB behaviour over a wide range of OLRs and pH setpoints.

The UASB reactor described by Matos et al. 2021 was defined as the calibration reactor and the UASB presented in this study was used as the validation reactor. Both reactors had the same configuration (see section 4.2.1 – Acidogenic reactor setup) and were fed with FW. The operating conditions of the calibration reactor were set as follows: temperature of 30.0 ± 0.5 °C, HRT of 1 d and variable pH (ranging between 4.04 and 5.18) and OLR (between 5.0 and 32.7 $gCOD.L^{-1}.d^{-1}$) (Matos et al. 2021).

ADM1 default kinetic parameters were used except for the lactic acid uptake rate, which was adopted from the study of Antonopoulou et al. 2012. The values adopted are summarized in Table C2 in Appendix C.

The monosaccharide and lactate degradation fractions ($\eta_{1,sug}$, $\eta_{2,sug}$, $\eta_{3,sug}$, $\eta_{1,lac}$, $\eta_{2,lac}$) were determined using the average concentrations of the respective SFP obtained from day 41 onwards of the calibration UASB (Matos et al., 2021). Day 41 corresponds to the day where no methane was detected in the gas outflow, and the first 37 d were considered a period of instability where the MMC was being selected (Matos et al., 2021). The estimated yields are presented in Table 4.6. These yield coefficients differed from those of Batstone, 2002 for the ADM1 model (Table 4.6), reflecting the different feedstock

fermented (fruit waste vs sewage sludge, respectively). Other stoichiometric parameters are ADM1 default values (see Table C2 in Appendix C).

Same kinetic and stoichiometric parameters were used for both calibration and validation reactors, no other parameter estimations or adjustments were made to fit the model in validation results.

Table 4.6 – Yields of the different fermentation products on monosaccharides and lactate calculated from the experimental data reported by Matos et al. 2021 versus the values proposed by Batstone, 2002.

Yields ($KgCOD.KgCOD^{-1}$)	Modified ADM1	ADM1[a]
$f_{AC,SUG}$	0.033	0.410
$f_{PROP,SUG}$	-	0.270
$f_{ET,SUG}$	0.057	-
$f_{BUT,SUG}$	0.549	0.130
$f_{LAC,SUG}$	0.235	-
$f_{H2,SUG}$	0.126	0.190
$f_{AC,LAC}$	0.525	-
$f_{PROP,LAC}$	0.133	-
$f_{VAL,LAC}$	0.214	-
$f_{H2,LAC}$	0.128	-

[a] from (Batstone, 2002)

The predictive power of the developed model was quantified by calculating the mean absolute error (MAE) and the root mean square error (RMSE) of the total SFP, 3-HB and 3-HV precursors production.

4.4 Results and discussion

4.4.1 Impact of acidogenic pH on the PHA precursors composition

The possibility of tailoring P(3HB-*co*-3HV) monomeric composition in a MMC-PHA production process fed with FW was assessed through manipulation of the acidogenesis pH. An UASB reactor was continuously operated for 318 days under dynamic pH changes and the corresponding performance and SFP profiles were analysed (Table 4.1).

The reactor was inoculated with granular biomass from a previous acidogenic UASB aiming to minimise the long and difficult start-up phases associated to granulation processes and methanogenesis inhibition (Lee et al., 2014; Matos et al., 2021). The initial 56 days of reactor operation corresponded to a gradual acclimatisation of the biomass to the increasing OLR, since the inoculum had been previously stored for a long period at cold temperatures to stop metabolic activity. After this start-up phase, the

reactor was operated at an average pH of 4.88 for 100 days (period 0, Table 4.1). This pH value was chosen as a previous study demonstrated that this pH was ideal to increase the overall PHA productivity and yield of the process (Matos et al., 2021). From the day 157 onwards, the pH was dynamically changed, testing a total of four different pH levels (phase I to IV, Table 4.1). At the end of this period, two of the pH setpoints were repeated to ensure process robustness (phase V and VI, Table 4.1). The SFP produced throughout the different phases of UASB operation are depicted in Figure 4.2 and the performance parameters are summarised in Table 4.1.

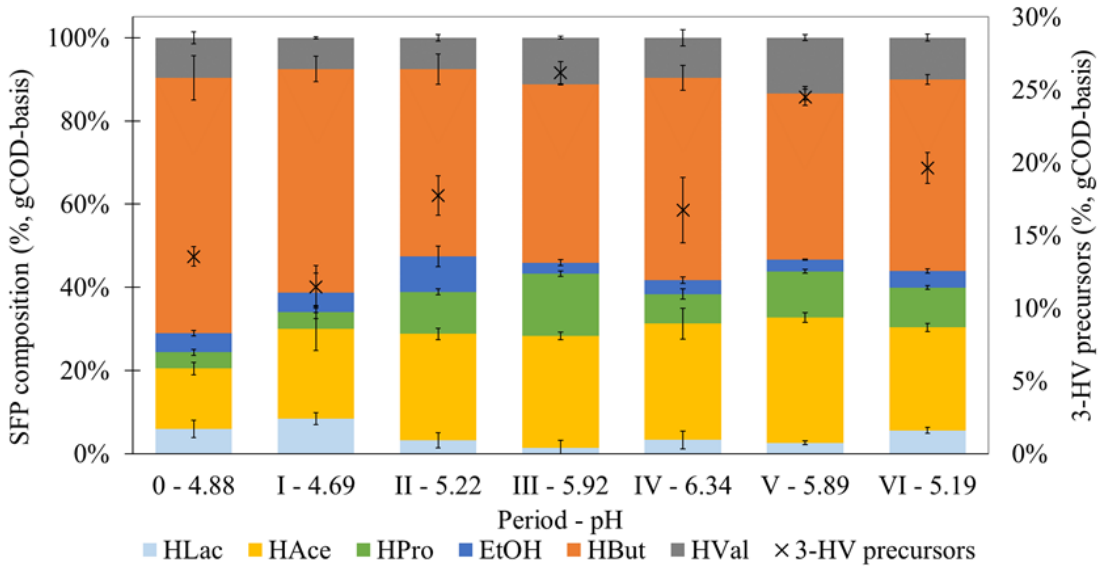

Figure 4.2 - SFP profiles and 3-HV precursors fraction obtained at each different pH setpoint.

During the whole operation time, the SFP end-stream was largely comprised of products capable to be converted into PHA by an acclimatised MMC (Figure 4.2). HLac, HAce, EtOH and HBut were reported to yield 3-HB monomers, while HPro and HVal contribute to increase the amount of 3-HV in the copolymer (Figure 4.2) (Jiang et al., 2011; Lemos et al., 2006; Zhang, 2015).

The total SFP concentration, as well as the fermentation yield and SFP productivity did not vary significantly with operating pH (Table 4.1), meaning that despite the continuous pH changes imposed, the microbial communities selected had the ability to respond with similar performance. The fermentation yields were in the same range as those reported for raspberry fruit waste fed to an acidogenic CSTR (0.75, 0.76 and 0.73, on a gCOD-basis, at pH 4.5, 5 and 5.5) by Mateus et al. 2020 and slightly higher than those reported by Gouveia et al. 2017 using cheese whey as substrate, also using a CSTR (0.33 to 0.68 for a pH range between 4 and 7).

The total SFP concentration varied between 19.5 and 22 $gCOD.L^{-1}$ (on average 560 ± 41 $Cmmol.L^{-1}$), resulting from the high OLR imposed and high fermentation yield attained. Overall, higher and more stable SFP productivity was observed as compared to other acidogenic reactors operated under dynamic

pH, which was likely due to the higher OLR imposed. For example, in the reactor treating cheese whey reported by Gouveia et al. 2017, the SFP concentration varied from 4.3 to 15.1 $gCOD.L^{-1}$ for pH ranging from 4 to 7, and a CSTR fed with sugar cane molasses showed a total SFP concentration between 194 and 238 $Cmmol.L^{-1}$ for pH setpoints between 5 and 7 (Albuquerque et al., 2007). Obtaining a high SFP concentration at the end of fermentation is a factor with high importance within the PHA producing process, since it allows to decrease reactor volumes of the further process steps, increasing the global PHA volumetric productivity, which has a strong impact on the operating and investment costs.

Unlike the other performance parameters, the SFP composition was strongly affected by pH (Figure 4.2). It is worth noting that the end-stream profile, and thus the 3-HV precursors fraction, was similar when the reactor was operated at similar pH conditions (Figure 4.2, period II/VI and III/V), showing the consistency of the UASB fermentation (i.e., the same metabolic products were obtained independently of the historical operational changes).

For all the pH setpoints, HBut was the dominant product of fermentation followed by HAce, while EtOH was present in the lowest relative amounts (Figure 4.2). Regarding HLac, it was also observed in low concentration during all the experimental phases (1-8%, gCOD-basis) (Figure 4.2). However, according to previous batch reactors (data not shown), inoculated with the same biomass and fed with FW at different pH setpoints (between 4.5 and 6.0), HLac was the SFP produced in larger amounts in an early stage of the fermentation. Then, it started to be consumed until being completely exhausted. Based on this, HLac was considered an intermediate product that can be degraded into HPro and HAce, as previously described by Costello et al. 1991 and Peiris et al. 2006, and confirmed by the increased concentration of those two compound in the batch assays (at the same time than HLac decreased). On the other hand, EtOH concentration achieved a maximum and remained approximately constant thereafter, suggesting that it is a final product of fermentation.

HVal was observed in considerable concentrations during fermentation (Figure 4.2). This result was unexpected in view of the inexistence of amino acids in FW, which are usually considered the feedstock for HVal instead of monossacharides (Batstone et al., 2002). Therefore, it was hypothesised that HVal was produced from HPro and carbon dioxide, a metabolic pathway that is thermodynamically possible, as described by Yu et al. 2004.

Despite being the most produced SFP, the HBut fraction tended to decrease from a maximum of 61% (gCOD-basis) at pH 4.88 to a minimum of 43/40% (gCOD-basis) when the pH increased to 5.92/5.89 (period III/V, Figure 4.2). Contrary behaviour was observed for the 3-HV precursors fraction (sum of HPro and HVal), which linearly increased from 11% to 26% when the pH increased from 4.66 to 5.92 (Figure 4.2). The fact that higher operating pH favoured the production of 3-HV precursors was expected, since higher pH seems to favour the production of HPro, a product that is more energetically favourable for acidogenic bacteria (Azbar et al., 2001). On contrary, reduced pH may cause environmental stress to acidogenic bacteria, forcing the microorganisms to produce SFP which reduce the net energy available for their metabolism, such as the case of HBut (Azbar et al., 2001), which is in

accordance with the results presented in this work. For the higher pH tested (pH 6.34), the 3-HV precursors abundance decreased again for 16%. This behaviour may be related with the fact that at this pH a higher amount of Archaea was detected in the granular sludge (see section 4.4.2 – UASB microbial community dynamics as a function of pH) which could have caused a change in the metabolic network. Similar SFP profile trends with pH were observed by Gouveia et al. 2017 in their CSTR fed with cheese whey, although in their case a narrow range of 3-HV precursors production was observed. In their CSTR, an increase of pH from 4.5 to 6 led to an increase of the 3-HV fraction from 0 to 10% (Cmol-basis), which decreased again for 6% at pH 7 (Gouveia et al., 2017).

After each pH change, the SFP profiles and reactor performance stabilised over a short period of time (between 3 and 15 d), indicating that the microbial culture was robust and capable to adapt to the different operating pH without necessity of a new acclimatisation period. Moreover, the response time was not quite different than that observed for acidogenic CSTR reactors treating food wastes and operated under dynamic pH, such as 4 d average response time observed for cheese whey (Gouveia et al., 2017) and 2 to 18 d observed for fruit pulp waste (Mateus et al., 2020), indicating that similar dynamic change in the SFP profile can be achieved when using a system with retained biomass, such as the UASB configuration.

The facts herein described show that a UASB configuration seems to be as effective as a CSTR on manipulating the 3-HV content of PHA copolymers through dynamically changing the acidogenic pH, with several design advantages (e.g., high OLR/SFP concentration, and simpler biomass separation process).

4.4.2 UASB microbial community dynamics as a function of pH

High throughput sequencing of the 16S rRNA gene was used to identify the bacterial population dynamics and qualitative FISH to detect the presence of Archaea in biomass samples collected under the different operating pH.

FISH results revealed that archaea organisms were “almost non-existent” during most of the operation period (Table 4.7). An exception was observed for pH 6.34, where Archaea were identified as “present” (Table 4.7), meaning that, despite the long period of time where Archaea were not able to thrive, those organisms were able to grow when favourable operational conditions were established (such as higher pH). Archaea are methane producers which may consume the available SFP, so their presence can unbalance/disturb the metabolic network of acidogenic bacteria, which is not desirable in a reactor producing precursors for further PHA production.

Table 4.7 – Qualitative FISH analysis using probe ARC915 to target Archaea.

pH	4.69	5.22	5.92	6.34	5.89	5.18
	+-	+-	+-	+	+-	+-

(-) not-detected; (+-) almost non-existent; (+) present; (++) abundant; (+++) dominant

The acidogenic bacterial community identified in the different samples showed similar diversities but different relative abundances (Figure 4.3 A). In total, 4 identified main phyla (> 96% of total reads in all the samples) were detected in the microbial community: *Firmicutes, Bacteriodetes, Saccharibacteria and Actinobacteria*. These phyla were frequently found in anaerobic reactors treating organic matters (Jang et al., 2014; Niu et al., 2013; Zhang et al., 2020). In particular, *Firmicutes and Bacteriodetes* accounted for more than 70% of the cultures selected at the different conditions, and were also identified as the most predominant phylum in waste activated sludge and food waste fermentation (Cheng et al., 2014; Cirne et al., 2012; Peng et al., 2018). *Firmicutes and Bacteriodetes* have low sensitivity to changes in the environmental conditions, such as pH (Venkiteshwaran et al., 2016), which can explain their permanence in the reactor at all the different pH tested.

Despite the changes of the community composition over the different pH, the most abundant OTUs were always *Clostridium sensu stricto 12, Ruminiclostridium 5, Prevotella 7, Megasphaera, Atopobium, Lactobacillus, Mitsuokella and Selenomonas* (Figure 4.3 A). These organisms accounted for more than 70 % of the total reads throughout the study (except for period V – pH 5.89, where the total identified genus were lower than for the other conditions).

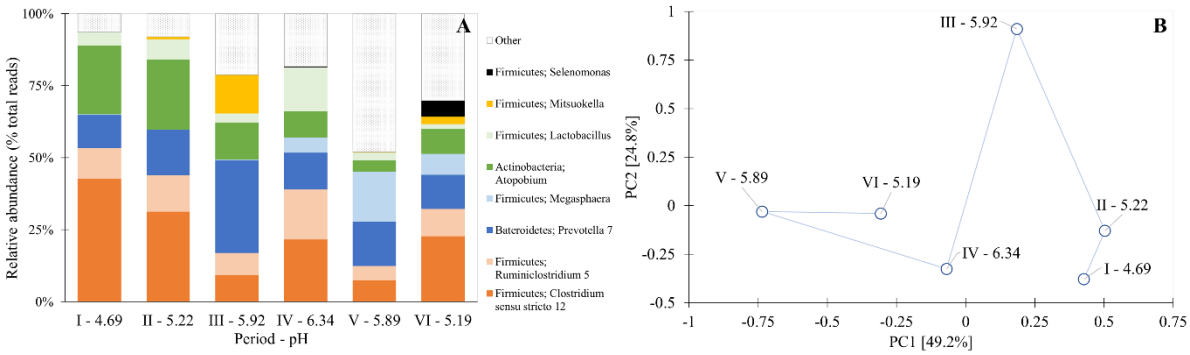

Figure 4.3 –Dynamics of the most relevant bacteria (A) and PCA ordination highlighting the differences/similarities in microbial communities (B) selected in the UASB reactor at the different pH setpoints (period – pH are represented in the data labels in B). The relative contribution (eigenvalue) of each axis to the total inertia in the data is indicated in percent at the axis titles.

It was observed that the presence of *Clostridium sensu stricto 12* and *Ruminiclostridium 5* seems to have a direct relation with HBut production (Figure 4.4 A) while the relative abundance of *Prevotella 7* and *Megasphaera* is directly correlated with the production of 3-HV precursors (HPro and HVal) (Figure 4.4 B). In fact, *Clostridium* was reported as the major HBut producing genera in the literature (Chai et

al., 2019) and *Ruminiclostridium 5* was demonstrated to be directly related with HBut production in other studies (Ribau Teixeira et al., 2020; Song et al., 2017). These two genera were observed in higher abundance at the periods I, II and IV (corresponding to pH 4.69, 5.22 and 6.34) (Figure 4.3 A), which were the periods of highest HBut production. On the other hand, *Prevotella* was associated to the production of HPro and HVal in anaerobic conditions (Precup and Vodnar, 2019; Tap et al., 2015) and *Megasphaera* was reported to convert HLac into HAce and HPro under glucose limiting conditions (Prabhu et al., 2012), a pathway that was discussed in this study (see section 4.4.1). *Prevotella 7* was present in increasing amounts as the pH increased from 4.69 to 5.92 (period I to III, Figure 4.3 A). Then, in phases V and VI (pH 5.89 and 5.19) the abundance of this genus significantly decreased when compared with similar pH phases (periods III and II, respectively) and it was instead observed an increase of *Megasphaera*.

Atopobium, Lactobacillus, Mitsuokella and Selenomonas are well-known HLac producers (Bryant, 1956; Dewhirst et al., 2001; Gouveia et al., 2017; Willems and Collins, 2015), which were present at an average relative abundance of more than 20% during all the operational period. The high fraction of those organisms in the community may indicate that, as hypothesised in section 4.4.1 – Impact of acidogenic pH on the PHA precursors composition, HLac is in lower amount in the fermentation broth because it is an intermediate for other SFP, such as HAce and HPro.

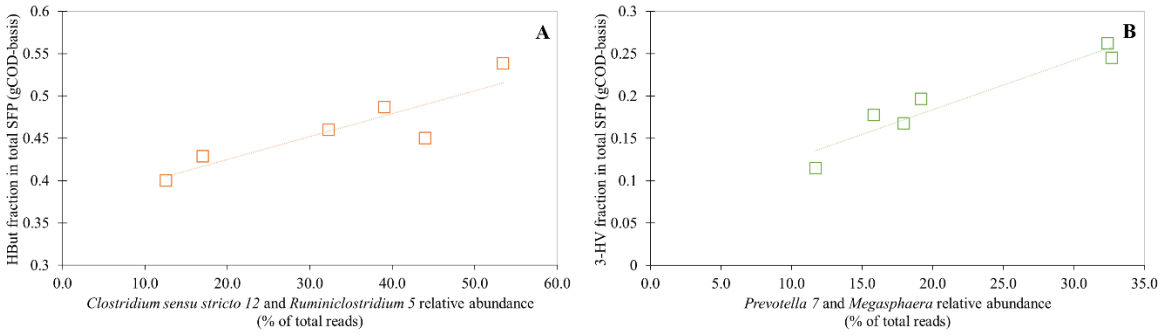

Figure 4.4 – HBut fraction as a function of the relative abundace of *Clostridium sensu stricto 12 and Ruminiclostridium 5* (A) and 3-HV precursors fraction relation with *Prevotella 7* and *Megasphaera* relative abundance (B)

The microbial profile enriched in the reactor clearly changed with the operating pH as evidenced by the distance of the corresponding points in the PCA plot (Figure 4.3 B). Additionally, despite the similar SFP profiles obtained at similar pH (period II/VI and III/V) those cultures greatly diverged in terms of composition, showing the functional redundancy of the microbial communities selected.

Overall, as observed in other studies using acidogenic CSTRs (Gouveia et al., 2017), in this case the granular microbial community varied dynamically in response to changes in pH, allowing the manipulation of the fraction of 3-HV bioprecursors.

4.4.3 Impact of pH on the polymer composition

The variation of the acidogenic pH imposed different SFP profiles production, which are, in their turn, precursors of P(3HB-*co*-3HV) with different monomeric compositions. Six fed batch PHA production assays were carried out using a selected PHA accumulating culture fed with the SFP produced at pH 4.69, 5.22 and 5.92 (Table 4.2).

As earlier hypothesised, it was observed that 3-HB monomers fraction was directly proportional to the fraction of HLac, HAce, EtOH and HBut (Figure 4.5 A) while the fraction of 3-HV monomers was directly proportional to the molar fraction of HPro and HVal (Figure 4.5 B). This is consistent with the metabolic pathways for SFP consumption and P(3HB-*co*-3HV) production that have been previously reported to predict the behaviour of mixed PHA producing cultures (Jiang et al., 2011; Lemos et al., 2006; Zhang, 2015). In total, it was possible to vary the fraction of 3-HV monomers of the polymer from 0.16 to 0.44, (gCOD-basis), which is correspondent to a variation of 27% in Cmol-basis. Those results are in the same order of magnitude than others obtained for acidogenic CSTRs operated under dynamic pH, e.g., the variation of 25% in 3-HV monomers fraction (Cmol-basis) achieved by Gouveia et al. 2017 using cheese whey or the 22% (Cmol-basis) achieved by Albuquerque et al. 2007 using sugar cane molasses.

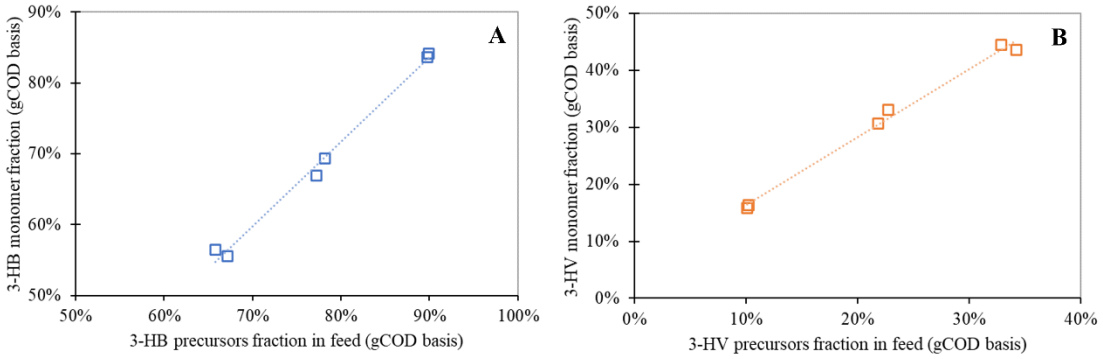

Figure 4.5 – 3-HB (A) and 3-HV (B) monomer fractions produced in the PHA production assays as a function of the corresponding different precursors present in the feed.

These assays clearly demonstrate that it was possible to manipulate the PHA monomeric composition through manipulating the pH of an acidogenic UASB reactor. As the 3-HV precursors production was linearly correlated with UASB pH (between 4.69 and 5.92), if a polymer with a higher 3-HV is required, the UASB should be operated at higher pH and vice-versa.

In a scenario of a real PHA production full-scale plant, the possibility of manipulating the PHA composition using the same feedstock by simply manipulating the operational pH of a UASB reactor could offer several advantages (e.g. simple solid/liquid separation process, high stability and reproducibility, high PHA volumetric productivity) that contribute to potential increase the economic feasibility of the process.

4.4.4 Model simulation results

4.4.4.1 Model calibration

A 251-day long-term dynamic simulation of the UASB experimental data reported by Matos et al. 2021was performed using both the original ADM1 and the modified ADM1 model developed in this study. The results for the total SFP, 3-HB and 3-HV precursors production are shown in Figure 4.6.

The original and modified ADM1 models exhibited substantial differences in the prediction of 3-HB and 3-HV precursors production (Figure 4.6). Both models did not describe well the first 37 d of reactor start-up, where the methanogenic culture present in the inoculum was active, causing perturbations in the system that are difficult to predict (Figure 4.6). This start-up period was not considered in the calculation of the average total SFP, 3-HB and 3-HV production values (observed and simulated) and respective MAEs and RMSEs represented in Table 4.8.

From day 41 onwards, the reactor pH ranged between 4.20 and 5.16 and both models were capable to reasonably predict total SFP production (Figure 4.6 A), as evidenced by the similar average, MAE and RMSE values represented in Table 4.8. However, as expected, the modified ADM1 developed in this study showed significant improvements with respect to the description of 3-HB and 3-HV bioprecursors production (Figure 4.6 B and C). The MAE and RMSE values for both precursors simulation using the modified ADM1 ranged between 2.2% and 2.9%, which is an acceptable range to accurately predict PHA monomeric composition, whereas ADM1 projected substantially higher 3-HV production, resulting in very high MAE and RMSE (around 22%) (Table 4.8). Between days 86 and 107, the OLR was increased from 17.6 until 30.1 $gCOD.L^{-1}.h^{-1}$ (Matos et al., 2021) and the developed model still described well total SFP and the different PHA precursors production.

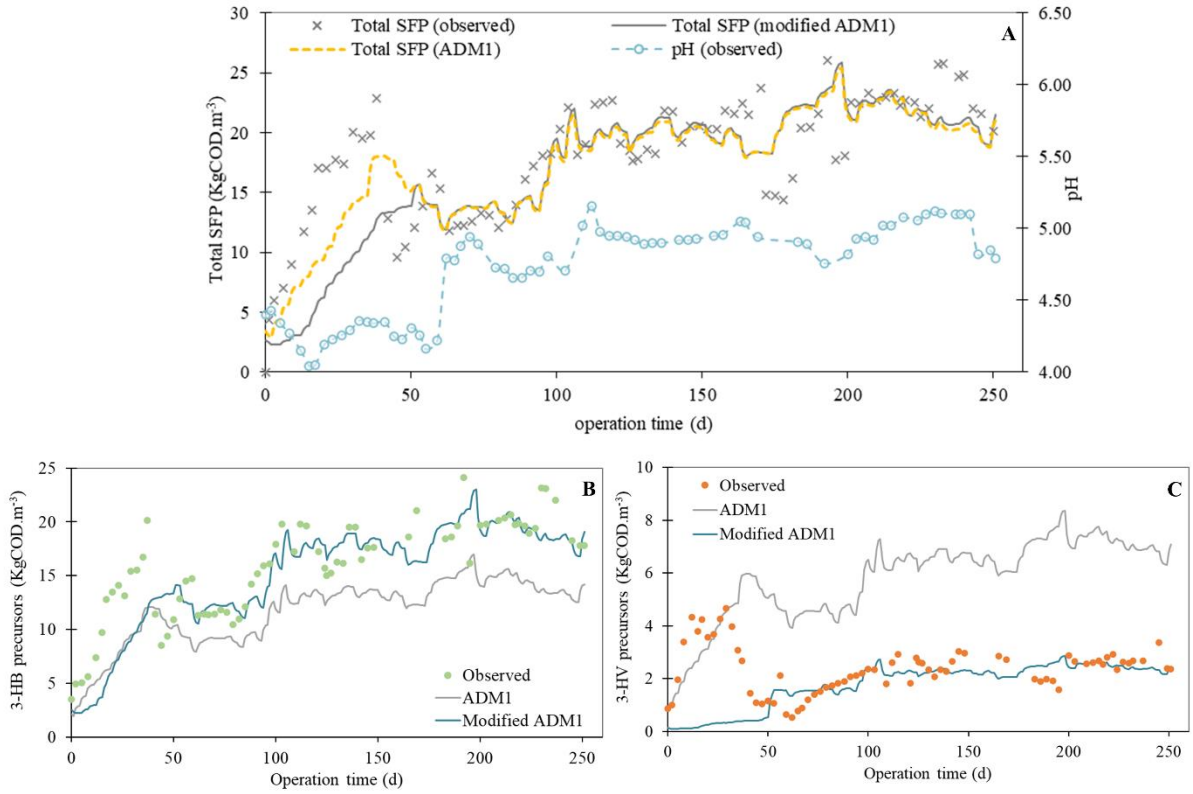

Figure 4.6 – Measured pH and observed total SFP (A), 3-HB (B) and 3-HV (C) bioprecursors production in calibration reactor and performance comparison between original ADM1 model and the modified ADM1 model developed in this study.

Table 4.8 – Model accuracy assessment for the period from day 41 onwards of the calibration reactor. Values are mean (standard deviation).

Variable	Observed	Predicted by modified ADM1	Predicted by ADM1	Modified ADM1		ADM1	
				MAE[a]	RMSE[b]	MAE[a]	RMSE[b]
Total SFP ($KgCOD.m^{-3}$)	19 (4)	19 (3)	20 (3)	2.00	2.63	2.21	2.92
3-HB precursors (% gCOD-basis)	89 (3)	89 (2)	66.7 (0.4)	2.21	2.91	21.87	22.01
3-HV precursors (% gCOD-basis)	11 (3)	11 (1)	33.3 (0.4)	2.19	2.89	21.87	22.01

[a] Mean absolute error

[b] Root mean square error

4.4.4.2 Model validation

The experimental data obtained from the UASB reactor presented in this study (see section 4.4.1 – Impact of acidogenic pH on the PHA precursors composition) was used to validate the model. This reactor was inoculated using previously acclimatised biomass (see section 4.2.1 – Acidogenic reactor setup), and the pH was set between 4.20 and 5.16 (Figure 4.7 A) during the first 178 days of operation, which is within the range observed for the period of UASB operation used for model calibration. For the following days of reactor operation (between 179 and 318), the pH varied between 5.16 and 6.41 (Figure 4.7 A). A comparison of predicted and experimental data, including total SFP, and 3-HB and 3-HV precursors production is shown in Figure 4.7.

The model developed in this work was capable to accurately predict total SFP production during the entire operating period (Figure 4.7 A), including the initial start-up phase, as evidenced by the low MAE and RMSE values of 1.56 and 1.97, respectively. The correlation between measured and modelled total SFP production is even more satisfactory than that observed for the calibration UASB (which displayed higher MAE and RMSE, Table 4.8). The fact that the model was capable to describe the SFP production for the start-up phase may have to do with the fact that previously acclimatised biomass was used in this case, which, contrasting to what happened for the calibration reactor, resulted in a negligible production of methane during this phase.

Regarding the specificity of precursors production during start-up, 3-HB predictions are quite satisfactory (Figure 4.7 B), while the simulated 3-HV precursors production was not well predicted during the first 35 d of operation (Figure 4.7 C). This behaviour may be related with the long storage period at cold temperatures at which the granules were subjected prior to inoculation and the difference between these conditions and the environmental conditions applied to the cells during reactor start-up.

From day 35 until day 178, the developed model was able to predict the microbial activity and PHA bioprecursors production for the validation UASB, as clearly observed in Figure 4.7 B and C, and supported by the low MAE and RMSE for both the 3-HB and 3-HV relative concentration, which were 2.0% and 2.5%, respectively. The model was even able to predict well the period where OLR was still being increased (from day 35 to 56, see section 4.4.1 – Impact of acidogenic pH on the PHA precursors composition), suggesting that the model is appropriate to describe PHA precursors production over a wide range of OLRs and for similar pH ranges than that observed in the calibration UASB. However, the 3-HV bioprecursors production was underestimated by the model for pH conditions different than that observed in the calibration UASB, such as for the higher pH values observed from day 179 onwards (Figure 4.7 C). At this stage, the MAE and RMSE for 3-HV relative concentration increased until 9.0% and 9.7%, respectively, which was considered to be unsatisfactory performance in predicting the 3-HV production by the expanded model. Previous studies have indicated that the type of SFP obtained during

acidogenesis is influenced by the operational conditions of hydrogen pressure (p_{H2}) and pH (Costello et al., 1991; Mosey, 1983; Shi et al., 2019). So, it can be hypothesised that to properly predict 3-HB and 3-HV production at a wider pH range, it is recommended to implement a variable acidogenic stoichiometric model approach in which acidogenesis is regulated by those two parameters, instead of the traditional assumptions where all the acidogenesis products are produced in constant proportions.

Overall, the results suggested that the modified model was capable to fully predict the long-term performance of the UASB reactors and achieved overall strong correlations with the experimental data for operational pH values ranging between 4.20 and 5.16. For pH setpoints above 5.16, the developed model describes well total SFP production, but not 3-HV precursors. Thus, if considering an appropriate pH range for model application, it can be a useful tool to support reactor design decisions, since it allows predicting important performance parameters (e.g., fermentation yield and SFP productivity) as a function of various pHs and OLRs observed.

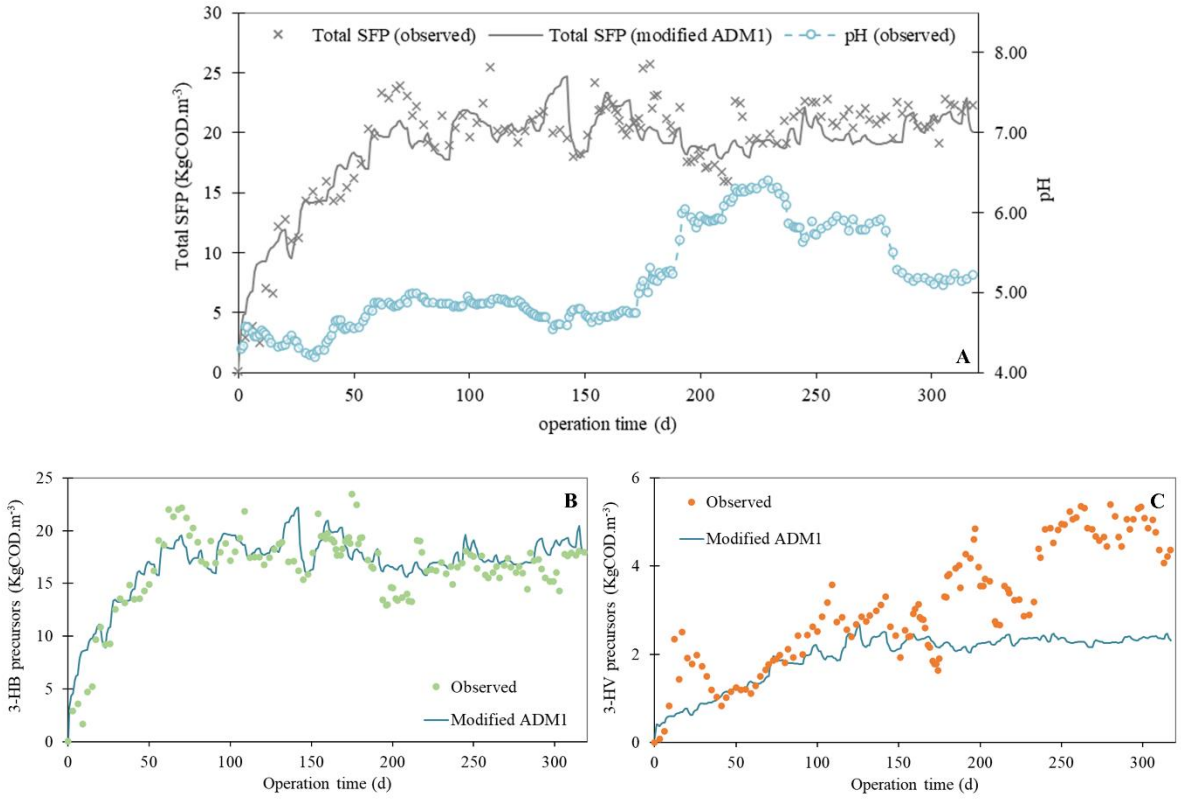

Figure 4.7 – Observed reactor pH and predicted versus measured results for total SFP (A), 3-HB (B) and 3-HV (C) precursors production in the validation UASB.

4.5 Conclusions

The production of 3-HV bioprecursors in an acidogenic UASB was manipulated using the operating pH as tuning parameter. The granular culture composition varied throughout the study, however it showed high levels of functional redundancy and stability, producing identical SFP composition for similar pH values.

Using the same 3-stage system and feedstock, operated in a continuous manner, it was possible to intentionally vary the 3-HV monomeric composition of P(3HB-*co*-3HV) from 0.16 to 0.44 (gCOD basis).

The pathway of production of valerate from lactate was, for the first time, incorporated in an ADM1 extension. The developed model was capable to achieve overall strong correlations with the measured total SFP production during all the operational periods of both calibration and validation UASBs. Additionally, the modified ADM1 predicted well the long-term performance of both reactors and achieved good correlations between predicted and measured 3-HB and 3-HV precursors production for the different OLRs tested over a limited range of operating pH values (between 4.20 and 5.16). The model still needs adjustments to predict 3-HV bioprecursors production at a wider range of pH conditions. Using a variable acidogenic stoichiometric model approach in which acidogenesis is regulated by pH and hydrogen pressure, instead of the traditional assumptions where all the acidogenesis products are produced in constant proportions, is recommended for future work.

4.6 References

Albuquerque, M.G.E., Eiroa, M., Torres, C., Nunes, B.R., Reis, M.A.M., 2007. Strategies for the development of a side stream process for polyhydroxyalkanoate (PHA) production from sugar cane molasses. J. Biotechnol. 130, 411–421. https://doi.org/10.1016/j.jbiotec.2007.05.011

Amann, R.I., 1995. In situ identification of micro-organisms by whole cell hybridization with rRNA-targeted nucleic acid probes, in: Molecular Microbial Ecology Manual. https://doi.org/10.1007/978-94-011-0351-0_23

Antonopoulou, G., Gavala, H.N., Skiadas, I. V., Lyberatos, G., 2012. Modeling of fermentative hydrogen production from sweet sorghum extract based on modified ADM1. Int. J. Hydrogen Energy 37, 191–208. https://doi.org/10.1016/j.ijhydene.2011.09.081

APHA, 1998. Standard Methods for Examination of Water and Wastewater, 20th ed, American Public Health Association, Washington, DC.

Atasoy, M., Eyice, O., Schnürer, A., Cetecioglu, Z., 2019. Volatile fatty acids production via mixed culture fermentation: Revealing the link between pH, inoculum type and bacterial composition. Bioresour. Technol. 292, 121889. https://doi.org/10.1016/j.biortech.2019.121889

Azbar, N., Ursillo, P., Speece, R.E., 2001. Effect of process configuration and substrate complexity on the performance of anaerobic processes. Water Res. 35, 817–829. https://doi.org/10.1016/S0043-1354(00)00318-3

Batstone, D.J. et al., 2002. Anaerobic Digestion Model No. 1 (ADM1). IWA Publishing.

Batstone, D.J., Keller, J., Angelidaki, I., Kalyuzhnyi, S. V., Pavlostathis, S.G., Rozzi, A., Sanders, W.T., Siegrist, H., Vavilin, V.A., 2002. The IWA Anaerobic Digestion Model No 1 (ADM1). Water Sci. Technol. https://doi.org/10.2166/wst.2002.0292

Bengtsson, S., Karlsson, A., Alexandersson, T., Quadri, L., Hjort, M., Johansson, P., Morgan-Sagastume, F., Anterrieu, S., Arcos-Hernandez, M., Karabegovic, L., Magnusson, P., Werker, A., 2017. A process for polyhydroxyalkanoate (PHA) production from municipal wastewater treatment with biological carbon and nitrogen removal demonstrated at pilot-scale. N. Biotechnol. 35, 42–53. https://doi.org/10.1016/j.nbt.2016.11.005

Bryant, M.P., 1956. The characteristics of strains of Selenomonas isolated from bovine rumen contents. J. Bacteriol. 72, 162–167. https://doi.org/10.1128/jb.72.2.162-167.1956

Campanari, S., Augelletti, F., Rossetti, S., Sciubba, F., Villano, M., Majone, M., 2017. Enhancing a multi-stage process for olive oil mill wastewater valorization towards polyhydroxyalkanoates and biogas production. Chem. Eng. J. 317, 280–289. https://doi.org/10.1016/j.cej.2017.02.094

Carvalheira, M., Duque, A., 2021. From Food Waste to Volatile Fatty Acids towards a Circular Economy, in: Fermentation - Processes, Benefits and Risks [Working Title]. IntechOpen, p. 13. https://doi.org/10.5772/intechopen.96542

Chai, L.-J., Lu, Z.-M., Zhang, X.-J., Ma, J., Xu, P.-X., Qian, W., Xiao, C., Wang, S.-T., Shen, C.-H., Shi, J.-S., Zheng-Hong, X., 2019. Zooming in on Butyrate-Producing Clostridial Consortia in the Fermented Grains of Baijiu via Gene Sequence-Guided Microbial Isolation. Front. Microbiol. 10. https://doi.org/10.3389/fmicb.2019.01397

Chen, H., Mao, Y.-Y., Jin, R.-C., 2020. What's the variation in anammox reactor performance after single and joint temperature based shocks? Sci. Total Environ. 713, 136609. https://doi.org/10.1016/j.scitotenv.2020.136609

Cheng, W., Chen, H., Yan, S.H., Su, J., 2014. Illumina sequencing-based analyses of bacterial communities during short-chain fatty-acid production from food waste and sewage sludge fermentation at different pH values. World J. Microbiol. Biotechnol. https://doi.org/10.1007/s11274-014-1664-6

Cirne, D.G., Bond, P., Pratt, S., Lant, P., Batstone, D.J., 2012. Microbial community analysis during continuous fermentation of thermally hydrolysed waste activated sludge. Water Sci. Technol. https://doi.org/10.2166/wst.2011.705

Costello, D.J., Greenfield, P.F., Lee, P.L., 1991. Dynamic modelling of a single-stage high-rate anaerobic reactor-I. Model derivation. Water Res. 25, 847–858. https://doi.org/10.1016/0043-1354(91)90166-N

Crocetti, G., Murto, M., Björnsson, L., 2006. An update and optimisation of oligonucleotide probes targeting methanogenic Archaea for use in fluorescence in situ hybridisation (FISH). J. Microbiol. Methods 65, 194–201. https://doi.org/10.1016/j.mimet.2005.07.007

Demirel, B., Yenigun, O., Onay, T.T., 2005. Anaerobic treatment of dairy wastewaters: a review. Process Biochem. 40, 2583–2595. https://doi.org/10.1016/j.procbio.2004.12.015

Dewhirst, F.E., Paster, B.J., Tzellas, N., Coleman, B., Downes, J., Spratt, D.A., Wade, W.G., 2001. Characterization of novel human oral isolates and cloned 16S rDNA sequences that fall in the family Coriobacteriaceae: description of olsenella gen. nov., reclassification of Lactobacillus uli as Olsenella uli comb. nov. and description of Olsenella profu. Int. J. Syst. Evol. Microbiol. 51, 1797–1804. https://doi.org/10.1099/00207713-51-5-1797

Duque, A.F., Oliveira, C.S.S., Carmo, I.T.D., Gouveia, A.R., Pardelha, F., Ramos, A.M., Reis, M.A.M., 2014. Response of a three-stage process for PHA production by mixed microbial cultures to feedstock shift: Impact on polymer composition. N. Biotechnol. 31, 276–288. https://doi.org/10.1016/j.nbt.2013.10.010

European Bioplastics, 2020. Bioplastics market data [WWW Document]. URL https://www.european-bioplastics.org/market/ (accessed 5.7.21).

Galí, A., Benabdallah, T., Astals, S., Mata-Alvarez, J., 2009. Modified version of ADM1 model for agro-waste application. Bioresour. Technol. 100, 2783–2790. https://doi.org/10.1016/j.biortech.2008.12.052

Girault, R., Rousseau, P., Steyer, J.P., Bernet, N., Béline, F., 2011. Combination of batch experiments with continuous reactor data for ADM1 calibration: Application to anaerobic digestion of pig slurry. Water Sci. Technol. 63, 2575–2582. https://doi.org/10.2166/wst.2011.594

Gouveia, A.R., Freitas, E.B., Galinha, C.F., Carvalho, G., Duque, A.F., Reis, M.A.M., 2017. Dynamic change of pH in acidogenic fermentation of cheese whey towards polyhydroxyalkanoates production: Impact on performance and microbial population. N. Biotechnol. 37, 108–116. https://doi.org/10.1016/j.nbt.2016.07.001

Greuter, D., Loy, A., Horn, M., Rattei, T., 2016. ProbeBase-an online resource for rRNA-targeted oligonucleotide probes and primers: New features 2016. Nucleic Acids Res. https://doi.org/10.1093/nar/gkv1232

Hassan, A.N., Nelson, B.K., 2012. Invited review: Anaerobic fermentation of dairy food wastewater. J. Dairy Sci. 95, 6188–6203. https://doi.org/10.3168/jds.2012-5732

Horiuchi, J.-I., Shimizu, T., Tada, K., Kanno, T., Kobayashi, M., 2002. Selective production of organic acids in anaerobic acid reactor by pH control. Bioresour. Technol. 82, 209–213. https://doi.org/10.1016/S0960-8524(01)00195-X

Jang, H.M., Kim, J.H., Ha, J.H., Park, J.M., 2014. Bacterial and methanogenic archaeal communities during the single-stage anaerobic digestion of high-strength food wastewater. Bioresour. Technol. 165, 174–182. https://doi.org/10.1016/j.biortech.2014.02.028

Jiang, Y., Marang, L., Kleerebezem, R., Muyzer, G., van Loosdrecht, M.C.M., 2011. Polyhydroxybutyrate production from lactate using a mixed microbial culture. Biotechnol. Bioeng. 108, 2022–2035. https://doi.org/10.1002/bit.23148

Jiang, Y., Marang, L., Tamis, J., van Loosdrecht, M.C.M., Dijkman, H., Kleerebezem, R., 2012. Waste to resource: Converting paper mill wastewater to bioplastic. Water Res. https://doi.org/10.1016/j.watres.2012.07.028

Lee, W.S., Chua, A.S.M., Yeoh, H.K., Ngoh, G.C., 2014. A review of the production and applications of waste-derived volatile fatty acids. Chem. Eng. J. https://doi.org/10.1016/j.cej.2013.09.002

Legendre, P., Gallagher, E.D., 2001. Ecologically meaningful transformations for ordination of species data. Oecologia. https://doi.org/10.1007/s004420100716

Lemos, P.C., Serafim, L.S., Reis, M.A.M., 2006. Synthesis of polyhydroxyalkanoates from different short-chain fatty acids by mixed cultures submitted to aerobic dynamic feeding. J. Biotechnol. https://doi.org/10.1016/j.jbiotec.2005.09.006

Lorini, L., Martinelli, A., Pavan, P., Majone, M., Valentino, F., 2020. Downstream processing and characterization of polyhydroxyalkanoates (PHAs) produced by mixed microbial culture (MMC) and organic urban waste as substrate. Biomass Convers. Biorefinery. https://doi.org/10.1007/s13399-020-00788-w

Mateus, S., Carvalheira, M., Cassidy, J., Freitas, E., Oehmen, A., Reis, M.A.M., 2020. Two-stage anaerobic digestion system treating different seasonal fruit pulp wastes: Impact on biogas and hydrogen production and total energy recovery potential. Biomass and Bioenergy 141. https://doi.org/10.1016/j.biombioe.2020.105694

Matos, M., Cruz, R.A.P., Cardoso, P., Silva, F., Freitas, E.B., Carvalho, G., Reis, M.A.M., 2021. Combined Strategies to Boost Polyhydroxyalkanoate Production from Fruit Waste in a Three-Stage Pilot Plant. ACS Sustain. Chem. Eng. acssuschemeng.1c02432. https://doi.org/10.1021/acssuschemeng.1c02432

Matos, M., Cruz, R.A.P., Cardoso, P., Silva, F., Freitas, E.B., Carvalho, G., Reis, M.A.M., 2021b. Sludge retention time impacts on polyhydroxyalkanoate productivity in uncoupled storage/growth processes. Sci. Total Environ. 799, 149363. https://doi.org/10.1016/j.scitotenv.2021.149363

Montiel-Jarillo, G., Carrera, J., Suárez-Ojeda, M.E., 2017. Enrichment of a mixed microbial culture for polyhydroxyalkanoates production: Effect of pH and N and P concentrations. Sci. Total Environ. 583, 300–307. https://doi.org/10.1016/j.scitotenv.2017.01.069

Moretto, G., Lorini, L., Pavan, P., Crognale, S., Tonanzi, B., Rossetti, S., Majone, M., Valentino, F., 2020. Biopolymers from urban organic waste: Influence of the solid retention time to cycle length ratio in the enrichment of a Mixed Microbial Culture (MMC). ACS Sustain. Chem. Eng. https://doi.org/10.1021/acssuschemeng.0c04980

Mosey, F.E., 1983. Mathematical modelling of the anaerobic digestion process: regulatory mechanisms for the forma tion of short-chain volatile acids from glucose. Wat. Sci.Tech. 15, 209–232.

Niu, Q., Qiao, W., Qiang, H., Li, Y.-Y., 2013. Microbial community shifts and biogas conversion computation during steady, inhibited and recovered stages of thermophilic methane fermentation on chicken manure with a wide variation of ammonia. Bioresour. Technol. 146, 223–233. https://doi.org/10.1016/j.biortech.2013.07.038

Parawira, W., Murto, M., Zvauya, R., Mattiasson, B., 2006. Comparative performance of a UASB reactor and an anaerobic packed-bed reactor when treating potato waste leachate. Renew. Energy 31, 893–903. https://doi.org/10.1016/j.renene.2005.05.013

Peiris, B.R.H., Rathnasiri, P.G., Johansen, J.E., Kuhn, A., Bakke, R., 2006. ADM1 simulations of hydrogen production. Water Sci. Technol. 53, 129–137. https://doi.org/10.2166/wst.2006.243

Peng, X., Zhang, S., Li, L., Zhao, X., Ma, Y., Shi, D., 2018. Long-term high-solids anaerobic digestion of food waste: Effects of ammonia on process performance and microbial community. Bioresour. Technol. 262, 148–158. https://doi.org/10.1016/j.biortech.2018.04.076

Pittmann, T., Steinmetz, H., 2013. Influence of operating conditions for volatile fatty acids enrichment as a first step for polyhydroxyalkanoate production on a municipal waste water treatment plant. Bioresour. Technol. 148, 270–276. https://doi.org/10.1016/j.biortech.2013.08.148

Prabhu, R., Altman, E., Eiteman, M.A., 2012. Lactate and Acrylate Metabolism by Megasphaera elsdenii under Batch and Steady-State Conditions. Appl. Environ. Microbiol. 78, 8564–8570. https://doi.org/10.1128/AEM.02443-12

Precup, G., Vodnar, D.-C., 2019. Gut Prevotella as a possible biomarker of diet and its eubiotic versus dysbiotic roles: a comprehensive literature review. Br. J. Nutr. 122, 131–140. https://doi.org/10.1017/S0007114519000680

Ribau Teixeira, M., Guarda, E.C., Freitas, E.B., Galinha, C.F., Duque, A.F., Reis, M.A.M., 2020. Valorization of raw brewers' spent grain through the production of volatile fatty acids. N. Biotechnol. 57, 4–10. https://doi.org/10.1016/j.nbt.2020.01.007

Sabapathy, P.C., Devaraj, S., Meixner, K., Anburajan, P., Kathirvel, P., Ravikumar, Y., Zabed, H.M., Qi, X., 2020. Recent developments in Polyhydroxyalkanoates (PHAs) production – A review. Bioresour. Technol. 306, 123132. https://doi.org/10.1016/j.biortech.2020.123132

Sagar, N.A., Pareek, S., Sharma, S., Yahia, E.M., Lobo, M.G., 2018. Fruit and Vegetable Waste: Bioactive Compounds, Their Extraction, and Possible Utilization. Compr. Rev. Food Sci. Food Saf. 17, 512–531. https://doi.org/10.1111/1541-4337.12330

Shi, E., Li, J., Zhang, M., 2019. Application of IWA Anaerobic Digestion Model No. 1 to simulate butyric acid, propionic acid, mixed acid, and ethanol type fermentative systems using a variable acidogenic stoichiometric approach. Water Res. 161, 242–250. https://doi.org/10.1016/j.watres.2019.05.094

Song, Y., Malmuthuge, N., Steele, M.A., Guan, L.L., 2017. Shift of hindgut microbiota and microbial short chain fatty acids profiles in dairy calves from birth to pre-weaning. FEMS Microbiol. Ecol. https://doi.org/10.1093/femsec/fix179

Tamis, J., Lužkov, K., Jiang, Y., Loosdrecht, M.C.M. va., Kleerebezem, R., 2014a. Enrichment of Plasticicumulans acidivorans at pilot-scale for PHA production on industrial wastewater. J. Biotechnol. https://doi.org/10.1016/j.jbiotec.2014.10.022

Tamis, J., Marang, L., Jiang, Y., van Loosdrecht, M.C.M., Kleerebezem, R., 2014b. Modeling PHA-producing microbial enrichment cultures—towards a generalized model with predictive power. N. Biotechnol. 31, 324–334. https://doi.org/10.1016/j.nbt.2013.11.007

Tap, J., Furet, J., Bensaada, M., Philippe, C., Roth, H., Rabot, S., Lakhdari, O., Lombard, V., Henrissat, B., Corthier, G., Fontaine, E., Doré, J., Leclerc, M., 2015. Gut microbiota richness promotes its stability upon increased dietary fibre intake in healthy adults. Environ. Microbiol. 17, 4954–4964. https://doi.org/10.1111/1462-2920.13006

Tedesco, D.E.A., Conti, C., Lovarelli, D., Biazzi, E., Bacenetti, J., 2019. Bioconversion of fruit and vegetable waste into earthworms as a new protein source: The environmental impact of earthworm meal production. Sci. Total Environ. 683, 690–698. https://doi.org/10.1016/j.scitotenv.2019.05.226

Venkiteshwaran, K., Bocher, B., Maki, J., Zitomer, D., 2016. Relating Anaerobic Digestion Microbial Community and Process Function. Microbiol. Insights. https://doi.org/10.4137/MBI.S33593

Wang, X., Carvalho, G., Reis, M.A.M., Oehmen, A., 2018. Metabolic modeling of the substrate competition among multiple VFAs for PHA production by mixed microbial cultures. J. Biotechnol. https://doi.org/10.1016/j.jbiotec.2018.06.342

Willems, A., Collins, M.D., 2015. Mitsuokella, in: Bergey's Manual of Systematics of Archaea and Bacteria. Wiley, pp. 1–9. https://doi.org/10.1002/9781118960608.gbm00698

Yu, H.Q., Mu, Y., Fang, H.H.P., 2004. Thermodynamic analysis of product formation in mesophilic acidogenesis of lactose. Biotechnol. Bioeng. 87, 813–822. https://doi.org/10.1002/bit.20190

Zhang, D., Wang, G., Wang, X., Zhao, J., Jia, B., Dai, X., 2020. Co-fermentation of waste activated sludge and agricultural waste for hydrogen production: effect of the carbon-to-nitrogen mass ratio. Desalin. WATER Treat. 173, 57–64. https://doi.org/10.5004/dwt.2020.24701

Zhang, Y., Ma, H., Niu, Q., Chen, R., Hojo, T., Li, Y.-Y., 2016. Effects of substrate shock on extracellular polymeric substance (EPS) excretion and characteristics of attached biofilm anammox granules. RSC Adv. 6, 113289–113297. https://doi.org/10.1039/C6RA20097D

Zhang, Y.P., 2015. The Influence of Different Carbon Sources for Polyhydroxyalkanoates Storage. Adv. Mater. Res. 1088, 587–590. https://doi.org/10.4028/www.scientific.net/AMR.1088.587

5

GENERAL CONCLUSIONS AND FUTURE WORK

5.1 General conclusions

This PhD Thesis was focused on solving the main bottlenecks (at the production level) that constrain the full-scale implementation of the PHA production process from waste-based feedstocks using MMCs: the high manufacturing costs associated to the low process performance and the ability to consistently manipulate, tailor and predict the polymer composition, and thus its properties.

The first part presented in this Thesis gave important insight about the impact of the SRT and OLR on the PHA producing MMC performance. These two parameters are known to greatly impact on the global process productivity and were poorly studied in the literature for selection reactors where the carbon (real feedstock) was fed uncoupled from the nitrogen source, as implemented in this study. It was observed that similar increase in PHA-producing biomass productivity was achieved for increasing OLR values, independently of the SRT used. However, higher-SRT cultures have faster storage kinetics and enhanced maximum accumulation capacity resulting in a global PHA productivity higher than that observed for lower-SRT communities. So, to maximise the global process performance, higher OLRs are preferred in the selection reactor, to increase biomass concentration, and should be combined with higher SRTs to increase polymer storage rates and microbial accumulation capacity.

Then, some optimal individual strategies investigated within the MMC PHA production process over the past twenty years were implemented as an integrated methodology to make PHA from MMC economically competitive. It was found that the pH of the acidogenic reactor can be manipulated at the same time to maximise fermentation yield and to fine-tune soluble fermentation products, in order to obtain a PHA precursors profile that benefits the PHA storing rate and yield. In the selection reactor it is important to feed the culture under uncoupled carbon and nitrogen availabilities to maintain the selection efficiency when using high operating OLRs (which are set to increase biomass productivity). And lastly, it was observed that a continuous feeding strategy should be applied to the PHA accumulation reactor to maximise PHA content on biomass. When using those optimal conditions combined in one single process, unprecedent global PHA productivities and overall yields could be obtained, having a direct impact on the investment and operational costs of the process. Therefore, it can be anticipated that, if these two critical parameters are maximised, a reduction of the final PHA production costs will be achieved. In the present study, using fruit waste as feedstock in a 3-stage process implemented at pilot scale, the combined strategies approach led to the highest performance values reported for MMC using complex feedstocks. Moreover, the selected culture was capable to produce a P(3HB-*co*-3HV) copolymer with a 3-HV content of 0.24 (g-basis) and a molecular weight of 311 KDa, which makes this material an ideal candidate for packaging applications, the largest market for bioplastic usage. Overall, the results obtained in this study clearly demonstrate the potential for full-scale implementation of the PHA production using fruit waste as substrate.

The third part of the thesis successfully demonstrated the possibility of manipulating PHA monomeric composition using the operating pH of a pilot-scale acidogenic UASB as tuning parameter

to obtain the desired PHA precursors. Additionally, it was observed that high levels of functional redundancy and stability in the PHA precursors profile could be obtained for similar pH setpoints implemented at different times of the operation. A model was developed to describe UASB performance as a function of pH and OLR. Although the model still needs improvements, a powerful predictive tool came out of this study. The extended AMD1 implemented was capable to achieve overall strong correlations with the measured total fermentation products obtained for all the pH and OLRs tested in the acidogenic reactor, and predicted well the 3-HB and 3-HV precursors production over a limited range of operating pH values.

This Thesis highlighted the importance of understanding the impact of key individual operating conditions on the overall performance of the MMC PHA integrated production process to increase its global feasibility. Moreover, it demonstrated that deeply knowing and accurately regulating and predicting the acidogenic process is essential to promote the production of the desired PHA monomeric composition, which are encouraging results towards the full-scale implementation of the PHA production from MMC and wastes.

5.2 Future work and perspectives

The results obtained during this PhD indicate that the main constrains for industrial application of the MMC PHA production process have been identified and substantial progress has been done towards overcoming them. Overall, the most important key performance parameters (PHA content on biomass, global productivity and overall yield) were clearly optimised, and the possibility of controlling the polymer composition at pilot scale level, using a reactor configuration that facilitates the production process, was proven. Nevertheless, some aspects that contribute to the minimisation of the product costs still need to be further assessed in future research.

First, it is important to evaluate more deeply the impact of some operating parameters in the selection reactor, for instance, the SRT should be increased above the values tested in this study and evaluate its impact on culture selection, polymer storage performance and global productivity; also, operating at higher HRTs reduce the necessity of diluting the feed stream, so, in this case, the impact of using higher HRTs should be further evaluated in order to decrease the working volume of the selection reactor as much as possible without jeopardizing the process performance, a strategy that will possibly reduce the global capital and operational costs significantly. Another critical point that may be further optimised to improve the economic viability of the process is the dosage of allylthiourea. This chemical was added in the pilot selection reactor used in this study as a way of preventing nitrification and reducing the amount of unknown factors, as it is not currently identified if the selected PHA-producing MMCs can be enriched on nitrate as nitrogen source instead of ammonium. However, allylthiourea dosage in a full-scale plant is not acceptable for economic and environmental reasons, so future research should evaluate the impact of not preventing nitrification at all or, in case of extremely necessity, propose cheaper and

eco-friendly alternatives. Lastly, one of the preconditions to establish a proper feast-famine regime in the selection stage is to avoid oxygen depletion during the feast phase, so oxygen transfer rate was promoted in excess (by using high air flow rates and high stirring speeds) during all the operating periods. Maintaining the oxygen transfer at high levels, especially in a reactor with high biomass concentration, is highly costly and involves expensive industrial fermentation reactors. To reduce process costs, the lowest threshold value of oxygen concentration (in both feast and famine phases) that promotes a successful MMC selection with a good PHA production performance should be identified as a guideline for future process implementation.

The PHA production using wastes as feedstock is an alternative to the conventional wastewater treatment process, so, besides the resource recovering objective there are also the compromise of delivery clean water to the environment at the end of the process. To evaluate if the global effluent meets the wastewater treatment practices, COD and nutrients should be measured in all the waste streams of the process. If those levels are above the established standards, solutions for treating those effluents should be investigated. Additionally, the possibility of recycling some of those streams should be investigated to prevent the wastage of large amounts of fresh water used for dilution and equipment cleaning.

The last future work suggestion targeting specifically the PHA production process has to do with the process economics. Although the results presented in this project suggest that the upstream part of the MMC PHA production process from wastes was reasonably optimised, a detailed techno-economic analysis is still required to effectively prove the feasibility of the process.

Regarding the modelling work, to properly predict 3-HB and 3-HV precursors production in the acidogenic reactor at a wider pH range, it is recommended to investigate the possibility of implementing a variable acidogenic stoichiometric model approach in which acidogenesis is regulated by hydrogen pressure and pH, instead of the traditional method where all the fermentation products are produced in constant proportions. Furthermore, ideally, the accuracy of the developed model should be tested for other agri-food feedstocks. However, due to the complexity of the selected microbial communities and the differences between fermentation products synthesis pathways observed for different microorganisms, the conversion of the variable types of organic carbon present in waste streams into PHA bioprecursors is not yet fully standardised. It could be difficult to investigate the individual performance for each population in a mixed culture. However, acidogenic cultures with similar microbial composition should share common tendencies when subjected to similar types of feed and reactor conditions. Future metabolic model work could be developed to link microbial profile to specific process parameters and stoichiometry in order to accurately describe PHA precursors production for a wider range of feedstock using the same model approach.

Besides the aspects specifically related with this Thesis project, there are still some aspects in the PHA production chain that require optimisation to enable full-scale implementation of waste based PHA production technology using MMCs. In particular, the development of cheaper and eco-friendly

downstream processes and managing the product characteristics in the context of commercial applications are crucial aspects that need further investigation to bring forward this sustainable approach for PHA production. Moreover, the evaluation of all the health, legislation and marketing aspects related to the usage of a waste-derived product should also be considered.

APPENDIX A

Supporting information for Chapter 2

A.1 Experimental section (Materials and Methods)

Experimental Setup

The upflow anaerobic sludge blanket (UASB) reactor was made of plexiglass with a height of 2.00 m and an internal diameter of 0.244 m.

The sequencial batch reactor (SBR) consisted of a cylindrical vessel made of stainless steel with 0.8 m of working height and a height-to-diameter ratio of 2. The culture was aerated by sparging air through a ring sparger (0.110 m diameter) and agitated with a six-blade Rushton turbine (0.135 m diameter and 0.035 m height) positioned in the bottom part of the reactor shaft and an upper Pitch blade (0.200 m diameter and 0.040 m height).

The accumulation assays were carried out in a stainless-steel cylindrical reactor with 0.63 m of working height and a height-to-diameter ratio of 2. Air was supplied through a ring sparger (0.085 m diameter) and the stirring system was composed by a six-blade Rushton turbine (0.110 m diameter and 0.030 m height) and a Pitch blade (0.160 m diameter and 0.032 m height).

Analytical methods

SFP concentrations were determined through high performance liquid chromatography (HPLC) using a VWR Hitachi Chromaster equipped with a Biorad pre-column, an Aminex column and a RI and UV detectors (wavelength of 210 nm). 99 µm of the filtered samples (0.45 µm) were eluted with 0.01 N H_2SO_4 at a flow rate of 0.5 $mL.min^{-1}$ and 30 °C of operating temperature. The SFP concentrations were calculated through calibration curves using 15-1000 $mg.L^{-1}$ standards.

Regarding PHA analysis, samples were processed using the method described by Lanham et al. (2013). 3-hydroxybutyrate (3-HB) and 3-hydroxyvalerate (3-HV) monomer concentrations of lyophilised biomass samples were quantified by gas chromatography (GC) using a flame ionization detector (GC-FID 430-GC, Bruker) and a Restek Stabilwax-column (60 m length, 0.53 mm ID, 1 µm d_f, Crossbond) and using helium as carrier gas (1.0 $mL.min^{-1}$). The monomers concentrations were calculated using two calibration curves, one for 3-HB and other for 3-HV, using standards (0.1 – 8.0 $g.L^{-1}$) of a commercial P(3-HB-*co*-3-HV) (88%:12%, 3-HB:3-HV, molar-basis) (Sigma) and corrected using heptadecane as internal standard (~1$g.L^{-1}$).

Microbiological analyses

The microbial community structure and the abundance of the different populations was analysed through semi-qualitative fluorescence *in situ* hybridization (FISH) on biomass samples fixed with 4% paraformaldehyde or ethanol (Nielsen, 2009) performed according to (Amann, 1995). More details about the following fluorescently labelled oligonucleotide probes used for the FISH experiments are available in the database probeBase 2016 (Greuter et al., 2016), unless specified: Fluorescein isothiocyanate (FITC)-labelled EUBmix probe for all Bacteria (mixture of EUB338, EUB338-II and EUB338-III) mixed with the cyanine 3 (Cy3) - labelled probes PAR651 for *Paracoccus*, LAMP444 for *Lampropedia* (Lee et al., 2004), AMAR839 for *Amaricoccus*, G Rb for *Rhodobacter* and *Roseobacter* and Meg983 and Meg1028 for *Meganema* (Thomsen et al., 2006).

Samples were observed using an Epifluorescence microscope Zeiss Imager D2 at 1000X.

Calculations

All concentrations (3-HB, 3-HV, SFP and X_a) were converted into COD in accordance with the following factors: 1.67 g-COD.g-3-HB^{-1}, 1.92 g-COD.g-3-HV^{-1}, 1.07 g-COD.g-HLac^{-1}, 1.07 g-COD.g-HAce^{-1}, 1.51 g-COD.g-HPro^{-1}, 2.08 g-COD.g-EtOH^{-1}, 1.82 g-COD.g-HBut^{-1}, 2.04 g-COD.g-HVaç$^{-1}$and 1.41 g-COD.g-X_a^{-1} (X_a formula of $C_5H_7NO_2$ (Gujer and Henze, 1991)).

A.2 Results and discussion

Feast to famine ratio along operation

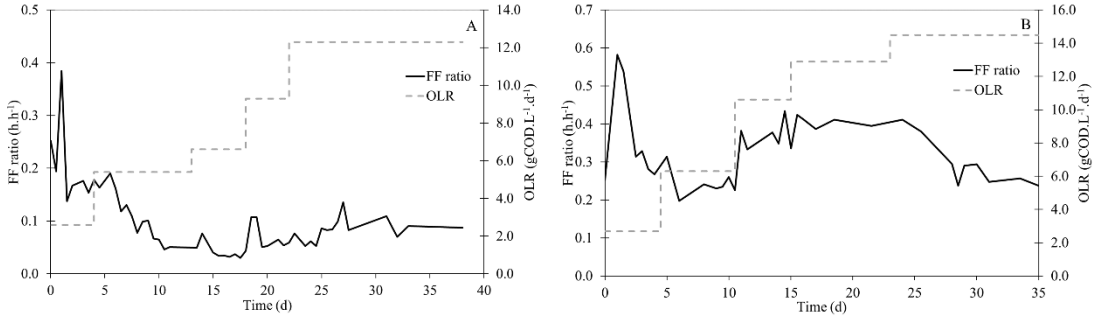

Figure A1 - Feast to famine ratio and OLR change over time in SBR 4d (A) and SBR 2d (B).

Microbial community results

Table A1 - High throughput 16S sequencing data of the most abundant bacterial populations present in the selection reactor at the different OLR tested and SRT of 4 days. (P_Phylum, c_class; genus level).

OLR ($gCOD.L^{-1}.d^{-1}$)	Inoculum	6.6	12.3
c_Alphaproteobacteria; Paracocccus	5.8	87.2	26.8
c_Alphaproteobacteria; Aminobacter	0.3	3.4	6.8
c_Alphaproteobacteria; o__DB1-14	0.0	0.2	12.2
c_Alphaproteobacteria; Thioclava	0.0	0.5	6.8
c_Alphaproteobacteria; Rhodobacter	6.4	0.3	0.1
c_Alphaproteobacteria; Amaricoccus	0.0	0.6	6.1
c_Alphaproteobacteria; Brevundimonas	0.0	0.4	5.9
c_Alphaproteobacteria; f__Rhodobacteraceae	2.0	0.2	8.6
c_Alphaproteobacteria; MNG7	6.1	0.0	0.0
P_Actinobacteria; Leucobacter	5.3	0.0	0.0
P_Firmicutes; Romboutsia	5.2	0.0	0.0
c_Alphaproteobacteria; f__Bradyrhizobiaceae	6.0	0.0	0.0
P_Actinobacteria; Nakamurella	0.0	1.1	3.8
c_Betaproteobacteria; Azoarcus	0.0	0.1	3.3
c_Alphaproteobacteria; f__Hyphomicrobiaceae	4.3	0.2	1.4
c_Alphaproteobacteria; Shinella	2.5	0.1	0.4
c_Gammaproteobacteria; Thermomonas	3.0	0.0	0.0
c_Alphaproteobacteria; Hyphomicrobium	2.9	0.0	0.0
P_Bacteroidetes; Flavobacterium	0.1	0.7	2.1
c_Alphaproteobacteria; f__Phyllobacteriaceae	2.1	0.3	0.6
c_Alphaproteobacteria; f__Rhizobiaceae	2.4	0.0	0.0
c_Alphaproteobacteria; Bosea	1.9	0.3	0.2
c_Betaproteobacteria; f__Comamonadaceae	0.0	0.5	2.9
P_Firmicutes; Clostridium sensu stricto	1.9	0.3	0.2
c_Alphaproteobacteria; Xanthobacter	1.4	0.0	0.1
P_Actinobacteria; Tetrasphaera	1.5	0.0	0.0
P_Actinobacteria; Fodinicola	1.4	0.0	0.0
P_Actinobacteria; f__Microthricaceae	2.4	0.0	0.0

Table A2 - High throughput 16S sequencing data of the most abundant bacterial populations present in the selection reactor at the different OLR tested and SRT of 2 days. (P_Phylum, c_class; genus level).

OLR ($gCOD.L^{-1}.d^{-1}$)	Inoculum	6.3	12.9	14.5
c_Betaproteobacteria; Lampropedia	0.0	0.0	0.2	33.0
c_Alphaproteobacteria; f__Rhodobacteraceae	3.3	4.1	21.7	20.2
P_Actinobacteria; Leucobacter	5.0	5.1	10.5	2.1
c_Alphaproteobacteria; f__Rhizobiales Incertae Sedis	0.7	18.5	3.9	0.8
c_Alphaproteobacteria; Gemmobacter	1.1	6.6	10.7	0.4
c_Alphaproteobacteria; Paracocccus	2.8	2.7	9.6	3.4
c_Alphaproteobacteria; Thioclava	0.0	1.5	4.2	11.4
c_Gammaproteobacteria; Thiothrix	14.9	0.2	0.0	0.0
c_Alphaproteobacteria; Amaricoccus	0.0	3.3	1.9	9.6
c_Alphaproteobacteria; Shinella	1.0	10.0	0.8	0.2
P_Actinobacteria; Microbacterium	0.2	2.7	6.9	0.4
c_Betaproteobacteria; Acidovorax	0.4	2.8	6.4	0.1
c_Alphaproteobacteria; f__Xanthobacteraceae	0.3	7.8	1.1	0.1
P_Bacteroidetes; Leadbetterella	0.0	0.1	5.2	1.2
c_Alphaproteobacteria; Rhodobacter	3.7	1.9	0.1	0.0
c_Alphaproteobacteria; f__Hyphomicrobiaceae	1.6	1.9	1.6	0.6
P_Actinobacteria; Marmoricola	4.7	0.1	0.0	0.0
c_Alphaproteobacteria; Meganema	0.6	0.4	0.3	3.4
c_Alphaproteobacteria; MNG7	4.1	0.1	0.0	0.0
c_Gammaproteobacteria; Pseudoxanthomonas	0.5	2.8	0.3	0.6
c_Alphaproteobacteria; Bosea	1.1	2.6	0.2	0.1
P_Firmicutes; Lactobacillus	0.2	0.1	1.3	1.9
c_Gammaproteobacteria; Thermomonas	3.2	0.2	0.1	0.0
c_Alphaproteobacteria; f__Phyllobacteriaceae	2.4	3.6	0.7	0.2
P_Firmicutes; Romboutsia	3.1	0.0	0.0	0.0
P_Bacteroidetes; Flavobacterium	0.0	1.3	1.5	0.2
c_Alphaproteobacteria; Devosia	0.3	0.8	1.4	0.5
c_Alphaproteobacteria; o__Rhizobiales	0.1	2.7	0.2	0.0
P_Actinobacteria; f__PeM15	2.7	0.1	0.0	0.0
c_Alphaproteobacteria; f__Bradyrhizobiaceae	3.1	0.1	0.0	0.0
c_Alphaproteobacteria; Hyphomicrobium	2.0	0.3	0.0	0.0

Table A3 - Identification of putative PHA-storers and respective relative abundance (% of total reads) determined by high throughput 16S sequencing. For each identified taxonomic group, a reference (Ref.) reporting the suggested PHA storing ability is provided.

		SBR 4d			SBR 2d				
family	**genus**	**I**[a]	**6.6**	**12.3**	**I**[a]	**6.3**	**12.9**	**14.5**	**Ref.**
Rhodobacteraceae[b]	-	2.0	0.2	8.6	3.3	4.1	21.7	20.2	-
Comamonadaceae	*Lampropedia*	0.0	0.0	0.0	0.0	0.0	0.2	33.0	(Koller et al., 2010)
Rhodobacteraceae	*Paracocccus*	5.8	87.2	26.8	2.8	2.7	9.6	3.4	(Koller et al., 2010)
Rhodobacteraceae	*Amaricoccus*	0.0	0.6	6.1	0.0	3.3	1.9	9.6	(Falvo et al., 2001)
Comamonadaceae	*Acidovorax*	0.0	0.0	0.0	0.4	2.8	6.4	0.1	(Schulze et al., 1999)
Spirosomaceae	*Leadbetterella*	0.0	0.0	0.0	0.0	0.1	5.2	1.2	(Shen et al., 2015)
Rhodobacteraceae	*Rhodobacter*	6.4	0.3	0.1	3.7	1.9	0.1	0.0	(Koller et al., 2010)
Neomegalonemataceae	*Meganema*	1.1	0.1	0.1	0.6	0.4	0.3	3.4	(D. Dionisi et al., 2005)
Xanthomonadaceae	*Pseudoxanthomonas*	0.0	0.0	0.0	0.5	2.8	0.3	0.6	(Mwamburi et al., 2019)
Flavobacteriaceae	*Flavobacterium*	0.1	0.7	2.1	0.0	1.3	1.5	0.2	(Davide Dionisi et al., 2005)
Phyllobacteriaceae	*Aminobacter*	0.3	3.4	6.8	0.0	0.0	0.0	0.0	(Wang et al., 2020)
Caulobacteraceae	*Brevundimonas*	0.0	0.4	5.9	0.0	0.0	0.0	0.0	(Bhuwal et al., 2013)
Zoogloeaceae	*Azoarcus*	0.0	0.1	3.3	0.0	0.0	0.0	0.0	(Carvalho et al., 2014)
Xanthobacteraceae	*Xanthobacter*	1.4	0.0	0.1	0.0	0.0	0.0	0.0	(Koller et al., 2010)
Boseaceae	*Bosea*	1.9	0.3	0.2	1.1	2.6	0.2	0.1	(Huang et al., 2012)
	TOTAL	18.9	93.3	60.2	12.3	21.9	47.4	71.8	

[a]Inoculum

[b]This family was characterised using FISH (results above) which suggested that it was mostly comprised of genera reported to contain PHA-storing organisms.

FISH was done with biomass samples taken at different OLRs to complement DNA sequencing results and to exclude some possible bias that can occur during the high throughput sequencing of the 16s rRNA gene (Větrovský and Baldrian, 2013). The probes applied were selected according with the high throughput sequencing data (Table C1 and C2).

Table A4 - FISH analysis of the bacterial community over time.

Reactor	OLR ($gCOD.L^{-1}.d^{-1}$)	PAR651 (*Paracoccus*)	LAMP444 (*Lampropedia*)	AMAR839 (*Amaricoccus*)	G Rb (*Rhodobacter* +*Roseobacter*)	Meg 983+1028 (*Meganema*)
SBR 4d	Inoculum	+-	-	+-	++	+-
	6.6	+++	-	+	+++	-
	12.3	++	-	+-	+++	+-
SBR 2d	Inoculum	+-	+-	-	+-	-
	6.3	+-	-	+-	++	+-
	12.9	+++	+	+-	+++	+
	14.5	++	++	+-	++	+

(-) not-detected; (+-) almost non-existent; (+) present; (++) abundant; (+++) dominant

The obtained FISH results corroborated the sequencing data and the enrichment of the SBR 4d with *Paracoccus*, with a strong positive signal of the PAR651 and G Rb over time (Table C4), noting that the latter probe also targets members of the genus *Paracoccus* and Rhodobactereaceae family.

For the SBR 2d, there was an increase in *Lampropedia* and *Meganema* at OLR of 12.9 and 14.5 $gCOD.L^{-1}.d^{-1}$ (Table C4), which was also indicated in the high throughput sequencing results.

The signal of the G Rb, PAR651 and AMAR839 over time indicates that the members targeted by the probe G Rb were mostly comprised of genera reported to contain PHA-storing organisms (namely *Paracoccus* and *Amaricoccus*). Due to this reason, the OTU belonging to the family Rhodobacteraceae previously identified in the high throughput sequencing analysis was considered to consist of putative PHA-storer (Table C3).

PHA monomers produced

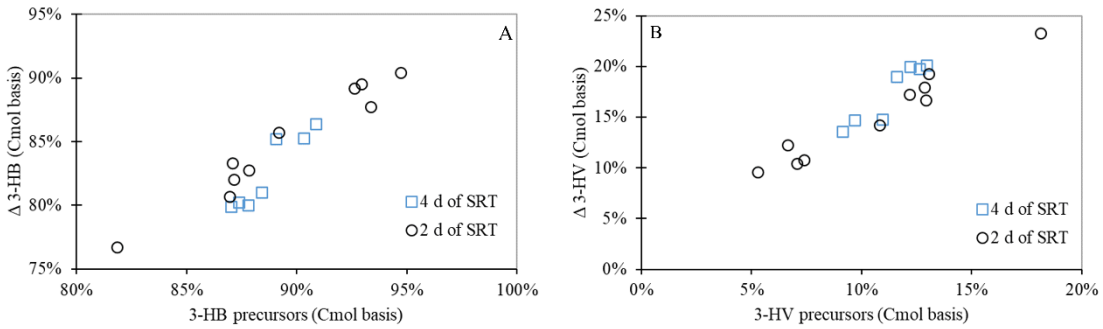

Figure A2 - Δ3-HB (A) and Δ3-HV (B) monomers produced during SBR cycles and accumulation assays as a function of the corresponding 3-HB and 3-HV precursors molar fraction in the feed.

A.3 References

Amann, R.I., 1995. In situ identification of micro-organisms by whole cell hybridization with rRNA-targeted nucleic acid probes, in: Molecular Microbial Ecology Manual. https://doi.org/10.1007/978-94-011-0351-0_23

Bhuwal, A.K., Singh, G., Aggarwal, N.K., Goyal, V., Yadav, A., 2013. Isolation and Screening of Polyhydroxyalkanoates Producing Bacteria from Pulp, Paper, and Cardboard Industry Wastes. Int. J. Biomater. 2013, 1–10. https://doi.org/10.1155/2013/752821

Carvalho, G., Oehmen, A., Albuquerque, M.G.E., Reis, M.A.M., 2014. The relationship between mixed microbial culture composition and PHA production performance from fermented molasses. N. Biotechnol. 31, 257–263. https://doi.org/10.1016/j.nbt.2013.08.010

Dionisi, Davide, Beccari, M., Gregorio, S.D., Majone, M., Papini, M.P., Vallini, G., 2005. Storage of biodegradable polymers by an enriched microbial community in a sequencing batch reactor operated at high organic load rate. J. Chem. Technol. Biotechnol. https://doi.org/10.1002/jctb.1331

Dionisi, D., Carucci, G., Papini, M.P., Riccardi, C., Majone, M., Carrasco, F., 2005. Olive oil mill effluents as a feedstock for production of biodegradable polymers. Water Res. 39. https://doi.org/10.1016/j.watres.2005.03.011

Falvo, A., Levantesi, C., Rossetti, S., Seviour, R.J., Tandoi, V., 2001. Synthesis of intracellular storage polymers by Amaricoccus kaplicensis, a tetrad forming bacterium present in activated sludge. J. Appl. Microbiol. 91, 299–305. https://doi.org/10.1046/j.1365-2672.2001.01384.x

Greuter, D., Loy, A., Horn, M., Rattei, T., 2016. ProbeBase-an online resource for rRNA-targeted oligonucleotide probes and primers: New features 2016. Nucleic Acids Res. https://doi.org/10.1093/nar/gkv1232

Gujer, W., Henze, M., 1991. Activated sludge modelling and simulation, in: Water Science and Technology. https://doi.org/10.2166/wst.1991.0553

Huang, Y.T., Chen, P.L., Semblante, G.U., You, S.J., 2012. Detection of polyhydroxyalkanoate-accumulating bacteria from domestic wastewater treatment plant using highly sensitive PCR primers. J. Microbiol. Biotechnol. 22, 1141–1147. https://doi.org/10.4014/jmb.1111.11040

Koller, M., Atlić, A., Dias, M., Reiterer, A., Braunegg, G., 2010. Microbial PHA Production from Waste Raw Materials. pp. 85–119. https://doi.org/10.1007/978-3-642-03287-5_5

Lanham, A.B., Ricardo, A.R., Albuquerque, M.G.E., Pardelha, F., Carvalheira, M., Coma, M., Fradinho, J., Carvalho, G., Oehmen, A., Reis, M.A.M., 2013. Determination of the extraction kinetics for the quantification of polyhydroxyalkanoate monomers in mixed microbial systems. Process Biochem. https://doi.org/10.1016/j.procbio.2013.07.023

Lee, N., Cellamare, C.M., Bastianutti, C., Rosselloó-Mora, R., Kämpfer, P., Ludwig, W., Schleifer, K.H., Stante, L., 2004. Emended description of the species Lampropedia hyalina. Int. J. Syst. Evol. Microbiol. https://doi.org/10.1099/ijs.0.02885-0

Mwamburi, S.M., Mbatia, B.N., Remmy, K., Kirwa, E.M., Noah, N.M., 2019. Production of polyhydroxyalkanoates by hydrocarbonaclastic bacteria. African J. Biotechnol. 18, 352–364. https://doi.org/10.5897/AJB2019.16763

Nielsen, P.H., 2009. FISH Handbook for Biological Wastewater Treatment. Water Intell. Online. https://doi.org/10.2166/9781780401775

Schulze, R., Spring, S., Amann, R., Huber, I., Ludwig, W., Schleifer, K.H., Kämpfer, P., 1999. Genotypic diversity of Acidovorax strains isolated from activated sludge and description of Acidovorax defluvii sp. nov. Syst. Appl. Microbiol. 22, 205–214. https://doi.org/10.1016/S0723-2020(99)80067-8

Shen, L., Hu, H., Ji, H., Zhang, C., He, N., Li, Q., Wang, Y., 2015. Production of poly(3-hydroxybutyrate-co-3-hydroxyhexanoate) from excess activated sludge as a promising substitute of pure culture. Bioresour. Technol. 189, 236–242. https://doi.org/10.1016/j.biortech.2015.04.007

Thomsen, T.R., Blackall, L.L., Aquino de Muro, M., Nielsen, J.L., Nielsen, P.H., 2006. Meganema perideroedes gen. nov., sp. nov., a filamentous alphaproteobacterium from activated sludge. Int. J. Syst. Evol. Microbiol. https://doi.org/10.1099/ijs.0.02916-0

Větrovský, T., Baldrian, P., 2013. The Variability of the 16S rRNA Gene in Bacterial Genomes and Its Consequences for Bacterial Community Analyses. PLoS One 8, 1–10. https://doi.org/10.1371/journal.pone.0057923

Wang, X., Oehmen, A., Carvalho, G., Reis, M.A.M., 2020. Community profile governs substrate competition in polyhydroxyalkanoate (PHA)-producing mixed cultures. N. Biotechnol. 58, 32–37. https://doi.org/10.1016/j.nbt.2020.03.003

APPENDIX B

Supporting information for Chapter 3

B.1 Experimental section (Materials and Methods)

Experimental Setup

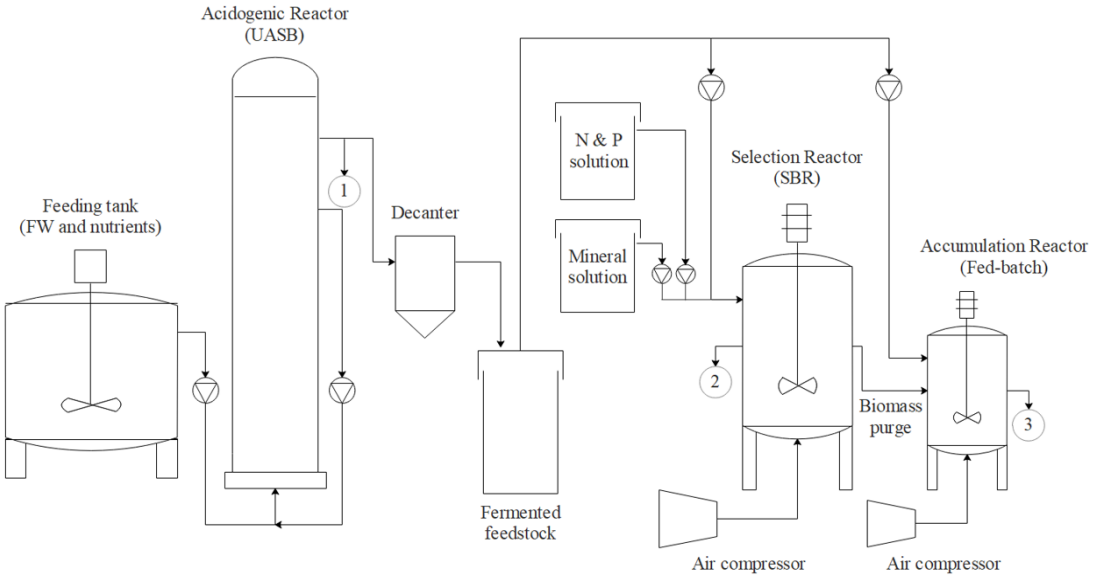

Figure B1 - Experimental setup of the pilot PHA production process using fruit waste as feedstock. Grey circles with 1, 2 and 3 identify the sampling points of the UASB (only effluent), SBR and accumulation reactors, respectively.

The upflow anaerobic sludge blanket (UASB) reactor was made of plexiglass with a height of 2.00 m and an internal diameter of 0.244 m.

The sequencial batch reactor (SBR) consisted of a cylindrical vessel made of stainless steel with 0.8 m of working height and a height-to-diameter ratio of 2. The culture was aerated by sparging air through a ring sparger (0.110 m diameter) and agitated with a six-blade Rushton turbine (0.135 m diameter and 0.035 m height) positioned in the bottom part of the reactor shaft and an upper Pitch blade (0.200 m diameter and 0.040 m height).

The accumulation assays were carried out in a stainless-steel cylindrical reactor with 0.63 m of working height and a height-to-diameter ratio of 2. Air was supplied through a ring sparger (0.085 m diameter) and the stirring system was composed by a six-blade Rushton turbine (0.110 m diameter and 0.030 m height) and a Pitch blade (0.160 m diameter and 0.032 m height).

Analytical methods

The concentration of the soluble fermentation products – SFP – (lactate, acetate, propionate, ethanol, butyrate and valerate) was determined in filtered samples (0.45 µm) through high performance liquid chromatography (HPLC) using a VWR Hitachi Chromaster equipped with a Biorad 125-0129 30 x 4.6 mm pre-column, Aminex HPX-87H 300 x 7.8 mm column and RI and UV (wavelength 210 nm) detectors. 0.01 N H_2SO_4 was used to elute 99 µm samples at a flow rate of 0.5 $mL.min^{-1}$ and 30 °C operating temperature. The concentrations of organic acids and ethanol were calculated through a standard curve with concentration between 15-1000 $mg.L^{-1}$ of each compound.

The biogas composition (H_2, N_2, O_2, CH_4 and CO_2) was determined on wet analysis through a gas chromatograph (Agilent 7890B, Agilent Technologies), equipped with a TCD detector. 0.25 mL of gas sample was injected on a 30 m Carbonex 1010 Plt column at 35 °C using helium as mobile phase at 1 $mL.min^{-1}$ during 50 min. The injector temperature was set at 200 °C.

Ammonium and phosphate were quantified by colorimetric methods implemented in a segmented flow analyser (Skalar San++, Skalar Analytical).

PHA was quantified by gas chromatography (GC) (430-GC, Bruker) using a flame ionization detector (FID) and a Restek Stabilwax-column (60 m length, 0.53 mm ID, 1 µm d_f, Crossbond).

The biomass concentration of SBR and MAP assays was determined using the volatile suspended solids (VSS) protocol described in standard methods.(APHA, 1998)

Microbiological analyses

Sludge samples were taken from the SBR reactor throughout the operating period and were phylogenetically characterized. DNA was extracted using the standard protocol for FastDNA Spin kit for soil (MP Biomedicals, USA) with the following exceptions: 500 µL of sample, 480 µL Sodium Phosphate Buffer and 120 µL MT Buffer were added to a Lysing Matrix E tube. 16S rRNA gene amplicon sequencing and bioinformatic processing was carried out using Illumina technology by DNASense (Aalborg, Denmark).

The microbial community structure and the abundance of the different populations was also analysed on biomass samples fixed with 4% paraformaldehyde or ethanol(Nielsen, 2009) through semi-qualitative fluorescence *in situ* hybridization (FISH) performed according to ref (Amann, 1995). More details about the following fluorescently labelled oligonucleotide probes used for the FISH experiments are available in the database probeBase 2016(Greuter et al., 2016), unless specified: Fluorescein isothiocyanate (FITC)-labelled EUBmix probe for all Bacteria (mixture of EUB338, EUB338-II and EUB338-III) mixed with the cyanine 3 (Cy3) - labelled probes PAR651 for *Paracoccus*, LAMP444 for

Lampropedia(Lee et al., 2004), AMAR839 for *Amaricoccus*, G Rb for *Rhodobacter* and *Roseobacter* and Meg983 and Meg1028 for *Meganema*(Thomsen et al., 2006).

Samples were observed using an Epifluorescence microscope Zeiss Imager D2 at 1000X.

Calculations

SFP, PHA monomers (3-HB and 3-HV) and active biomass (X_a) concentrations were converted into COD in accordance with the following oxidation stoichiometry: 1.07 gCOD.g-lactate^{-1}, 1.07 gCOD.g-acetate^{-1}, 1.51 gCOD.g-propionate^{-1}, 2.08 gCOD.g-ethanol^{-1}, 1.82 gCOD.g-butyrate^{-1}, 2.04 gCOD.g-valerate^{-1}, 1.67 gCOD.g-3-HB^{-1}, 1.92 gCOD.g-3-HV^{-1} and 1.41 gCOD.g-X_a^{-1}, considering the chemical biomass formula $C_5H_7NO_2$ (Gujer and Henze, 1991).

The feast to famine length ratio (FF ratio, h.h^{-1}) was calculated as the fraction between the lengths of feast and famine phases observed in each cycle.

The percentages of PHA content in biomass (%, g-basis) were determined by dividing quantified PHA by measured VSS concentration. The active biomass concentrations (X_a, g.L^{-1}) were calculated by the difference between VSS (g.L^{-1}) and PHA (g.L^{-1}).

The biomass volumetric productivities (P_X, g-X_a.L^{-1}.d^{-1}) were calculated by dividing active biomass concentration (g-X_a.L^{-1}) by sludge retention time (SRT, d).

Specific uptake rates (-q_{SFP}, gCOD-SFP.gCOD-X_a^{-1}.L^{-1}) and specific storage rates ($q_{PHA,}$ gCOD-PHA.gCOD-X_a^{-1}.h^{-1}) were determined from the linear regression of total and individual SFP and PHA specific concentrations, respectively, plotted over time.

The storage yields ($Y_{PHA/SFP}$, gCOD-PHA.gCOD-SFP^{-1}) were calculated as the ratio between q_{PHA} and -q_{SFP}.

The growth yields on PHA ($Y_{X/PHA}$, gCOD-X_a.gCOD-PHA^{-1}) were calculated by dividing active biomass formed by total amount of PHA consumed.

The global PHA productivity (g-PHA.L^{-1}.d^{-1}) takes in consideration the second and third steps of the process and can be calculated as:

$$global\ PHA\ productivity = P_X * \frac{PHA^{Acc}}{X_a^{Acc}}$$

where,

P_X (g-X_a.L^{-1}.d^{-1}) is the biomass volumetric productivity in the selection reactor;

PHA^{Acc} (g-PHA.L^{-1}) is the maximum concentration of PHA achieved at the end of accumulation assay;

X_a^{Acc} (g-X_a.L^{-1}) is the active biomass concentration inoculated in the accumulation assay that produced the corresponding PHA^{Acc} amount;

B.2 Results and discussion

Acidogenic reactor results

Table B1 - Operating conditions applied and performance parameters determined at pseudo-steady-state of UASB reactor. Values presented are mean (standard deviation).

operating conditions	value
HRT (d)	1
OLR ($gCOD.L^{-1}.d^{-1}$)	29.2 (2)
C:N:P ratio (g-basis)	100:0.5:0.1
reactor performance	**value**
SFP concentration ($gCOD.L^{-1}$)	21.7 (2)
SFP [HLac/HAce/HPro/EtOH/HBut/HVal] ($gCOD.L^{-1}$)	2/4.0/1.5/1.1/12/1.2 (2/0.4/0.2/0.8/2/0.4)
$Y_{SFP/S}$ (gCOD-basis)	0.74 (0.09)
Biogas productivity ($L.L^{-1}.d^{-1}$)	7.4 (0.9)
Gas composition [$H_2/O_2/N_2/CH_4/CO_2$] (% molar-basis)	16/1.4/5/0/77 (3/0.4/2/0/3)

Microbial community results

Samples were taken from the inoculum and after achieving pseudo-steady-state with OLRs of 3.4 and 5.4 $gCOD.L^{-1}.d^{-1}$ to characterise the microbial communities. The results (Table S2) showed that an initially diverse community, containing many members of the *Proteobacteria*, *Firmicutes* and *Actinobacteria*, gave place to a more enriched community in the subsequent samples. *Paracoccus* increased from a low relative abundance (2.2%) to a dominant presence inside the SBR during operation at an OLR of 3.4 $gCOD.L^{-1}.d^{-1}$ (81.2%) and 5.4 $gCOD.L^{-1}.d^{-1}$ (75.3%). Semi-quantitative FISH analyses done on samples taken throughout the five different OLR phases confirmed the enrichment of the community in *Paracoccus* over time (Table S3). *Paracoccus* is a well-known bacterial genus with PHA storing capacity, its enrichment is strongly related with high concentration of HBut in the feed.(Albuquerque et al., 2013) *Paracoccus was* described in the literature as consuming a wide range of substrates with higher specific uptake rates, with the exception for HAce consumption which was only moderate.(Albuquerque et al., 2013; Moretto et al., 2020) The same behaviour was

observed in this work. Overall, there were only small changes in the microbial community along operation indicates that the culture was capable to deal with the increasing OLR and changes in substrate composition.

Table B2 - Most abundant bacterial populations present in the microbial community identified by 16S rRNA gene amplicon sequencing of the cultures enriched in the selection reactor at the different OLR tested. (P_Phylum, c_class; genus level).

OLR ($gCOD.L^{-1}.d^{-1}$)	Inoculum	3.4	5.4
c_Alphaproteobacteria; Paracocccus	2.2	81.2	75.3
c_Gammaproteobacteria; Thiothrix	11.9	0.0	0.0
P_Firmicutes; Leuconostoc	9.1	0.0	0.0
P_Firmicutes; Romboutsia	6.0	0.0	0.0
P_Planctomycetes; f_Planctomycetaceae*	4.3	0.1	0.2
P_Chloroflexi; Candidatus Defluviifilum	3.4	0.0	0.0
c_Alphaproteobacteria; Hyphomicrobium	3.2	0.3	0.2
P_Actinobacteria; Leucobacter	2.9	0.0	0.0
c_Alphaproteobacteria; Rhodobacter	2.9	0.2	0.3
P_Firmicutes; Clostridium sensu stricto	2.6	0.1	0.4
c_Alphaproteobacteria; MNG7	2.6	0.0	0.1
P_Actinobacteria; Marmoricola	2.2	0.0	0.0
c_Alphaproteobacteria; Gemmobacter	0.6	0.1	0.1
c_Alphaproteobacteria; Meganema	0.3	1.9	4.0
c_Alphaproteobacteria; Shinella	0.3	0.2	0.5
P_Firmicutes; Lactobacillus	0.2	0.2	0.6
Actinobacteria; Actinomyces	0.1	0.0	0.0
P_Actinobacteria; Microbacterium	0.1	0.6	0.2
c_Alphaproteobacteria; Aminobacter	0.0	5.1	6.2
c_Alphaproteobacteria; Amaricoccus	0.0	1.6	0.4
c_Betaproteobacteria; Lampropedia	0.0	0.3	0.0
P_Actinobacteria; Atopobium	0.0	0.2	0.4
c_Alphaproteobacteria; Thioclava	0.0	0.2	0.1
P_Bacteroidetes; Prevotella	0.0	0.1	0.2
P_Firmicutes; Ruminiclostridium	0.0	0.0	0.1

*Lowest phylogenetic category assigned for the OUT

Table B3 - FISH analysis of the bacterial community over time during the increased OLR imposed in the SBR.

OLR ($gCOD.L^{-1}.d^{-1}$)	**Par651** (Paracoccus)	**Lamp444** (Lampropedia)	**Amar839** (Amaricoccus)	**G Rb** (Rhodobacter+ Roseobacter)	**Meg 983+1028** (Meganema)
Inoculum	+-	-	+-	+-	+-
1.7	++	-	+	+++	-
2.4	+++	-	+	+++	-
3.4	+++	-	+-	+++	+-
5.4	+++	-	+-	+++	+-
8.7	+++	-	+-	+++	+-

Assumptions for global COD mass balance

The COD mass balance was based on the calculation of amount of active biomass needed to inoculate the accumulation reactor in order to produce 1 Kg of P(3HB-co-3HV) (with 0.24 g-basis of 3-HV monomers). All the experimental individual parameters used in the overall yield calculation are represented in Table S4.

Taking in consideration the average PHA content on biomass of 80.5% (g basis), obtained in the MAP tests for the biomass selected at an OLR of 5.4 $gCOD.L^{-1}.d^{-1}$, the SBR will need to generate 0.34 KgCOD of X_a. Using the storage yield observed in the accumulation runs (0.98 $gCOD.gCOD^{-1}$), it was calculated the SFP amount needed to produce 1 Kg of PHA (1.68 KgCOD of SFP). The calculations for the selection reactor were done considering the results obtained for the OLR of 5.4 $gCOD.L^{-1}.d^{-1}$, in this case the average X_a was 9.72 $gCOD.L^{-1}$ generated at a growth yield of 0.45 $KgCOD\text{-}X_a.KgCOD\text{-}SFP^{-1}$ and 25 L-purge is collected every day. Considering the applied OLR, 0.76 KgCOD of SFP will be necessary to generate 0.34 KgCOD of total purged X_a (, which result in a final amount of 2.44 KgCOD of SFP needed to feed the second and third stage of the process. The biomass was purged at the end of the cycle with a PHA content of 16% (g-basis) on average. The usage of the decanter unit reduced the SFP amount in 15%, trough reducing the SFP-reach stream flow. At last, the acidogenic fermentation showed a yield of 0.74 ($gCOD.gCOD^{-1}$) which means that, to have the 2.44 KgCOD of SFP after decanter step, an initial amount of 3.87 KgCOD of fruit waste (FW) should be fed into the system.

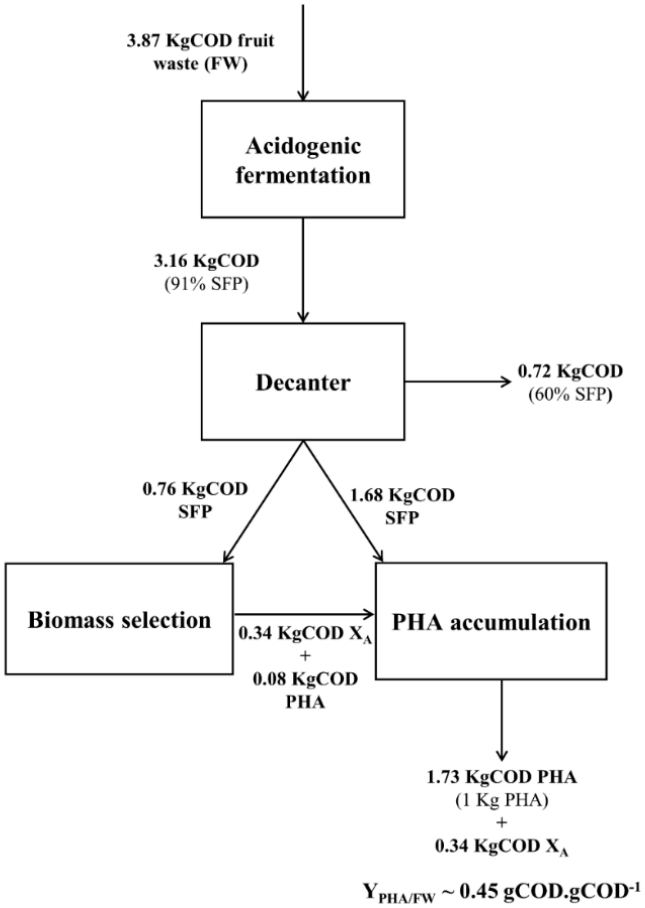

Figure B2 - COD flow in the 3-step PHA production process using fruit waste as carbon source and applying the combined effective strategies.

Table B4 - Process parameters used in the calculation of the overall PHA yield and comparison with literature studies.

Parameter	This study	References		
		Tamis et al. 2014	Tamis et al. 2018	Valentino et al. 2017
Feedstock	Fruit waste	Mars candy factory wastewaters	Paper mill wastewater	Synthetic feedstock
Fermentation yield (gCOD-SFP.gCOD-feed^{-1})	0.74	~0.74[a]	0.68	0.80
Growth yield of biomass on SFP (gCOD-X_a.gCOD-SFP^{-1})	0.45	0.39	0.42	0.30
Storage yield (gCOD-PHA.gCOD-SFP^{-1})	0.98	0.63	0.68	0.82
Max. PHA content (%, g-basis)	80.5	70	75	70
Overall PHA yield (gCOD-PHA.gCOD-feed^{-1})	0.45	0.30	0.34	0.42[b]

[a] estimated from the authors' results

[b] theoretical value that may be achieved considering best laboratory scale results (at that time)

B.3 References

Albuquerque, M.G.E., Carvalho, G., Kragelund, C., Silva, A.F., Barreto Crespo, M.T., Reis, M.A.M., Nielsen, P.H., 2013. Link between microbial composition and carbon substrate-uptake preferences in a PHA-storing community. ISME J. 7, 1–12. https://doi.org/10.1038/ismej.2012.74

Amann, R.I., 1995. In situ identification of micro-organisms by whole cell hybridization with rRNA-targeted nucleic acid probes, in: Molecular Microbial Ecology Manual. https://doi.org/10.1007/978-94-011-0351-0_23

APHA, 1998. Standard Methods for Examination of Water and Wastewater, 20th ed, American Public Health Association, Washington, DC.

Greuter, D., Loy, A., Horn, M., Rattei, T., 2016. ProbeBase-an online resource for rRNA-targeted oligonucleotide probes and primers: New features 2016. Nucleic Acids Res. https://doi.org/10.1093/nar/gkv1232

Gujer, W., Henze, M., 1991. Activated sludge modelling and simulation, in: Water Science and Technology. https://doi.org/10.2166/wst.1991.0553

Lee, N., Cellamare, C.M., Bastianutti, C., Rosselloó-Mora, R., Kämpfer, P., Ludwig, W., Schleifer, K.H., Stante, L., 2004. Emended description of the species Lampropedia hyalina. Int. J. Syst. Evol. Microbiol. https://doi.org/10.1099/ijs.0.02885-0

Moretto, G., Lorini, L., Pavan, P., Crognale, S., Tonanzi, B., Rossetti, S., Majone, M., Valentino, F., 2020. Biopolymers from urban organic waste: Influence of the solid retention time to cycle length ratio in the enrichment of a Mixed Microbial Culture (MMC). ACS Sustain. Chem. Eng. https://doi.org/10.1021/acssuschemeng.0c04980

Nielsen, P.H., 2009. FISH Handbook for Biological Wastewater Treatment. Water Intell. Online. https://doi.org/10.2166/9781780401775

Tamis, J., Lužkov, K., Jiang, Y., Loosdrecht, M.C.M. va., Kleerebezem, R., 2014. Enrichment of Plasticicumulans acidivorans at pilot-scale for PHA production on industrial wastewater. J. Biotechnol. https://doi.org/10.1016/j.jbiotec.2014.10.022

Tamis, J., Mulders, M., Dijkman, H., Rozendal, R., van Loosdrecht, M.C.M.M., Kleerebezem, R., 2018. Pilot-Scale Polyhydroxyalkanoate Production from Paper Mill Wastewater: Process Characteristics and Identification of Bottlenecks for Full-Scale Implementation. J. Environ. Eng. (United States). https://doi.org/10.1061/(ASCE)EE.1943-7870.0001444

Thomsen, T.R., Blackall, L.L., Aquino de Muro, M., Nielsen, J.L., Nielsen, P.H., 2006. Meganema perideroedes gen. nov., sp. nov., a filamentous alphaproteobacterium from activated sludge. Int. J. Syst. Evol. Microbiol. https://doi.org/10.1099/ijs.0.02916-0

Valentino, F., Morgan-Sagastume, F., Campanari, S., Villano, M., Werker, A., Majone, M., 2017. Carbon recovery from wastewater through bioconversion into biodegradable polymers. N. Biotechnol. 37, 9–23. https://doi.org/10.1016/j.nbt.2016.05.007

APPENDIX C

Supporting information for Chapter 4

C.1 Kinetic matrix of the model

Table C1 - Kinetic matrix of the model. Description of kinetic and stoichiometric parameters can be found in Table C2.

j	Symbol	Name	S_{SUG}	S_{AA}	S_{LCFA}	S_{VAL}	S_{BUT}	S_{LAC}	S_{ET}	S_{PROP}	S_{AC}
1	r1	Hydrolysis of Carbohydrates	1.0								
2	r2	Hydrolysis of Proteins		1.0							
3	r3	Hydrolysis of Lipids	$1-f_{LCFA,LIP}$		$f_{LCFA,LIP}$						
4	r4	Uptake of Sugars	-1.0				$(1-Y_{SUG})*f_{BUT,SUG}$	$(1-Y_{SUG})*f_{LAC,SUG}$	$(1-Y_{SUG})*f_{ET,SUG}$		$(1-Y_{SUG})*f_{AC,SUG}$
5	r5	Uptake of Amino Acids		-1.0		$(1-Y_{AA})*f_{VAL,AA}$	$(1-Y_{AA})*f_{BUT,AA}$			$(1-Y_{AA})*f_{PROP,AA}$	$(1-Y_{AA})*f_{AC,AA}$
6	r6	Uptake of LCFA			-1.0						$(1-Y_{LCFA})*0.7$
7	r7	Uptake of Lactate				$(1-Y_{LAC})*f_{VAL,LAC}$		-1.0		$(1-Y_{LAC})*f_{PROP,LAC}$	$(1-Y_{LAC})*f_{AC,LAC}$
8	r8	Uptake of Valerate				-1.0				$(1-Y_{C4})*0.54$	$(1-Y_{C4})*0.31$
9	r9	Uptake of Butyrate					-1.0				$(1-Y_{C4})*0.8$
10	r10	Uptake of Propionate								-1.0	$(1-Y_{PROP})*0.57$
11	r11	Uptake of Acetate									-1.0
12	r12	Uptake of Hydrogen									
13	r13	Decay of X_{SUG}									
14	r14	Decay of X_{AA}									
15	r15	Decay of X_{LCFA}									
16	r16	Decay of X_{LAC}									
17	r17	Decay of X_{C4}									
18	r18	Decay of X_{PRO}									
19	r19	Decay of X_{AC}									
20	r20	Decay of X_{H2}									

Table C1 – Kinetic matrix of the model (cont.). Description of kinetic and stoichiometric parameters can be found in Table C2.

j	Symbol	Name	S_{H2}	S_{CH4}	S_U	X_{CH}	X_{PROT}	X_{LIP}	X_{SUG}	X_{AA}	X_{LCFA}
1	r1	Hydrolysis of Carbohydrates				-1.0					
2	r2	Hydrolysis of Proteins					-1.0				
3	r3	Hydrolysis of Lipids						-1.0			
4	r4	Uptake of Sugars	$(1-Y_{SUG})*f_{H2,SUG}$						Y_{SUG}		
5	r5	Uptake of Amino Acids	$(1-Y_{AA})*f_{H2,AA}$							Y_{AA}	
6	r6	Uptake of LCFA	$(1-Y_{LCFA})*0.3$								Y_{LCFA}
7	r7	Uptake of Lactate	$(1-Y_{LAC})*f_{H2,LAC}$								
8	r8	Uptake of Valerate	$(1-Y_{C4})*0.15$								
9	r9	Uptake of Butyrate	$(1-Y_{C4})*0.2$								
10	r10	Uptake of Propionate	$(1-Y_{PROP})*0.43$								
11	r11	Uptake of Acetate		$(1-Y_{AC})$							
12	r12	Uptake of Hydrogen	-1.0	$(1-Y_{H2})$							
13	r13	Decay of X_{SUG}			$f_{Su,BM}$	$f_{CH,BM}$	$f_{PROT,BM}$	$f_{LIP,BM}$	-1.0		
14	r14	Decay of X_{AA}			$f_{Su,BM}$	$f_{CH,BM}$	$f_{PROT,BM}$	$f_{LIP,BM}$		-1.0	
15	r15	Decay of X_{LCFA}			$f_{Su,BM}$	$f_{CH,BM}$	$f_{PROT,BM}$	$f_{LIP,BM}$			-1.0
16	r16	Decay of X_{LAC}			$f_{Su,BM}$	$f_{CH,BM}$	$f_{PROT,BM}$	$f_{LIP,BM}$			
17	r17	Decay of X_{C4}			$f_{Su,BM}$	$f_{CH,BM}$	$f_{PROT,BM}$	$f_{LIP,BM}$			
18	r18	Decay of X_{PRO}			$f_{Su,BM}$	$f_{CH,BM}$	$f_{PROT,BM}$	$f_{LIP,BM}$			
19	r19	Decay of X_{AC}			$f_{Su,BM}$	$f_{CH,BM}$	$f_{PROT,BM}$	$f_{LIP,BM}$			
20	r20	Decay of X_{H2}			$f_{Su,BM}$	$f_{CH,BM}$	$f_{PROT,BM}$	$f_{LIP,BM}$			

Table C1– Kinetic matrix of the model (cont.). Description of kinetic and stoichiometric parameters can be found in Table C2.

j	Symbol	Name	X_{C4}	X_{LAC}	X_{PROP}	X_{AC}	X_{H2}	$X_{E,AN}$	Rates [a]
1	r1	Hydrolysis of Carbohydrates							$k_{hyd,CH}*X_{CH}$
2	r2	Hydrolysis of Proteins							$k_{hyd,PROT}*X_{PROT}$
3	r3	Hydrolysis of Lipids							$k_{hyd,LIP}*X_{LIP}$
4	r4	Uptake of Sugars							$k_{m,SUG}*Msat_{SSUG,Ks,SUG}*X_{SUG}*I_{pH,acid}*Noncompinh_{SNHx,IIN,BAC}$
5	r5	Uptake of Amino Acids							$k_{m,AA}*Msat_{SAA,Ks,AA}*X_{AA}*I_{pH,acid}*Noncompinh_{SNHx,IIN,BAC}$
6	r6	Uptake of LCFA							$k_{m,LCFA}*Msat_{SLCFA,Ks,LCFA}*X_{LCFA}*I_{pH,acet}*Noncompinh_{SNHx,IIN,BAC}*Noncompinh_{SH2,IH2\_Xlcfa}$
7	r7	Uptake of Lactate		Y_{LAC}					$k_{m,LAC}*Msat_{SLAC,Ks,LAC}*X_{LAC}*I_{pH,lac}*Noncompinh_{SNHx,IIN,BAC}$
8	r8	Uptake of Valerate	Y_{C4}						$k_{m,C4}*Msat_{SVAL,Ks,C4}*Lim_{SBUT,SVAL}*I_{pH,acet}*Noncompinh_{SNHx,IIN,BAC}*Noncompinh_{SH2,IH2\_Xc4}$
9	r9	Uptake of Butyrate	Y_{C4}						$k_{m,C4}*Msat_{SBUT,Ks,C4}*Lim_{SVAL,SBUT}*I_{pH,acet}*Noncompinh_{SNHx,IIN,BAC}*Noncompinh_{SH2,IH2\_Xc4}$
10	r10	Uptake of Propionate			Y_{PROP}				$k_{m,PROP}*Msat_{SPROP,Ks,PROP}*X_{PROP}*I_{pH,acet}*Noncompinh_{SNHx,IIN,BAC}*Noncompinh_{SH2,IH2\_Xprop}$
11	r11	Uptake of Acetate				Y_{AC}			$k_{m,AC}*Msat_{SAC,Ks,AC}*X_{AC}*I_{pH,AC}*Noncompinh_{SNHx,IIN,BAC}*Noncompinh_{SNH3,INH3,BAC}$
12	r12	Uptake of Hydrogen					Y_{H2}		$k_{m,H2}*Msat_{SH2,Ks,H2}*X_{H2}*I_{pH,H2}*Noncompinh_{SNHx,IIN,BAC}$
13	r13	Decay of X_{SUG}						$f_{XE,BM}$	$k_{dec,Xsug}*X_{SUG}$
14	r14	Decay of X_{AA}						$f_{XE,BM}$	$k_{dec,Xaa}*X_{AA}$
15	r15	Decay of X_{LCFA}						$f_{XE,BM}$	$k_{dec,Xlcfa}*X_{LCFA}$
16	r16	Decay of X_{LAC}		-1.0				$f_{XE,BM}$	$k_{dec,Xlac}*X_{LAC}$
17	r17	Decay of X_{C4}	-1.0					$f_{XE,BM}$	$k_{dec,Xc4}*X_{C4}$
18	r18	Decay of X_{PRO}			-1.0			$f_{XE,BM}$	$k_{dec,Xprop}*X_{PROP}$
19	r19	Decay of X_{AC}				-1.0		$f_{XE,BM}$	$k_{dec,Xac}*X_{AC}$
20	r20	Decay of X_{H2}					-1.0	$f_{XE,BM}$	$k_{dec,Xh2}*X_{H2}$

[a] definition of saturation and inhibition terms used in the process rates can be found in Table C3 and state variables are in Table C5

Table C2 - Description of kinetic and stoichiometric parameters and values used in the simulations.

Symbol	Unit	Name	Value
Hydrolysis			
k_{dis}	d^{-1}	First-order of Disintegration Rate Constant	0.5
$k_{hyd,CH}$	d^{-1}	Hydrolysis Rate Constant of Carbohydrates	10
$k_{hyd,PROT}$	d^{-1}	Hydrolysis Rate Constant of Proteins	10
$k_{hyd,LIP}$	d^{-1}	Hydrolysis Rate Constant of Lipids	10
Kinetic parameters			
$k_{m,SUG}$	Kg COD_S.Kg COD $_X^{-1}.d^{-1}$	Monod Max. Specific Uptake Rate of Sugars	30
$k_{m,AA}$	Kg COD_S.Kg COD $_X^{-1}.d^{-1}$	Monod Max. Specific Uptake Rate of Amino Acids	50
$k_{m,LCFA}$	Kg COD_S.Kg COD $_X^{-1}.d^{-1}$	Monod Max. Specific Uptake Rate of LCFA	6
$k_{m,C4}$	Kg COD_S.Kg COD $_X^{-1}.d^{-1}$	Monod Max. Specific Uptake Rate of Valerate/Butyrate	20
$k_{m,LAC}$	Kg COD_S.Kg COD $_X^{-1}.d^{-1}$	Monod Max. Specific Uptake Rate of Lactate	11
$k_{m,PROP}$	Kg COD_S.Kg COD $_X^{-1}.d^{-1}$	Monod Max. Specific Uptake Rate of Propionate	13
$k_{m,AC}$	Kg COD_S.Kg COD $_X^{-1}.d^{-1}$	Monod Max. Specific Uptake Rate of Acetate	8
$k_{m,H2}$	Kg COD_S.Kg COD $_X^{-1}.d^{-1}$	Monod Max. Specific Uptake Rate of Hydrogen	35
$K_{s,SUG}$	Kg $COD_S.m^{-3}$	Half Saturation Value of Uptake of Sugars	0.5
$K_{s,AA}$	Kg $COD_S.m^{-3}$	Half Saturation Value of Uptake of Amino Acids	0.3
$K_{s,LCFA}$	Kg $COD_S.m^{-3}$	Half Saturation Value of Uptake of LCFA	0.4
$K_{s,C4}$	Kg $COD_S.m^{-3}$	Half Saturation Value of Uptake of Valerate/Butyrate	0.2
$K_{s,LAC}$	Kg $COD_S.m^{-3}$	Half Saturation Value of Uptake of Lactate	0.5
$K_{s,PROP}$	Kg $COD_S.m^{-3}$	Half Saturation Value of Uptake of Propionate	0.1
$K_{s,AC}$	Kg $COD_S.m^{-3}$	Half Saturation Value of Uptake of Acetate	0.15
$K_{s,H2}$	Kg $COD_S.m^{-3}$	Half Saturation Value of Uptake of Hydrogen	7.00E-06
$k_{dec,all}$	d^{-1}	Decay rates	0.02
Yields of biomass on substrate			
Y_{SUG}	Kg COD.Kg COD^{-1}	Yield of Biomass on Sugars	0.1
Y_{AA}	Kg COD.Kg COD^{-1}	Yield of Biomass on Amino Acids	0.08
Y_{LCFA}	Kg COD.Kg COD^{-1}	Yield of Biomass on LCFA	0.06
Y_{C4}	Kg COD.Kg COD^{-1}	Yield of Biomass on Valerate/Butyrate	0.06
Y_{LAC}	Kg COD.Kg COD^{-1}	Yield of Biomass on Lactate	0.1
Y_{PROP}	Kg COD.Kg COD^{-1}	Yield of Biomass on Propionate	0.04
Y_{AC}	Kg COD.Kg COD^{-1}	Yield of Biomass on Acetate	0.05
Y_{H2}	Kg COD.Kg COD^{-1}	Yield of Biomass on Hydrogen	0.06
Stoichiometric coefficients			
$f_{LCFA,LIP}$	Kg COD.Kg COD^{-1}	Yield of lipids to LCFA	0.95
$f_{VAL,AA}$	Kg COD.Kg COD^{-1}	Yield of amino acids to valerate	0.23
$f_{BUT,AA}$	Kg COD.Kg COD^{-1}	Yield of amino acids to butyrate	0.26
$f_{PROP,AA}$	Kg COD.Kg COD^{-1}	Yield of amino acids to propionate	0.05
$f_{AC,AA}$	Kg COD.Kg COD^{-1}	Yield of amino acids to acetate	0.4
$f_{H2,AA}$	Kg COD.Kg COD^{-1}	Yield of amino acids to hydrogen	0.06
$f_{CH,BM}$	Kg COD.Kg COD^{-1}	Yield of Biomass to carbohydrates	0.26
$f_{PROT,BM}$	Kg COD.Kg COD^{-1}	Yield of Biomass to proteins	0.26
$f_{LIP,BM}$	Kg COD.Kg COD^{-1}	Yield of Biomass to lipids	0.33

$f_{Su,BM}$	Kg COD.Kg COD^{-1}	Yield of Biomass to soluble inerts	0.05
$f_{XE,BM}$	Kg COD.Kg COD^{-1}	Yield of Biomass to Endogenous Decay Products	0.1
$f_{AC,SUG}$	Kg COD.Kg COD^{-1}	Yield of monosaccharides to acetate	0.033
$f_{PROP,SUG}$	Kg COD.Kg COD^{-1}	Yield of monosaccharides to propionate	0
$f_{ET,SUG}$	Kg COD.Kg COD^{-1}	Yield of monosaccharides to ethanol	0.057
$f_{BUT,SUG}$	Kg COD.Kg COD^{-1}	Yield of monosaccharides to butyrate	0.549
$f_{LAC,SUG}$	Kg COD.Kg COD^{-1}	Yield of monosaccharides to lactate	0.235
$f_{H2,SUG}$	Kg COD.Kg COD^{-1}	Yield of monosaccharides to hydrogen	0.126
$f_{AC,LAC}$	Kg COD.Kg COD^{-1}	Yield of lactate to acetate	0.525
$f_{PROP,LAC}$	Kg COD.Kg COD^{-1}	Yield of lactate to propionate	0.133
$f_{VAL,LAC}$	Kg COD.Kg COD^{-1}	Yield of lactate to valerate	0.214
$f_{H2,LAC}$	Kg COD.Kg COD^{-1}	Yield of lactate to hydrogen	0.128

Table C3 - Saturation and inhibition terms used in the process rates.

Symbol	Name	Expression
$Msat_{SSUG,Ks,SUG}$	Saturation term of monosaccharides	$S_{SUG}/(K_{s,SUG}+S_{SUG})$
$Msat_{SAA,Ks,AA}$	Saturation term of amino acids	$S_{AA}/(K_{s,AA}+S_{AA})$
$Msat_{SLCFA,Ks,LCFA}$	Saturation term of long chain fatty acids	$S_{LCFA}/(K_{s,LCFA}+S_{LCFA})$
$Msat_{SVAL,Ks,C4}$	Saturation term of valerate	$S_{VAL}/(K_{s,C4}+S_{VAL})$
$Msat_{SBUT,Ks,C4}$	Saturation term of butyrate	$S_{BUT}/(K_{s,C4}+S_{BUT})$
$Msat_{SLAC,Ks,LAC}$	Saturation term of lactate	$S_{LAC}/(K_{s,LAC}+S_{LAC})$
$Msat_{SPROP,Ks,PROP}$	Saturation term of propionate	$S_{PROP}/(K_{s,PROP}+S_{PROP})$
$Msat_{SAC,Ks,AC}$	Saturation term of acetate	$S_{AC}/(K_{s,AC}+S_{AC})$
$Msat_{SH2,Ks,H2}$	Saturation term of dissolved hydrogen	$S_{H2}/(K_{s,H2}+S_{H2})$
$Lim_{SBUT,SVAL}$	Butyrate/Valerate limitation	$X_{C4}/(1+S_{BUT}/S_{VAL})$
$Lim_{SVAL,SBUT}$	Valerate/Butyrate limitation	$X_{C4}/(1+S_{VAL}/S_{BUT})$
$Noncompinh_{SNHx,IIN,BAC}$	Ammonia inhibition	$1/(1+ I_{IN,BAC}/S_{NHx})$
$Noncompinh_{SH2,IH2\_Xlcfa}$	Hydrogen inhibition (X_LCFA)	$1/(1+ S_{H2}/I_{H2\_Xlcfa})$
$Noncompinh_{SH2,IH2\_Xc4}$	Hydrogen inhibition (X_C4)	$1/(1+ S_{H2}/I_{H2\_Xc4})$
$Noncompinh_{SH2,IH2\_Xprop}$	Hydrogen inhibition (X_PROP)	$1/(1+ S_{H2}/I_{H2\_Xprop})$
$Noncompinh_{SNH3,INH3,BAC}$	Ammonia inhibition	$1/(1+ S_{NHx}/I_{NH3,BAC})$
$I_{pH,acid}$	Calculated pH Inhibition for Acidogens	$If(pH>=I_{pHUL,acid}; 1; Exp(-3*((pH-I_{pHUL,acid})/(I_{pHUL,acid}-I_{pHLL,acid}))^2))$
$I_{pH,acet}$	Calculated pH Inhibition for Acetogens	$If(pH>=I_{pHUL,acet}; 1; Exp(-3*((pH-I_{pHUL,acet})/(I_{pHUL,acet}-I_{pHLL,acet}))^2))$
$I_{pH,lac}$	Calculated pH Inhibition for Lactate Degraders	$If(pH>=I_{pHUL,lac}; 1; Exp(-3*((pH-I_{pHUL,lac})/(I_{pHUL,lac}-I_{pHLL,lac}))^2))$
$I_{pH,AC}$	Calculated pH Inhibition for Aceticlastic Methanogens	$If(pH>=I_{pHUL,AC}; 1; Exp(-3*((pH-I_{pHUL,AC})/(I_{pHUL,AC}-I_{pHLL,AC}))^2))$
$I_{pH,H2}$	Calculated pH Inhibition for Hydrogen-utilising Methanogens	$If(pH>=I_{pHUL,H2}; 1; Exp(-3*((pH-I_{pHUL,H2})/(I_{pHUL,H2}-I_{pHLL,H2}))^2))$

C.2 Influent characterisation

Table C4 - Measurements needed for the characterisation of the influent.

Parameter	Average (std)
COD_{Total} (g COD.m^{-3}) [a]	29095 (2445)
$COD_{Soluble}$ (g COD.m^{-3}) [a]	24089 (2024)
SFP_{Total} (g COD.m^{-3}) [a]	104 (102)
Lactate (g COD.m^{-3}) [a]	47 (69)
Acetate (g COD.m^{-3}) [a]	27 (9)
Propionate (g COD.m^{-3}) [a]	30 (91)
Ethanol (g COD.m^{-3}) [a]	0 (0)
Butyrate (g COD.m^{-3}) [a]	0.16 (0.98)
Valerate (g COD.m^{-3}) [a]	0 (0)
N_{Total} (g N.m^{-3}) [b]	144 (12)
NH_x-N (g N.m^{-3}) [a]	104 (12)
P_{Total} (g P.m^{-3}) [b]	49 (4)
PO_4-P (g P.m^{-3}) [a]	41 (7)
TSS (g TSS.m^{-3}) [b]	5645 (474)
VSS (g VSS.m^{-3}) [b]	5239 (440)
Carbohydrates (g COD.m^{-3}) [c]	3841
Proteins (g COD.m^{-3}) [c]	517
Lipids (g COD.m^{-3}) [c]	567

[a] measurements from reactor weekly monitoring
[b] measurements from the extra sampling campaign
[c] assumed from the study of Gali et. al 2009

Table C5 - Equations used in total COD, total nitrogen and total phosphorous mass balances.

Parameter	Description	Mass balance
COD_{Total}	Total COD	$COD_{particulate} + COD_{Soluble}$
$COD_{particulate}$	Particulate COD	$X_{CH} + X_{PROT} + X_{LIP} + X_{bac} + X_U$
$COD_{Soluble}$	Soluble COD	$S_{SUG} + S_{AA} + S_{LCFA} + SFP_{Total} + S_U$
X_{bac}	COD of all biomasses	$X_{SUG} + X_{AA} + X_{LCFA} + X_{LAC} + X_{PROP} + X_{AC} + X_{H2}$
SFP_{Total}	Total SFPs	$S_{AC} + S_{BUT} + S_{PROP} + S_{VAL} + S_{LAC} + S_{ET}$
N_{Total}	Total nitrogen	$S_{NHx} + N_{bac} + N_{AA} + N_{XU} + N_{SU}$
P_{Total}	Total phosphorous	$S_{PO4} + P_{bac} + P_{XLIP} + P_{XCH} + P_{XU} + P_{SU}$

Table C6 - State variables of the modified ADM1 model developed.

State variable	Description	Value	State variable	Description	Value
S_{SUG} (g COD.m^{-3})	Monosaccharides	23974	$X_{E,AN}$ (g COD.m^{-3})	Anaerobic Decay Products	82
S_{AA}(g COD.m^{-3})	Amino Acids	0	S_{NHx} (g N.m^{-3})	Ammonia	0
S_{LCFA} (g COD.m^{-3})	Long Chain Fatty Acids	0	N_{bac} (g N.m^{-3})	Nitrogen from biomass	105
S_{VAL} (g COD.m^{-3})	Total Valerate	0	N_{AA} (g N.m^{-3})	Nitrogen from amino acids	38
S_{BUT} (g COD.m^{-3})	Total Butyrate	0	N_{XU} (g N.m^{-3})	Nitrogen from particulate inerts	2
S_{PROP} (g COD.m^{-3})	Total Propionate	30	N_{SU} (g N.m^{-3})	Nitrogen from soluble inerts	0.5
S_{AC} (g COD.m^{-3})	Total Acetate	27	S_{PO4} (g P.m^{-3})	Orthophosphate	41
S_{LAC} (g COD.m^{-3})	Total Lactate	47	P_{bac} (g P.m^{-3})	Phosphorus from biomass	0
S_{ET} (g COD.m^{-3})	Ethanol	0	P_{XLIP} (g P.m^{-3})	Phosphorus from lipids	0
S_{U} (g COD.m^{-3})	Soluble Inerts	10	P_{XCH} (g P.m^{-3})	Phosphorus from carbohydrates	12
X_{COMP} (g COD.m^{-3})	Composites	0	P_{XU} (g P.m^{-3})	Phosphorus from particulate inerts	0.8
X_{CH} (g COD.m^{-3})	Carbohydrates	3841	P_{SU} (g P.m^{-3})	Phosphorus from soluble inerts	0.0
X_{PROT} (g COD.m^{-3})	Proteins	517	X_{CH} (g TSS.m^{-3})	Carbohydrates	3600
X_{LIP} (g COD.m^{-3})	Lipids	566	X_{PROT} (g TSS.m^{-3})	Proteins	317
X_{SUG} (g COD.m^{-3})	Sugar Degraders	0	X_{LIP} (g TSS.m^{-3})	Lipids	197
X_{AA} (g COD.m^{-3})	Amino Acids Degraders	0	X_{SUG} (g TSS.m^{-3})	Sugar Degraders	0
X_{LCFA} (g COD.m^{-3})	LCFA Degraders	0	X_{AA} (g TSS.m^{-3})	Amino Acids Degraders	0
X_{C4} (g COD.m^{-3})	Valerate and Butyrate Degraders	0	X_{LCFA} (g TSS.m^{-3})	LCFA Degraders	0
X_{PROP} (g COD.m^{-3})	Propionate Degraders	0	X_{PROP} (g TSS.m^{-3})	Propionate Degraders	0
X_{AC} (g COD.m^{-3})	Acetate Degraders	0	X_{AC} (g TSS.m^{-3})	Acetate Degraders	0
X_{H2} (g COD.m^{-3})	Hydrogen Degraders	0	X_{H2} (g TSS.m^{-3})	Hydrogen Degraders	0
X_{LAC} (g COD.m^{-3})	Lactate Degraders	0	X_{LAC} (g TSS.m^{-3})	Lactate Degraders	0
X_{bac} (g COD.m^{-3})	Total Biomass	0	X_{bac} (g TSS.m^{-3})	Total Biomass	0
X_{U} (g COD.m^{-3})	Particulate Inerts	0	X_{U} (g TSS.m^{-3})	Particulate Inerts	63

C.3 References

Galí, A., Benabdallah, T., Astals, S., Mata-Alvarez, J., 2009. Modified version of ADM1 model for agro-waste application. Bioresour. Technol. 100, 2783–2790. https://doi.org/10.1016/j.biortech.2008.12.052

2021

MARIANA CAMPOS DE MATOS

POLYHYDROXYALKANOATE (PHA) BIOSYNTHESIS FROM FRUIT WASTE AT PILOT SCALE: PRODUCTIVITY MAXIMISATION AND POLYMER TAILORING